Spectrum Awareness for Cognitive Radio Systems

by

©Yahia Y. Ahmed Eldemerdash Ahmed

A dissertation submitted to the School of Graduate Studies
in partial fulfillment of the requirements for the degree of

Doctor of Philosophy

Faculty of Engineering and Applied Science
Memorial University of Newfoundland

October 2015

St. John's, Newfoundland

Abstract

Spectrum scarcity is an obstacle to deploy emerging high speed wireless services that require more frequency spectrum. Cognitive radio (CR) appears as a promising solution for the spectral congestion by allowing spectrum sharing between primary and secondary users in which optimum utilization of the available spectrum is achieved. Efficient coexistence between different users requires full knowledge of the activities in the spectrum of interest. Spectrum awareness is the terminology used to describe the techniques that detect the presence of signals in certain frequency bands, as well as identify the main parameters of such signals, e.g., modulation scheme. These two tasks are commonly referred by the terms spectrum sensing and signal identification, respectively.

Blind signal identification was initially used by military applications, such as radio surveillance and electronic warfare, and has recently been extended to civilian applications. This problem becomes more challenging in multiple-input multiple-output (MIMO) scenarios due to the diverse transmission schemes that can be employed, e.g., spatial multiplexing (SM) and space-time block codes (STBCs). A large number of studies have been carried out for developing blind signal identification algorithms in single-input single-output (SISO) scenarios, including identification of the modulation format and recognition of single-carrier (SC) versus multicarrier transmissions. However, the problem of signal identification for MIMO systems remains at an incipient stage. In this dissertation, we develop novel algorithms to blindly identify the MIMO transmission scheme of the received signal.

More specifically, in Chapters 2 and 3, we address the problem of identifying STBCs for the SC transmission. Unlike most of the work done to date, we show that STBC identification can be performed using a single receive antenna. Four algorithms are proposed in Chapter 2 to identify SM and Alamouti STBC. Then, the idea is extended to include additional STBCs in Chapter 3. The proposed algorithms show improved performance when compared with other algorithms in the literature. Moreover, neither modulation identification nor channel and noise power estimation are required by these algorithms.

In Chapter 4 we investigate the identification of SM and Alamouti coded orthogonal frequency division multiplexing (OFDM) signals. A new discriminating feature and a novel decision criterion are developed. The proposed algorithm outperforms the algorithms in the literature with the advantages of requiring neither modulation identification nor channel and noise power estimation, and being more robust to the carrier frequency offset impairment.

Furthermore, in Chapter 5, the problem of identifying SM and Alamouti SC frequency division multiple access (SC-FDMA) signals is studied when the receiver is equipped with a single antenna. To the best of our knowledge, this is the first work devoted to the identification of MIMO SC-FDMA signals. The theoretical performance analysis of the proposed algorithm is presented. Simulation results show the agreement between theoretical and simulation findings. The proposed algorithm requires neither modulation identification nor channel and noise power estimation.

Finally, conclusions are drawn and possible extensions to signal identification in MIMO scenarios are discussed in Chapter 6.

To the soul of my parents ...

To my wife and my kids, Yassin and Mohamed ...

Acknowledgements

After thanking Almighty "ALLAH" for his blessing and guidance to complete this work, I would like to offer my sincere thanks to my supervisor Prof. Octavia Dobre for the amazing opportunity she provided me with. Her valuable guidance, dedication, and encouragement have pushed me far beyond my expectations.

I would like to acknowledge the financial support provided by my supervisor, the Faculty of Engineering and Applied Science, the School of Graduate Studies, and Defence Research and Development Canada (DRDC).

I would like to thank the staff of the Department of Electrical and Computer Engineering. I thank all my group members and lab colleagues; it was fun working with all of you.

I would like to acknowledge the most impactful persons in my life, my parents. I would have never been in this position without your love, care, and support. I wish you were with me to share this moment.

Finally, I would like to acknowledge a lot of sincere and loving people I have been blessed with, who have strongly contributed to this success. Starting with my brother Khaled Ahmed, for taking care of everything back home on my behalf, my brother and sister, for their love, my father and mother in law, what can I say to express my gratitude to you, my lovely wife, without you nothing is complete, and my kids, Yassin and Mohamed, you add a great value to everything.

Co-Authorship Statement

I, Yahia Y. Ahmed Eldemerdash Ahmed, hold a principle author status for all the manuscript chapters (Chapter 2 - 5) in this dissertation. However, each manuscript is co-authored by my supervisor and co-researchers, whose contributions have facilitated the development of this work as described below.

- Paper 1 in Chapter 2: Yahia A. Eldemerdash, Mohamed Marey, Octavia A. Dobre, Gorge Karagiannidis, and Robert Inkol, "Fourth-Order Statistics for Blind Classification of Spatial Multiplexing and Alamouti Space-Time Block Code Signals," IEEE Transactions on Communications, vol. 61, pp. 2420-2431, June 2013.
  I was the primary author, with authors 2 - 5 contributing to the idea, its formulation and development, and refinement of the presentation.

- Paper 2 in Chapter 3: Yahia A. Eldemerdash, Mohamed Marey, Octavia A. Dobre, Gorge Karagiannidis, and Robert Inkol, "An Efficient Algorithm for Space-Time Block Code Classification," in Proceeding of IEEE Globecom, 2013, pp. 3329-3334.
  I was the primary author, with authors 2 - 5 contributing to the idea, its formulation and development, and refinement of the presentation.

- Paper 3 in Chapter 4: Yahia A. Eldemerdash, Octavia A. Dobre, and Bruce Liao, "Blind Identification of SM and Alamouti STBC-OFDM Signals," IEEE Transactions on Wireless Communications, vol. 14, pp. 972-982, February 2015.

I was the primary author, with authors 2 - 3 contributing to the idea, its formulation and development, and refinement of the presentation.

- Paper 4 in Chapter 5: Yahia A. Eldemerdash and Octavia A. Dobre, "On The Identification of SM and Alamouti Coded SC-FDMA Signals: A Statistical-Based Approach," submitted to IEEE Transactions on Vehicular Technology, June 2015.
  I was the primary author, with the second author contributing to the idea, its formulation and development, and refinement of the presentation.

_____ _____

Yahia Y. Ahmed Eldemerdash Ahmed Date

Table of Contents

List of Tables

List of Figures

List of Abbreviations

AL	Alamouti
AWGN	Additive White Gaussian Noise
CC	Cyclic Cross-correlation
CF	Cycle Frequency
CoP	Code Parameter
CP	Cyclic Prefix
CR	Cognitive Radio
DFT	Discrete Fourier Transform
FB	Feature-based
FBMC	Filter Bank Multicarrier
FFT	Fast Fourier Transform
FOLP	Fourth-Order Lag Product
FOM	Fourth-Order Moment
IFFT	Inverse Fast Fourier Transform

LB	Likelihood-based
LRT	Likelihood Ratio Test
MIMO	Multiple-Input Multiple-Output
ML	Maximum Likelihood
OFDM	Orthogonal Frequency Division Multiplexing
QAM	Quadrature Amplitude Modulation
QPSK	Quadrature Phase-Shift Keying
SC	Single Carrier
SC-FDMA	Single Carrier Frequency Division Multiple Access
SISO	Single-Input Single-Output
SM	Spatial Multiplexing
SNR	Signal-to-Noise Ratio
SOS	Second-Order Statistics
STBCs	Space-Time Block Codes
SVM	Support Vector Machine

Chapter 1

Introduction and Overview

1.1 Background

Wireless technologies have evolved remarkably since Guglielmo Marconi first demonstrated the radio's ability to provide continuous contact with ships sailing in the English channel in 1897. New theories and applications of wireless technologies have been developed by thousands of scientists and engineers throughout the world ever since. Wireless communications can be regarded as the most important development that has an extremely wide range of applications: from TV remote control and cordless phones to cellular phones and satellite-based systems. It has changed people's life style in every respect. Especially during the last decade, the mobile radio communications industry has grown at an exponential rate, fueled by the digital and radio frequency (RF) circuit design, fabrication and integration techniques and more computing power in electronic chips. This trend will continue with an even greater pace in the future.

In wireless communications, the radio spectrum is a scarce resource due to the ceaseless demands of spectrum by new applications and services [1]. Cognitive radio (CR) has arisen as a promising solution to the spectral scarcity problem by introducing op-

portunistic usage of the frequency bands that are not heavily utilized by the primary/ incumbent radios [1–3]. CR can be considered to be an adaptive communication system, which has the capability to learn from the surrounding environment and adapt its parameters accordingly. The basic features of CR are intelligence, adaptability, learning, accuracy, reconfigurability, and reliability [4]. Due to the CR ability to autonomously detect and react to the changes in the environment, spectrum sensing and awareness is a fundamental component in the CR architecture [5, 6]. This is not simply the problem of deciding whether there is an available frequency band to use or not, but also of blindly (non-data-aided) identifying the signal type of the radios transmitting in the frequency bands adjacent to the available band. This enables the CR to design a transmission strategy that minimizes interference to and from those radios. Since different signals are able to tolerate different amounts of interference, the signal type of other radios sharing the environment has to be identified. Blind signal identification has other important applications in electronic warfare, spectrum monitoring, radio surveillance, and parameter configuration in software-defined radios [7, 8].

Signal identification for single-input single-output (SISO) and single-input multiple-output (SIMO) systems has been intensively investigated in the existing literature. Modulation identification has been considered in [9–16], whereas discrimination between single carrier (SC) and orthogonal frequency division multiplexing (OFDM) signals has been investigated in [17–21], and detection of the number of sources transmitting in the frequency band of interest has been considered in [22–27].

Due to the increasing complexity and diversity of techniques used in digital wireless communications both in civilian and military communications, methods employed in signal identification need to be constantly extended and improved to include newly emerging transmission techniques. Each emerging transmission method presents new parameters to identify and new challenges to overcome. The multiple-input multiple-output (MIMO)

systems, which have become popular in the last decade, represent such an example.

The main difference between the MIMO systems and conventional SISO systems is that the former employs multiple antennas for transmission and reception. This is done by either multiplexing the data symbols to multiple transmit antennas or introducing redundancy to the signal by employing space-time codes. These two approaches allow MIMO systems to achieve a distinct advantage when compared with SISO systems in terms of data rates and robustness in fading environments, respectively.

With the deployment of the MIMO technology [28, 29], new and challenging signal identification problems have emerged, which do not exist for single antenna systems, such as the identification of the space-time block code (STBC) and detection of the number of transmit antennas employed in the MIMO transmission. Furthermore, existing modulation identification algorithms developed with the assumption of single antenna transmission cannot be directly applied when multiple transmit antennas are used. Hence, the modulation identification problem needs to be completely reconsidered for MIMO systems. Research efforts on signal identification for MIMO signals, which have found considerable interest in the last couple of years, have been concentrating on these three particular problems [30–53]. Throughout this dissertation, we focus on the STBC identification for different transmission systems.

The work devoted to STBC identification can be divided into two categories: likelihood-based (LB) [30] and feature-based (FB) [31–45] algorithms. Both approaches have been investigated for the identification of STBC for SC systems [30–42], whereas only FB methods have been employed for the identification of STBC for OFDM systems [43–45]. The basic idea of the LB algorithms is to calculate the likelihood function of the received signal, and then employ the maximum likelihood (ML) criterion to make a decision. In case of the FB algorithms, the space-time redundancy induced in the transmit signal by the space-time coding operation is exploited to identify STBCs with different code lengths.

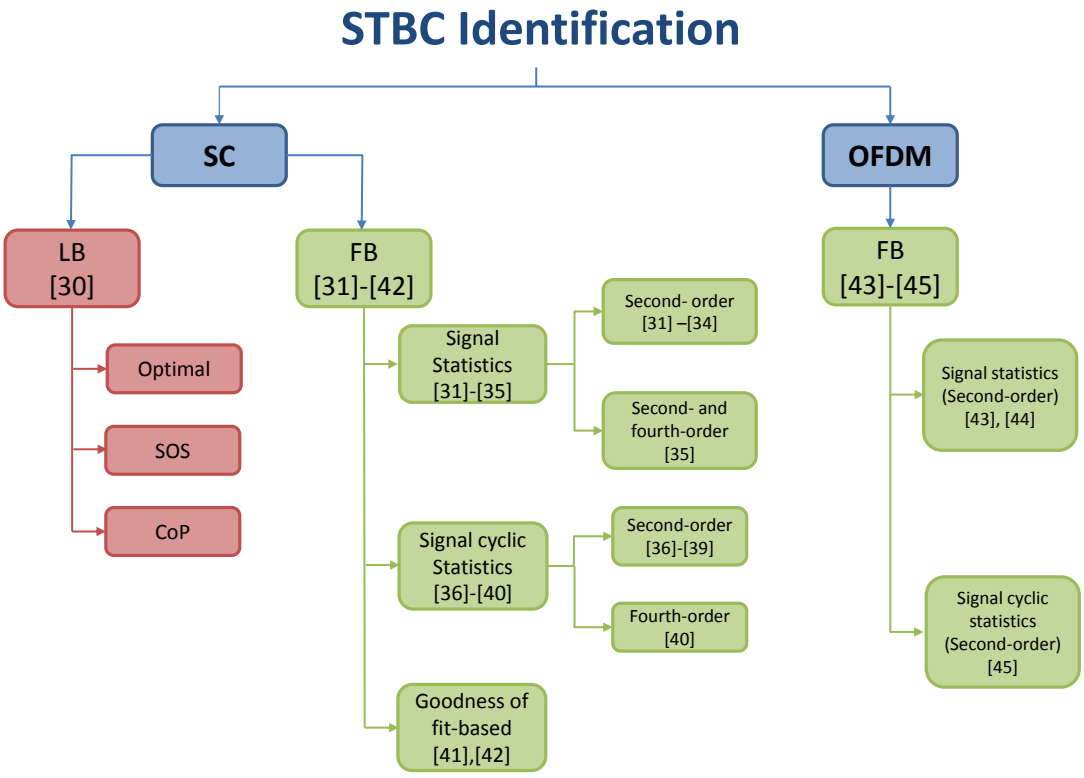

Fig. 1.1: Summary of the existing STBC identification algorithms for SC and OFDM systems. Here, SOS and CoP refer to the second-order statistics and code parameter algorithms, respectively.

Various features have been considered for discriminating between different STBCs, such as second- [31–34, 43, 44], and both second- and fourth-order [35] signal statistics, as well as second- [36–39, 45] and fourth-order [40] signal cyclic statistics. A summary of existing STBC identification algorithms for the SC and OFDM systems is provided in Fig. 1.1, and more details are presented in the next two sections of this chapter.

1.2 STBC identification for SC systems

1.2.1 Likelihood-based algorithms

The authors in [30] propose three LB approaches for STBC identification assuming a frequency-flat block fading channel: the optimal algorithm in the sense of maximizing the average probability of correct identification, its second-order statistics (SOS) approximation, and the code parameter (CoP) algorithm.

The STBC $\hat{C}$ is recognized at the receive-side among a set Θ_C of STBC candidates with equal *a priori* probabilities as

$$\hat{C} = \arg \max_{C \in \Theta_C} \log(\Lambda[\mathbf{Y}|C, \mathbf{H}, \mathcal{M}, \sigma_w^2]), \tag{1.1}$$

where $\log(\Lambda[\mathbf{Y}|C, \mathbf{H}, \mathcal{M}, \sigma_w^2])$ is the log-likelihood function of the $N_r \times K$ matrix $\mathbf{Y}$ corresponding to the received signal, conditioned on the transmitted STBC C, the $N_r \times N_t$ channel matrix $\mathbf{H}$, the modulation $\mathcal{M}$, and the noise power σ_w^2 at the receiver, with N_r, K, and N_t denoting the number of receive antennas, the number of received samples, and the number of transmit antennas, respectively. The log-likelihood function in (1.1) is calculated by averaging over the data symbols considered as independent and identically distributed (i.i.d.) variables drawn from the alphabet corresponding to the constellation points of modulation $\mathcal{M}$; thus, the algorithm is referred to as the average likelihood ratio test (ALRT).

The ALRT algorithm requires knowledge of the channel matrix $\mathbf{H}$, the modulation $\mathcal{M}$, and the noise power at the receiver σ_w^2, as well as perfect timing, block, and frequency synchronization, which makes it impractical. In addition, it suffers from high computational complexity. On the other hand, it provides an optimal solution in the sense of maximizing the average probability of correct identification and represents an upper bound for the STBC identification performance.

In the SOS algorithm, the received symbols are modeled as i.i.d. Gaussian variables, with zero-mean and covariance $\mathbf{\Psi}_{C,\mathbf{H},\sigma_w^2}$, regardless of the modulation type. Accordingly, the log-likelihood function is expressed as $\log(\Lambda[\mathbf{Y}|\mathbf{\Psi}_{C,\mathbf{H},\sigma_w^2}])$, and $\hat{C}$ is selected as the STBC candidate which maximizes this function. When compared with the optimal algorithm, SOS has reduced complexity. The algorithm can be extended to the blind context by estimating the unknown parameters $\mathbf{H}$ and σ_w^2 under the hypothesis that the STBC C is transmitted. Then, the STBC $\hat{C}$ is chosen as the one for which the log-likelihood function with the associated estimated parameters is maximum. Several techniques are reported in the literature for estimating $\mathbf{H}$ and σ_w^2 for various STBCs [54, 55]. Apparently, the estimation accuracy affects the performance of the blind SOS algorithm and the computational complexity increases (depending on the estimation method).

In the CoP algorithm, a parameterized likelihood function is constructed using the STBC parameters, i.e., code length, L, and number of transmitted symbols for each block, N_s, and knowledge of the modulation and channel is not required. This algorithm is suitable for STBCs with different parameters, i.e., different code lengths or different numbers of symbols per space-time block. For example, SM ($N_t = 2$) and AL-STBC can be differentiated by their respective code length. On the other hand, if two codes have the same code length, they can be identified if they have a different numbers of symbols per space-time block. In this case, the parameterized log-likelihood function can be written as a function of N_s and L, i.e., $\log(\Lambda[\mathbf{Y}|\mathbf{\Psi}_{N_s,L}])$, where $\mathbf{\Psi}_{N_s,L}$ is the parameterized covariance matrix of the received sequence [30]. Finally, the STBC $\hat{C}$ is chosen as the one that maximizes $\log(\Lambda[\mathbf{Y}|\mathbf{\Psi}_{N_s,L}])$. The CoP algorithm has less computational complexity when compared with the optimal and SOS algorithms.

All LB algorithms presented above require timing, block, and frequency synchronization. Furthermore, both SOS (blind) and CoP algorithms require that the number of receive antennas satisfies $N_r \geq N_s/L$; thus, these algorithms cannot be employed in

receivers with a single antenna.

1.2.2 Feature-based algorithms

The FB STBC identification algorithms found in the literature mainly exploit the space-time redundancy induced in the transmit signal to identify STBCs with different code lengths. This inherent property of the STBC coded signals is employed by several algorithms, which can be categorized into three distinct subcategories: *signal statistics-based* [31–35], *signal cyclic statistics-based* [36–40], and *goodness of fit-based* [41, 42] algorithms. A brief presentation of these algorithms is provided as follows.

Signal statistics-based algorithms

A second-order/ zero-conjugate space-time correlation is used in [31] and [32] to provide a feature for STBC identification. The zero-conjugate is used, as the encoding matrices of STBCs other than SM already contain conjugation. It has been shown that the Frobenius norm of the space-time second-order correlation matrix exhibits peaks whose positions depend on the STBC. Detecting the presence of a peak at a certain delay is formulated as a binary hypothesis testing problem, i.e., there exists no peak under hypothesis $\mathcal{H}_0$, while a peak is present under hypothesis $\mathcal{H}_1$. In [31], the decision whether a peak is present or not is made based on the minimum distance between the theoretical and estimated features. In [32], such a decision is made by comparing the feature estimate with a threshold corresponding to a certain probability of false alarm, which is defined as the probability to decide that a peak exists, when it does not. The main drawback of the algorithms in [31] and [32] is that they require multiple receive antennas $N_r \geq N_t$; in practical applications, size, power, and cost constraints on the intelligent radio receivers may favor single receive antenna solutions for STBC identification.

The identification features in [32] are employed in [33], where the correlations at several

delays are considered and feature vectors are formed accordingly. Based on these vectors, a support vector machine (SVM) is trained to identify various STBCs. The algorithm in [33] shows better performance when compared with those in [31] and [32], as the identification process relies on feature vectors containing multiple features corresponding to different delays. Note that the algorithm in [33] has the same limitation on the number of receive antennas as [31] and [32], i.e., $N_r \geq N_t$.

Furthermore, a second-order/ zero-conjugate cross-correlation between the signals received with two different antennas is exploited as an identification feature in [34] under frequency-selective channel conditions. The authors show that for AL-STBC, the cross-correlation exhibits peaks at delays related to the symbol duration and the multiple propagation paths, whereas no peaks are present for SM. The decision is made on the maximum of the estimated cross-correlations for all pairs of receive antennas by comparing the maximum cross-correlation with a threshold corresponding to a certain probability of false alarm. Apparently, this algorithm requires at least two receive antennas, and it cannot be used with single antenna receivers.

As previously discussed, second-order statistics of the signal cannot provide an identification feature when a single antenna is available at the receive-side; in such a case, the authors in [35] resort to fourth-order statistics for STBC signal identification.

In [35], the vector of the received samples is re-arranged to form specific two-rows and four-rows matrices. The authors show that at zero-delay, the second-order/ one-conjugate and the fourth-order/ two-conjugate statistics of these matrices provide suitable features for STBC identification. The statistics are mapped into a high dimensional space using a trained SVM to identify the candidate STBCs.

Signal cyclic statistics-based algorithms

Cyclic statistics-based features are proposed in [36–40] for STBC identification. The second-order/ zero-conjugate cyclic cross-correlation (CC) of the signals received by two

antennas is used in [36–38] for STBC identification. It was shown that this CC exhibits peaks at cycle frequencies (CFs) and delays depending on the transmitted STBC. No CFs exist for SM, while CFs equal multiple integers of $\frac{1}{\rho L}$ are exhibited by other STBCs, with ρ an integer representing the oversampling factor. Detecting the presence of peaks at a single CF is done by using the cyclostationarity test developed by Dandawate and Giannakis in [56], while the test proposed in [57] can be used to detect the presence of peaks at multiple CFs.

In [39], the second-order/ zero-conjugate and second-order/ one-conjugate CCs of the N_t components of the transmit signal vector are employed for STBC identification. Since the choice of the discriminating features is based on the CCs of the transmit signal vector, its reconstruction is required at the receive-side prior to estimating the features. As such, the estimation of the number of transmit antennas is performed first, for which the authors apply the Gaussian minimum description length algorithm [22]. This knowledge leads to a reduction in the number of the STBC candidates, since only the codes characterized by the estimated N_t need to be considered for identification. Subsequently, the joint approximate diagonalization of eigen-matrices algorithm [58] is employed to separate the N_t transmit signals, from which the CCs are estimated. The decision on the STBC is made by detecting the existence of CFs at specific delays, based on the cyclostationarity test in [56]. The algorithm in [39] has the capability of identifying a large pool of STBCs, including codes with the same code length. However, it suffers from higher computational complexity when compared with other signal cyclic statistics-based algorithms due to the pre-processing steps required for the reconstruction of the transmit signals.

The previously presented second-order CCs are not suitable for receivers equipped with a single antenna. For this case, the fourth-order/ two-conjugate cyclic cumulant at CF $\frac{1}{2\rho}$ and delay vector $[0, 0, \rho, \rho]$ is employed to identify SM and AL-STBC [40], with the decision criterion based on the cyclostationarity test in [56]. The algorithm in [40]

was investigated under AWGN channel conditions; for practical fading channels, this algorithm does not provide an adequate performance.

Goodness of fit-based algorithms

A non-parametric goodness of fit test is adopted in [41, 42] to identify STBCs with a single receive antenna. In [41], the identification of SM and AL-STBC is done by constructing two vectors from the received sequence. The authors show that such vectors are i.i.d. with the same distribution for SM, whereas this does not hold for AL-STBC. The Kolmogorov-Smirnov test is employed to measure the distance between the empirical cumulative distributions of the two sequences, and thus, to decide whether SM or AL-STBC is present. The main advantage of this approach is that it is robust to time and frequency offsets. The method was extended in [42] to include additional STBCs; however, a larger observation period is required to obtain a good performance when compared with the identification of SM and AL-STBC.

1.3 STBC identification for OFDM systems

The problem of STBC identification for OFDM systems is investigated in [43–45], by following the FB approach. Features based on the second-order/ zero-conjugate cross-correlation are employed in [43, 44], while the second-order/ zero-conjugate cyclic cross-correlation is used in [45]. Note that the cross-correlation functions are estimated between the signal components received by different antenna pairs ($N_r \geq 2$). It should be noted that the inverse fast Fourier transform (IFFT) block in the MIMO-OFDM transmitter [59] makes the problem of STBC-OFDM signal identification more challenging when compared with the case of the SC systems [43–45].

The authors in [43, 44] propose a second-order/ zero-conjugates cross-correlation between the signals received by two antennas, $N_r = 2$. The idea is to calculate the cross-

correlation between the two received signals on each subcarrier. The authors show that the proposed cross-correlation exhibits at least two peaks on two subcarriers separated by $N/2$, with N as the number of subcarriers; on the other hand, no peaks exist in case of SM [43]. The decision about the presence of such discriminating peaks is made by comparing the maximum of the cross-correlations with a threshold corresponding to a desired probability of false alarm. The idea is extended in [44] to include other STBCs with different code lengths. The main drawback of this approach is that it requires a large observation time and suffers from high sensitivity to frequency offset.

In [45], an approach based on the second-order/ zero-conjugate cyclic cross-correlation is proposed to identify SM and AL-STBC by using different antennas ($N_r \geq 2$). The cyclostationarity test proposed in [56] is employed as a decision criterion. This algorithm is applicable for OFDM signals with a reduced number of subcarriers and has the same disadvantage of sensitivity to frequency offset as the algorithms in [43] and [44].

1.4 Motivation and Outline

Motivation:

Based on the aforementioned discussion, the following observations can be made:

- Most of the STBC identification algorithms require multiple antennas at the receive-side. Since this requirement cannot always be met due to size and cost limitations, solutions for STBC blind identification when a single receive antenna is available are of interest.

- The existing STBC identification algorithms for the OFDM system require a large observation period and suffer from high sensitivity to frequency offset.

- While STBC identification has been investigated for both SC and OFDM systems,

there is no work in the literature devoted to study this problem for the SC-FDMA systems.

Motivated by the aforementioned observations, in this thesis we have addressed the following research problems:

Research problems:

- **P1**- Developing STBC identification algorithms for SC signals with a single receive antenna.
- **P2**- Developing an identification algorithm for STBC-OFDM signals which requires shorter observation period, and hence is less sensitive to the frequency offset.
- **P3**- Developing an algorithm to identify STBC SC-FDMA signals.

Thesis structure:

Chapters 2 and 3 address **P1**, i.e., we propose algorithms to blindly identify STBCs when a single receive antenna is available. In particular, identification of SM and Alamouti STBCs are considered in Chapter 2, where the fourth-order moment and the discrete Fourier transform of the fourth-order lag product (FOLP) are used as discriminating features. For the former, an optimal algorithm is proposed by employing the likelihood ratio test (LRT) to maximize the average probability of correct identification; however, it requires knowledge of several parameters, e.g., channel coefficients and noise power. Three FOLP-based algorithms, named FOLP-A, -B, and -C, are then proposed to relax such requirements. It was shown that the FOLP-C algorithm is robust to frequency offset when compared with the other proposed algorithms. Therefore, this algorithm is extended to include additional STBCs in Chapter 3. The proposed algorithms show an improved performance when compared with algorithms in the literature.

Chapter 4 addresses **P2**, by considering the problem of identifying SM and Alamouti coded OFDM signals with multiple receive antennas. A new discriminating feature, based on the cross-correlation between the sequences received by two antennas, is developed. A decision criterion based on the statistic of the feature estimate is proposed. Simulation results show the superiority of the proposed algorithm over the other two algorithms found in the literature. The proposed algorithm achieves a very good performance with a short observation period and is less sensitive to the frequency offset impairment.

Chapter 5 addresses **P3**, by investigating the identification of STBC SC-FDMA signals for the first time in the literature. Considering a single receive antenna, we propose a discriminating feature based on a fourth-order statistic of the received sequence to blindly identify SM and Alamouti SC-FDMA signals. A constant false alarm decision criterion is developed based on the statistical properties of the feature estimate. Moreover, the theoretical performance analysis of the proposed identification algorithm is presented. Simulation results show the validity of the proposed algorithm and a very good agreement with the theoretical findings.

1.5 Contributions

This dissertation presents the following novel contributions to the STBC identification:

- We propose novel algorithms to identify SM and Alamouti STBCs for SC systems with a single receive antenna. More specifically, fourth-order statistics are employed as discriminating features, and four algorithms are proposed. It was shown that the first algorithm is optimal; however, it requires knowledge of the transmission parameters. The other algorithms do not have such a requirement. It is also shown that one of these algorithms is robust to the frequency offset impairment.

- We extend the algorithm which is more robust to model mismatches to a larger pool of STBCs.

- We develop a new cross-correlation that provides a discriminating feature to identify SM and Alamouti-coded OFDM signals. A novel decision criterion is also provided. Accordingly, a new identification algorithm is developed based on the proposed cross-correlation and decision criterion. This algorithm has the advantages of requiring neither modulation identification nor channel and noise power estimation.

- We study, for the first time in the literature, the identification of MIMO SC-FDMA signals. More specifically, we investigate the identification of SM and Alamouti SC-FDMA signals when a single antenna is employed at the receive-side. We also provide the theoretical performance analysis for the proposed signal identification algorithm. This algorithm requires neither modulation identification nor channel and noise power estimation. Moreover, it is robust to spatially correlated fading.

- We set up various simulation experiments to investigate the performance of the proposed algorithms under diverse scenarios, e.g., when signals are affected by spatially correlated fading, Doppler frequency, and timing and frequency offsets.

- We provide comparisons with the existing STBC identification algorithms for different scenarios and show the superiority of our proposed algorithms over most of the algorithms in the literature.

References

[1] S. Haykin, "Cognitive radio: brain-empowered wireless communications," *IEEE J. Sel. Areas Commun.*, vol. 23, pp. 201–220, Feb. 2005.

[2] B. Wang and K. Liu, "Advances in cognitive radio networks: A survey," *IEEE J. Sel. Topics Signal Process.*, vol. 5, pp. 5–23, Feb. 2011.

[3] D. Cabric, "Cognitive Radios: System Design Perspective," Ph.D. dissertation, University of California, Berkeley, USA, 2007.

[4] T. Yucek and H. Arslan, "A survey of spectrum sensing algorithms for cognitive radio applications," *IEEE Commun. Surveys Tuts.*, vol. 11, pp. 116–130, Mar. 2009.

[5] H. Celebi, I. Guvenc, S. Gezici, and H. Arslan, "Cognitive-radio systems for spectrum, location, and environmental awareness," *IEEE Antennas Propag. Mag.*, vol. 52, pp. 41–61, Aug. 2010.

[6] E. Axell, G. Leus, E. G. Larsson, and H. Poor, "Spectrum sensing for cognitive radio: State-of-the-art and recent advances," *IEEE Signal Process. Mag.*, vol. 29, pp. 101–116, May 2012.

[7] J. L. Xu, W. Su, and M. Zhou, "Software-defined radio equipped with rapid modulation recognition," *IEEE Trans. Veh. Technol.*, vol. 59, pp. 1659–1667, May 2010.

[8] O. A. Dobre, A. Abdi, Y. Bar-Ness, and W. Su, "Survey of automatic modulation classification techniques: Classical approaches and new trends," *IET Commun.*, vol. 1, pp. 137–156, Apr. 2007.

[9] F. Hameed, O. Dobre, and D. Popescu, "On the likelihood-based approach to modulation classification," *IEEE Trans. Wireless Commun.*, vol. 8, pp. 5884–5892, Dec. 2009.

[10] Q. Shi and Y. Karasawa, "Noncoherent maximum likelihood classification of quadrature amplitude modulation constellations: Simplification, analysis, and extension," *IEEE Trans. Wireless Commun.*, vol. 10, pp. 1312–1322, Apr. 2011.

[11] A. Swami and B. M. Sadler, "Hierarchical digital modulation classification using cumulants," *IEEE Trans. Commun.*, vol. 48, pp. 416–429, Mar. 2000.

[12] H.-C. Wu, M. Saquib, and Z. Yun, "Novel automatic modulation classification using cumulant features for communications via multipath channels," *IEEE Trans. Wireless Commun.*, vol. 7, pp. 3098–3105, Aug. 2008.

[13] M. Pedzisz and A. Mansour, "Automatic modulation recognition of MPSK signals using constellation rotation and its 4th order cumulant," *Elsevier: Digital Signal Processing*, vol. 15, pp. 295–304, Jan. 2005.

[14] W. Su, "Feature space analysis of modulation classification using very high-order statistics," *IEEE Commun. Lett.*, vol. 17, pp. 1688–1691, Sep. 2013.

[15] O. A. Dobre, M. Oner, S. Rajan, and R. Inkol, "Cyclostationarity-based robust algorithms for QAM signal identification," *IEEE Commun. Lett.*, vol. 16, pp. 12–15, Jan. 2012.

[16] K. Hassan, I. Dayoub, W. Hamouda, and M. Berbineau, "Automatic modulation recognition using wavelet transform and neural networks in wireless systems," *EURASIP J. Adv. Sig. Proc.*, vol. 2010, pp. 1–13, 2010.

[17] T. Yucek and H. Arslan, "Ofdm signal identification and transmission parameter estimation for cognitive radio applications," in *Proc. IEEE GLOBCOM*, 2007, pp. 4056–4060.

[18] M. Shi, A. Laufer, Y. Bar-Ness, and W. Su, "Fourth order cumulants in distinguishing single carrier from ofdm signals," in *Proc. IEEE MILCOM*, 2008, pp. 1–6.

[19] A. Punchihewa, Q. Zhang, O. A. Dobre, C. Spooner, S. Rajan, and R. Inkol, "On the cyclostationarity of OFDM and single carrier linearly digitally modulated signals in time dispersive channels: theoretical developments and application," *IEEE Trans. Wireless Commun.*, vol. 9, pp. 2588–2599, Aug. 2010.

[20] P. D. Sutton, K. E. Nolan, and L. E. Doyle, "Cyclostationary signatures in practical cognitive radio applications," *IEEE J. Sel. Areas Commun.*, vol. 26, pp. 13–24, Jan. 2008.

[21] A. Al-Habashna, O. A. Dobre, R. Venkatesan, and D. C. Popescu, "Second-order cyclostationarity of mobile WiMAX and LTE OFDM signals and application to spectrum awareness in cognitive radio systems," *IEEE J. Sel. Topics Signal Process.*, vol. 6, pp. 26–42, Feb. 2012.

[22] M. Wax and T. Kailath, "Detection of signals by information theoretic criteria," *IEEE Trans. Acoust., Speech, Signal Process.*, vol. 33, pp. 387–392, Apr. 1985.

[23] S. Valaee and P. Kabal, "An information theoretic approach to source enumeration in array signal processing," *IEEE Trans. Signal Process.*, vol. 52, pp. 1171–1178, May 2004.

[24] B. Nadler, "Nonparametric detection of signals by information theoretic criteria: performance analysis and an improved estimator," *IEEE Trans. Signal Process.*, vol. 58, pp. 2746–2756, May 2010.

[25] L. Huang and S. Wu, "Low-complexity MDL method for accurate source enumeration," *IEEE Signal Process. Lett.*, vol. 14, pp. 581–584, Sep. 2007.

[26] E. Fishler, M. Grosman, and H. Messer, "Determining the number of discrete alphabet sources from sensor data," *EURASIP J. Adv. Sig. Proc.*, vol. 2005, pp. 4–12, Jan. 2005.

[27] F. Haddadi, M. Malek-Mohammadi, M. M. Nayebi, and M. R. Aref, "Statistical performance analysis of MDL source enumeration in array processing," *IEEE Trans. Signal Process.*, vol. 58, pp. 452–457, Jan. 2010.

[28] R. Nee, V. K. Jones, G. Awater, A. Zelst, J. Gardner, and G. Steele, "The 802.11n MIMO-OFDM standard for wireless LAN and beyond," *Wireless Personal Comm.*, vol. 37, pp. 445–453, May 2006.

[29] A. Ghosh and R. Ratasuk, *Essentials of LTE and LTE-A*. Cambridge University Press, 2011.

[30] V. Choqueuse, M. Marazin, L. Collin, K. C. Yao, and G. Burel, "Blind recognition of linear space–time block codes: A likelihood-based approach," *IEEE Trans. Signal Process.*, vol. 58, pp. 1290–1299, Mar. 2010.

[31] V. Choqueuse, K. Yao, L. Collin, and G. Burel, "Blind recognition of linear space time block codes," in *Proc. IEEE ICASSP*, 2008, pp. 2833–2836.

[32] V. Choqueuse, K. Yao, L. Collin, and G. Burel, "Hierarchical space-time block code recognition using correlation matrices," *IEEE Trans. Wireless Commun.*, vol. 7, pp. 3526–3534, Sep. 2008.

[33] M. Luo, L. Gan, and L. Li, "Blind recognition of space-time block code using correlation matrices in a high dimensional feature space," *J. Inf. Comput. Sci*, vol. 9, pp. 1469–1476, Jun. 2012.

[34] M. Marey, O. A. Dobre, and B. Liao, "Classification of STBC systems over frequency-selective channels," *IEEE Trans. Veh. Technol.,* DOI: 10.1109/TVT.2014.2335415, 2014.

[35] G. Qian, L. Li, M. Luo, H. Liao, and H. Zhang, "Blind recognition of space-time block code in MISO system," *EURASIP JWCN*, vol. 1, pp. 164–176, Jun. 2013.

[36] M. Shi, Y. Bar-Ness, and W. Su, "STC and BLAST MIMO modulation recognition," in *Proc. IEEE GLOBECOM*, 2007, pp. 3034–3039.

[37] M. Marey, O. A. Dobre, and R. Inkol, "Cyclostationarity-based blind classification of stbcs for cognitive radio systems," in *Proc. IEEE ICC*. IEEE, 2012, pp. 1715–1720.

[38] ——, "Classification of space-time block codes based on second-order cyclostationarity with transmission impairments," *IEEE Trans. Wireless Commun.*, vol. 11, pp. 2574–2584, Jul. 2012.

[39] A. Turan, M. Oner, and H. Cirpan, "Space time block code classification for MIMO signals exploiting cyclostationarity," *accepted in IEEE ICC*, 2015.

[40] M. DeYoung, R. Heath, and B. Evans, "Using higher order cyclostationarity to identify space-time block codes," in *Proc. IEEE GLOBECOM*, 2008, pp. 1–5.

[41] M. Mohammadkarimi and O. A. Dobre, "Blind identification of spatial multiplexing and Alamouti space-time block code via Kolmogorov-Smirnov (KS) test," *IEEE Commun. Lett.*, vol. 18, pp. 1711–1714, Oct. 2014.

[42] ——, "A novel non-parametric method for blind identification of STBC codes," in *Proc. IEEE CWIT*, 2015.

[43] M. Marey, O. A. Dobre, and R. Inkol, "Novel algorithm for stbc-ofdm identification in cognitive radios," in *Proc. IEEE ICC*. IEEE, 2013, pp. 2770–2774.

[44] ——, "Blind STBC identification for multiple-antenna OFDM systems," *IEEE Trans. Commun.*, vol. 62, pp. 1554–1567, May 2014.

[45] E. Karami and O. A. Dobre, "Identification of SM-OFDM and AL-OFDM signals based on their second-order cyclostationarity," *IEEE Trans. Veh. Technol.*, vol. 64, pp. 942–953, Mar. 2015.

[46] O. Somekh, O. Simeone, Y. Bar-Ness, and W. Su, "Detecting the number of transmit antennas with unauthorized or cognitive receivers in MIMO systems," in *Proc. IEEE MILCOM*, 2007, pp. 1–5.

[47] K. Hassan, C. N. Nzeza, R. Gautier, E. Radoi, M. Berbineau, and I. Dayoub, "Blind detection of the number of transmitting antennas for spatially-correlated MIMO systems," in *Proc. IEEE ITST*, 2011, pp. 458–462.

[48] M. Shi, Y. Bar-Ness, and W. Su, "Adaptive estimation of the number of transmit antennas," in *Proc. IEEE MILCOM*, 2007, pp. 1–5.

[49] K. Hassan, I. Dayoub, W. Hamouda, C. N. Nzeza, and M. Berbineau, "Blind digital modulation identification for spatially-correlated MIMO systems," *IEEE Trans. Wireless Commun.*, vol. 11, pp. 683–693, Feb. 2012.

[50] M. S. Mühlhaus, M. Öner, O. A. Dobre, H. U. Jäkel, and F. K. Jondral, "Automatic modulation classification for MIMO systems using fourth-order cumulants," in *Proc. IEEE VTC(Fall)*, 2012, pp. 1–5.

[51] M. Muhlhaus, M. Oner, O. A. Dobre, H. Jakel, and F. K. Jondral, "A novel algorithm for mimo signal classification using higher-order cumulants," in *Proc. IEEE RWS*, 2013, pp. 7–9.

[52] M. S. Mühlhaus, M. Öner, O. A. Dobre, and F. K. Jondral, "A low complexity modulation classification algorithm for MIMO systems," *IEEE Commun. Lett.*, vol. 17, pp. 1881–1884, Oct. 2013.

[53] S. Kharbech, I. Dayoub, M. Zwingelstein-Colin, E. Simon, and K. Hassan, "Blind digital modulation identification for time-selective mimo channels," *IEEE Wireless Commun. lett.*, vol. 3, pp. 373–376, Aug. 2014.

[54] J. Vía and I. Santamaría, "Correlation matching approaches for blind ostbc channel estimation," *IEEE Trans. Signal Process.*, vol. 56, pp. 5950–5961, Aug. 2008.

[55] V. Choqueuse, A. Mansour, G. Burel, L. Collin, and K. Yao, "Blind channel estimation for STBC systems using higher-order statistics," *IEEE Trans. Wireless Commun.*, vol. 10, pp. 495–505, Feb. 2011.

[56] A. V. Dandawate and G. B. Giannakis, "Statistical tests for presence of cyclostationarity," *IEEE Trans. Signal Process.*, vol. 42, pp. 2355–2369, Sep. 1994.

[57] J. Lundén, V. Koivunen, A. Huttunen, and H. V. Poor, "Spectrum sensing in cognitive radios based on multiple cyclic frequencies," in *Proc. IEEE CrownCom*, 2007, pp. 37–43.

[58] J.-F. Cardoso and A. Souloumiac, "Blind beamforming for non-gaussian signals," in *Proc. IEE FRSP)*, vol. 140, no. 6, 1993, pp. 362–370.

[59] Y. G. Li, J. H. Winters, and N. R. Sollenberger, "MIMO-OFDM for wireless communications: signal detection with enhanced channel estimation," *IEEE Trans. Commun.*, vol. 50, pp. 1471–1477, Sep. 2002.

Chapter 2

Fourth-Order Statistics for Blind Classification of Spatial Multiplexing and Alamouti Space-Time Block Code Signals

2.1 Abstract

Blind signal classification, a major task of intelligent receivers, has important civilian and military applications. This problem becomes more challenging in multi-antenna scenarios due to the diverse transmission schemes that can be employed, e.g., spatial multiplexing (SM) and space-time block codes (STBCs). This paper presents a class of novel algorithms for blind classification of SM and Alamouti STBC (AL-STBC) transmissions. Unlike the prior art, we show that signal classification can be performed using a single receive antenna by taking advantage of the space-time redundancy. The first proposed algorithm relies on the fourth-order moment as a discriminating feature and employs the

likelihood ratio test for achieving maximum average probability of correct classification. This requires knowledge of the channel coefficients, modulation type, and noise power. To avoid this drawback, three algorithms have been further developed. Their common idea is that the discrete Fourier transform of the fourth-order lag product exhibits peaks at certain frequencies for the AL-STBC signals, but not for the SM signals, and thus, provides the basis of a useful discriminating feature for signal classification. The effectiveness of these algorithms has been demonstrated in extensive simulation experiments, where a Nakagami-m fading channel and the presence of timing and frequency offsets are assumed.

2.2 Introduction

Blind signal classification, an important task of intelligent receivers, finds applications in both military and commercial communications, such as electronic warfare, radio surveillance, civilian spectrum monitoring, and cognitive radio systems [1–7]. For example, the strategies employed by cognitive radio systems to opportunistically exploit the available spectrum require knowledge of signals in the environment to evaluate the likelihood of interfering with them [4–7].

Most previous work on blind signal classification has focused on single-input single-output scenarios [8–16]. However, the advent and rapid adoption of multiple-input multiple-output techniques adds a further level of complexity. These multiple antenna systems introduce new and challenging signal classification problems, such as estimation of the number of transmit antennas and the space-time code. Signal classification in the context of multiple antenna systems has been addressed by a relatively small number of papers [17–26]. The problems considered by these papers included the estimation of the number of transmit antennas [17, 18], modulation classification [19, 20], and the

classification of linear space-time block codes (STBCs) [21–26].

Regarding STBC classification algorithms, they can be divided in two general categories: likelihood-based [21] and feature-based [22–26]. Likelihood-based algorithms calculate the likelihood function of the received signal, and employ the maximum likelihood criterion to make a decision [21]. These algorithms require channel estimation, time, block, and frequency synchronization, and knowledge of the modulation format, while they suffer from high computational complexity. In [22, 23], the space-time second-order correlation function is used as a discriminating signal feature, with the decision being made by comparing the feature with a threshold [22] or based on the minimum distance between the theoretical and estimated features [23]. Signal cyclostationarity-based features are used in [24–26], with the decision made based on a cyclostationarity test. Most of the previous research [22–25] require multiple receive antennas. However, in many practical applications, size, power, and cost constraints on the receivers may favor single receive antenna solutions for STBC classification.

In this work, the goal is to investigate the classification capability of a radio equipped with a single receive antenna. Given the assumption that either spatial multiplexing (SM) or Alamouti (AL) STBC is used by the received signal, it is shown that the fourth-order moment (FOM) and the discrete Fourier transform (DFT) of a fourth-order lag product (FOLP) can be efficiently used to blindly classify these signals[1]. Based on this result, four classification algorithms are proposed. The first algorithm is FOM-based and employs the likelihood ratio test (LRT) for decision making. Unfortunately, its practical implementation is complicated by the requirement for knowledge of the channel coefficients, modulation type, and noise power. To avoid this requirement, we propose three further algorithms which are based on the DFT of the FOLP and are referred to as FOLP-based

[1]Note that the second-order signal statistics can be employed as discriminating features with multiple receive antennas [22–25]. Hence, the direct extension of a fourth-order statistic-based algorithm to multiple receive antennas makes little sense.

algorithms. Furthermore, we investigate the performance of the proposed algorithms in the presence of diverse model mismatches, such as timing and frequency offsets, Doppler frequency, and spatially correlated fading.

The rest of this paper is organized as follows: Section 2.3 introduces the system model. Sections 2.4 and 2.5 develop the FOM and FOLP-based classification algorithms, respectively. Simulation results are presented in Section 2.6. Finally, conclusions are drawn in Section 2.7.

2.3 System Model

We consider a wireless communication system which employs linear space-time block coding with multiple transmit antennas. Each block of N_s modulated symbols is encoded to generate N_t parallel signal sequences of length L. These sequences are transmitted simultaneously with N_t antennas in L consecutive time periods [27,28]. We denote the bth block of N_s complex symbols to be transmitted by the column vector $\mathbf{X}_b = [x_{b,0}, ..., x_{b,N_s-1}]^T$, with the superscript T denoting transposition. The data symbols are assumed to belong to an M-point signal constellation and consist of independent and identically distributed random variables with zero mean and second-order statistics[2] $\mathrm{E}\{|x|^2\} = 1$ and $\mathrm{E}\{x^2\} = \mathrm{E}\{(x^*)^2\} = 0$. Here, $\mathrm{E}\{.\}$ and $*$ denote statistical expectation and complex conjugate operations, respectively. Further, we denote the $N_t \times L$ space-time coding matrix and the $(l+1)$th column of this matrix by $\mathbb{G}(\mathbf{X}_b)$ and $\mathbb{G}_l(\mathbf{X}_b)$, $0 \leq l < L$, respectively.

For SM, a block of $N_s = N_t$ symbols is transmitted simultaneously via the N_t antennas in a single time period ($L = 1$), with the coding matrix given as [27]

[2]Results for the fourth-order statistics of SM and AL-STBC, given in Sections 2.4 and 2.5, are obtained under the assumption that $\mathrm{E}\left[x^2\right] = \mathrm{E}\left[(x^*)^2\right] = 0$; this corresponds to M-ary phase-shift-keying (PSK) and quadrature amplitude modulation (QAM) constellations with $M \geq 4$ [8].

$$\mathbb{G}^{\mathrm{SM}}(\mathbf{X}_b) = [x_{b,0}, ..., x_{b,N_t-1}]^T . \tag{2.1}$$

For the AL-STBC, a block of two symbols ($N_s = 2$) is transmitted via two antennas ($N_t = 2$) in two consecutive time periods ($L = 2$), with the coding matrix given as [29]

$$\mathbb{G}^{\mathrm{AL}}(\mathbf{X}_b) = \begin{bmatrix} x_{b,0} & -x_{b,1}^* \\ x_{b,1} & x_{b,0}^* \end{bmatrix}, \tag{2.2}$$

where the rows and columns correspond to the transmit antennas and time periods, respectively.

We consider a receiver with a single antenna, and assume that the length and time alignment of the STBC blocks are unknown. Without loss of generality, we assume that the first received symbol, denoted by $r(0)$, intercepts the $(k_1 + 1)$th column, $0 \leq k_1 < L$, of the bth transmitted block, denoted by $\mathbb{G}_{k_1}(\mathbf{X}_b)$. Under these assumptions, the kth intercepted symbol, $r(k)$, $k \geq 0$, is expressed as [22]

$$r(k) = \mathbf{H}\mathbf{S}(k) + w(k), \tag{2.3}$$

where $\mathbf{S}(k) = \mathbb{G}_p(\mathbf{X}_q)$, with $p = (k + k_1) \bmod L$, $q = b + (k + k_1) \operatorname{div} L$, and $z \bmod L$ and $z \operatorname{div} L$ denoting respectively the remainder and the quotient of the division z/L, $w(k)$ represents the complex additive white Gaussian noise (AWGN) with zero-mean and variance σ_w^2, and $\mathbf{H} = [h_0, ..., h_{N_t-1}]$ is the vector of the fading channel coefficients, which are considered to be constant over the observation period.

The objective is to blindly classify the SM and AL-STBC from K received symbols, $r(k)$, $0 \leq k \leq K - 1$, when $N_t = 2$ and a single receive antenna is available. This is formulated as a binary hypothesis testing problem: under hypothesis $\mathcal{H}_0$, the decision that SM is received is made, while the AL-STBC is selected under hypothesis $\mathcal{H}_1$.

Since lower-order statistics do not provide discriminating signal features for the SM and AL-STBC with M-ary PSK and QAM, $M \geq 4$, we resort to fourth-order statistics. Next, we show how the FOM and FOLP of the received signal can be exploited in the four proposed classification algorithms.

2.4 FOM-based Algorithm

The first algorithm relies on the fourth-order moment of the received signal, and applies the LRT to obtain the maximum average probability of correct classification. More specifically, we employ the fourth-order/ zero-conjugate (4,0) moment at a delay-vector $[0, 0, 1, 1]$, defined as [30]

$$m_{r,4,0} = \mathrm{E}\left\{r^2(k)r^2(k+1)\right\}. \tag{2.4}$$

Note that for simplicity, the delay-vector is not specified in the moment notation. Theoretical values of this moment are subsequently derived, and the LRT is formulated based on the moment sample estimate distribution.

By using (2.1)-(2.3), the second-order statistics of data symbols, and the independence of the symbol and noise sequences, the respective expressions for $m_{r,4,0}$ of the SM and AL-STBC can be obtained as,

$$m_{r,4,0}^{\mathrm{SM}} = 0, \quad \text{and} \quad m_{r,4,0}^{\mathrm{AL}} = h_0^2 h_1^2 c_{x,4,2}, \tag{2.5}$$

where h_0 and h_1 are the channel coefficients, and $c_{x,4,2} = \mathrm{E}\{|x|^4\} - 2(\mathrm{E}\{|x|^2\})^2$ represents the (4,2) cumulant corresponding to the signal constellation.

In practice, we estimate $m_{r,4,0}$ based on K observed symbols (equal here to the number of samples) as [30],

Table 2.1: Moment and cumulant values for various signal constellations.

	QPSK	8-PSK	16-QAM	64-QAM
$m_{x,2,1} = c_{x,2,1}$	1	1	1	1
$m_{x,4,2}$	1	1	1.32	1.38
$c_{x,4,2}$	-1	-1	-0.68	-0.619
$m_{x,6,3}$	1	1	1.96	2.2
$c_{x,6,3}$	4	4	2.08	1.7972

$$\hat{m}_{r,4,0} = \frac{1}{K}\sum_{k=0}^{K-1} r^2(k)r^2(k+1). \tag{2.6}$$

Following the same procedure as [31], the sample estimate can be shown to be unbiased and asymptotically Gaussian distributed. Furthermore, by applying some mathematical manipulations to (2.1)-(2.3), and (2.6), we obtain the respective expressions for the variance of $\hat{m}_{r,4,0}$ for the SM and AL-STBC given by

$$\begin{aligned}\sigma^2_{\mathrm{SM}} = \tfrac{1}{K}\{&16|h_0|^4|h_1|^4 + (m_{x,4,2})^2(|h_0|^4+|h_1|^4)^2 + 8m_{x,4,2}(|h_0|^6|h_1|^2 + |h_0|^2|h_1|^6)\\ &+4\sigma_w^8 + 8\sigma_w^6(|h_0|^2+|h_1|^2) + 40\sigma_w^4|h_0|^2|h_1|^2 + 32\sigma_w^2(|h_0|^4|h_1|^2 + |h_0|^2|h_1|^4)\\ &+18m_{x,4,2}\sigma_w^4(|h_0|^4+|h_1|^4) + 8m_{x,4,2}\sigma_w^2(|h_0|^6 + |h_0|^4|h_1|^2 + |h_0|^2|h_1|^4 + |h_1|^6)\}.\end{aligned} \tag{2.7}$$

$$\begin{aligned}\sigma^2_{\mathrm{AL}} = \tfrac{1}{K}\{&(m_{x,4,2})^2(|h_0|^8+|h_1|^8) + 4(m_{x,6,3}+m_{x,4,2})(|h_0|^6|h_1|^2 + |h_0|^2|h_1|^6) + 4\sigma_w^8\\ &+8\sigma_w^6(|h_0|^2+|h_1|^2) + 8m_{x,4,2}\sigma_w^2(|h_0|^6+|h_1|^6) + 2m_{x,4,2}\sigma_w^4(5|h_0|^4 + 8|h_0|^2|h_1|^2 + 5|h_1|^4)\\ &+4\sigma_w^2(m_{x,6,3}+5m_{x,4,2}+4)(|h_0|^4|h_1|^2 + |h_0|^2|h_1|^4) + 8\sigma_w^4(|h_0|^4 + 3|h_0|^2|h_1|^2 + |h_1|^4)\}.\end{aligned} \tag{2.8}$$

where $m_{x,\alpha,\beta} = \mathrm{E}\{x^{\alpha-\beta}(x^*)^\beta\}$ represents the (α,β) moment corresponding to the signal constellation. Examples of moments and cumulants corresponding to different signal constellations are provided in Table 2.1, for $\alpha = 2, 4, 6$, and diverse βs [8].

Based on the statistical properties of the fourth-order moment sample estimate, $\hat{m}_{r,4,0}$,

it is straightforward to write the following expressions for the probability density functions conditional on the hypothesis $\mathcal{H}_0$ (SM signal) and $\mathcal{H}_1$ (AL-STBC signal), respectively as

$$p\left(\hat{m}_{r,4,0}\left|\mathcal{H}_0\right.\right)=\frac{1}{\pi\sigma_{\mathrm{SM}}^2}\exp\left(\frac{-\left|\hat{m}_{r,4,0}\right|^2}{\sigma_{\mathrm{SM}}^2}\right), \tag{2.9}$$

and

$$p\left(\hat{m}_{r,4,0}\left|\mathcal{H}_1\right.\right)=\frac{1}{\pi\sigma_{\mathrm{AL}}^2}\exp\left(\frac{-\left|\hat{m}_{r,4,0}-h_0^2h_1^2c_{x,4,2}\right|^2}{\sigma_{\mathrm{AL}}^2}\right). \tag{2.10}$$

Under the assumption of equally likely hypotheses and after simple mathematical manipulations, the LRT becomes

$$\frac{\left|\hat{m}_{r,4,0}\right|^2}{\sigma_{\mathrm{SM}}^2}-\frac{\left|\hat{m}_{r,4,0}-h_0^2h_1^2c_{x,4,2}\right|^2}{\sigma_{\mathrm{AL}}^2}\underset{\mathcal{H}_0}{\overset{\mathcal{H}_1}{\gtrless}}\ln\frac{\sigma_{\mathrm{AL}}^2}{\sigma_{\mathrm{SM}}^2}. \tag{2.11}$$

The distributions of $\hat{m}_{r,4,0}$ conditional on hypothesis $\mathcal{H}_0$ and $\mathcal{H}_1$, given in (2.9) and (2.10), can be used to analytically determine the probability of correct classification for SM and AL-STBC signals, respectively. From statistical communication theory [32], it follows that

$$P(\lambda=\xi|\xi,h_0,h_1)=1-Q\left(\frac{|h_0^2h_1^2c_{x,4,2}|}{\sqrt{2\sigma_\xi^2}}\right),\ \xi\in\{\mathrm{SM},\ \mathrm{AL}\}, \tag{2.12}$$

where λ is the estimated signal type, $P(\lambda=\xi|\xi,h_0,h_1),\xi\in\{\mathrm{SM},\ \mathrm{AL}\}$, is the probability of correct classification of ξ conditional on the channel coefficients, and $Q(.)$ is the Q-function, defined as $Q(x)=\int_x^\infty\frac{1}{\sqrt{2\pi}}e^{-\frac{t^2}{2}}dt$ [32]. Furthermore, the probability of correct classification, $P(\lambda=\xi|\xi)$, can be obtained by averaging (2.12) over the channel coefficients h_0 and h_1 as,

$$P(\lambda=\xi|\xi)=1-\int_0^\infty\int_0^\infty Q\left(\frac{\gamma_0^2\gamma_1^2|c_{x,4,2}|}{\sqrt{2\sigma_\xi^2}}\right)p\left(\gamma_0\right)p\left(\gamma_1\right)d\gamma_0d\gamma_1, \tag{2.13}$$

where γ_i represents the magnitude of $h_i, i=0,1$. Note that, according to (2.7) and (2.8),

σ_ξ^2 is a function of γ_0 and γ_1. As there is no closed-form solution for (2.13), we used the trapezoidal numerical method described in [33] to solve the integration.

The FOM-based algorithm employs the LRT for achieving a maximum average probability of correct classification [34],

$$P_c = \frac{1}{2} \sum_{\xi \in \{\text{SM, AL}\}} P\left(\lambda = \xi | \xi\right). \tag{2.14}$$

However, this requires knowledge of the channel coefficients, modulation type, and noise power. Given perfect estimates of such parameters, this result represents a performance upper bound that is useful for evaluating the performance of other proposed algorithms. The FOM-based algorithm is summarized below.

The FOM-based algorithm

Required signal pre-processing: Blind carrier frequency and timing synchronization, blind classification of the modulation type, blind estimation of the channel coefficients, and estimation of the noise power.
Input: The observed symbols $r(k)$, $k = 0, 1, ..., K-1$, modulation type, channel coefficients, frequency and timing information, and noise power.
- Compute the reference FOM of AL as $h_0^2 h_1^2 c_{x,4,2}$.
- Estimate the FOM of the received signal using (2.6).
- Compute σ_{SM}^2 using (2.7).
- Compute σ_{AL}^2 using (2.8).

if $\frac{|\hat{m}_{r,4,0}|^2}{\sigma_{\text{SM}}^2} - \frac{\left|\hat{m}_{r,4,0} - h_0^2 h_1^2 c_{x,4,2}\right|^2}{\sigma_{\text{AL}}^2} > \ln \frac{\sigma_{\text{AL}}^2}{\sigma_{\text{SM}}^2}$ **then**
- AL-STBC is declared present ($\mathcal{H}_1$ true).

else
- SM is declared present ($\mathcal{H}_0$ true).

end if

2.5 FOLP-based Algorithms

Based on the DFT of the FOLP at delay-vector [0,0,1,1], three classification algorithms for the SM and AL-STBC are developed. The main advantage of these algorithms is that they do not require knowledge of the channel coefficients, modulation type, and noise

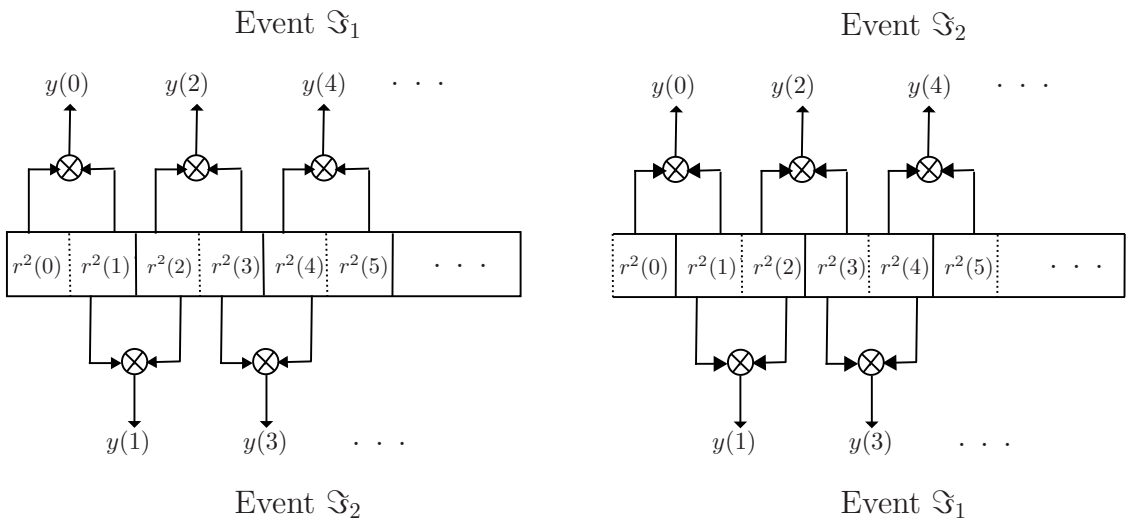

Fig. 2.1: Illustration of events $\Im_1$ and $\Im_2$ when (a) $r(0)$ corresponds to the beginning of the AL-STBC block, (b) $r(0)$ does not correspond to the beginning of the AL-STBC block. Solid lines are used to delimitate symbols which do not belong to the same block and dashed lines to delimitate symbols which belong to the same block.

power.

Consider the sequence $\mathbf{y} = [y(0), y(1), ..., y(K-1)]$, with $y(k) = r^2(k)r^2(k+1),\ k = 0, 1, ..., K-1$. Since a random variable can be expressed as the sum of its mean and another zero-mean random variable which represents the deviation from the mean [35], $y(k)$ can be written for the SM and AL-STBC respectively as,

$$y^{\mathrm{SM}}(k) = \mathrm{E}\{y^{\mathrm{SM}}(k)\} + \psi^{\mathrm{SM}}(k), \tag{2.15}$$

and

$$y^{\mathrm{AL}}(k) = \mathrm{E}\{y^{\mathrm{AL}}(k)\} + \psi^{\mathrm{AL}}(k), \tag{2.16}$$

where $\mathrm{E}\{y^{\xi}(k)\}$ is the mean of $y^{\xi}(k)$, and $\psi^{\xi}(k)$ is its deviation from the mean, $\xi \in \{\mathrm{SM}, \mathrm{AL}\}$.

Based on (2.2)-(2.5), one can easily show that $\mathrm{E}\{y^{\mathrm{AL}}(k)\}$ equals $2h_0^2h_1^2c_{x,4,2}$ when $r(k)$ and $r(k+1)$ belong to the same transmitted data block (event $\Im_1$), and zero when they do not (event $\Im_2$). The difference between events $\Im_1$ and $\Im_2$ is illustrated in Fig. 2.1. Apparently, under the event $\Im_1$, $\mathrm{E}\{y^{\mathrm{AL}}(k)\}$ is a constant, $C = 2h_0^2h_1^2c_{x,4,2}$, which depends on the modulation type and channel coefficients. Further, $\psi^{\mathrm{AL}}(k)$ can be considered as a noise component that hides the presence of C if $y^{\mathrm{AL}}(k)$ is received. Furthermore, based on (2.1), (2.3)-(2.5), it is easy to show that $\mathrm{E}\{y^{\mathrm{SM}}(k)\} = 0$; thus, $\psi^{\mathrm{SM}}(k)$ can be seen as a noise component which hides the absence of C if $y^{\mathrm{SM}}(k)$ is received. In the absence of such noise components, i.e., $\psi^{\mathrm{SM}}(k) = \psi^{\mathrm{AL}}(k) = 0$, the FOLP sequence for the AL-STBC code would be either $[C, 0, C, 0, C, 0, C, ...]$ or $[0, C, 0, C, 0, C, 0, ...]$, depending on whether or not $r(0)$ and $r(1)$ correspond to the same data block, and the FOLP sequence for SM would be $[0, 0, 0, 0, 0, 0, ...]$. The following discussion shows how this property can be exploited as a feature for distinguishing between the SM and AL-STBC in the frequency domain.

Let $\mathbf{Y} = [Y(0), Y(1), ..., Y(K-1)]$ denote the K-point DFT[3] of $\mathbf{y}$, with

$$Y(n) = \frac{1}{\sqrt{K}} \sum_{k=0}^{K-1} y(k) e^{-j2\pi kn/K}, \qquad n = 0, 1, ..., K-1. \tag{2.17}$$

By replacing (2.15) and (2.16) in (2.17), it follows that

$$Y^{\mathrm{SM}}(n) = \Psi^{\mathrm{SM}}(n),\ n = 0, 1, ..., K-1, \tag{2.18}$$

and

$$Y^{\mathrm{AL}}(n) = \begin{cases} \mathcal{E} + \Psi^{\mathrm{AL}}(n), & n = 0, K/2, \\ \Psi^{\mathrm{AL}}(n), & \text{otherwise}, \end{cases} \tag{2.19}$$

where $\Psi^{\mathrm{SM}}(n)$ and $\Psi^{\mathrm{AL}}(n)$ represent the DFT of $\psi^{\mathrm{SM}}(k)$ and $\psi^{\mathrm{AL}}(k)$, respectively. $\mathcal{E} =$

[3]Note that, without loss of generality, K is assumed to be even.

$\frac{\sqrt{K}}{2}C$ if $r(0)$ and $r(1)$ belong to the same transmitted data block, and $\mathcal{E} = \pm\frac{K-2}{2\sqrt{K}}C \approx \pm\frac{\sqrt{K}}{2}C$ otherwise; the plus sign corresponds to $n = 0$ and the minus sign to $n = K/2$. Clearly, (2.18) and (2.19) indicate that $|Y(n)|$ does not exhibit peaks for SM, but it does for the AL-STBC at $n = 0, K/2$.

From (2.17), $Y(n)$ is composed of a large number of contributions when K is large. Consequently, the central limit theorem indicates that $Y(n)$ should have a Gaussian distribution when K tends to infinity. A closer look at (2.17) and (2.18) reveals that the asymptotic distribution of $Y(n)$, $n = 0, \cdots K-1$, for SM is Gaussian with zero mean. In addition, further consideration of (2.17) and (2.19) indicates that the asymptotic distribution of $Y(n)$ for the AL-STBC is also Gaussian with zero mean at $n = 0, \cdots K-1$, $n \neq 0, K/2$, and non-zero mean, $\mathcal{E}$, at $n = 0, K/2$.

The following subsections describe the development of the decision criteria that form the basis of the three proposed FOLP-based classification algorithms.

2.5.1 FOLP-A classification algorithm

The basic idea of the FOLP-A classification algorithm is to test for the existence of peaks in $|Y(n)|$, either at $n = 0$ or $n = K/2$, as follows. We define n_1 as the value of n that maximize $|Y(n)|$,

$$n_1 = \arg\max_n |Y(n)|, \qquad n = 0, 1, ..., K-1. \tag{2.20}$$

If $n_1 \in \{0, K/2\}$, the AL-STBC is declared present ($\mathcal{H}_1$ true); otherwise, SM is declared present ($\mathcal{H}_0$ true). A summary of the proposed FOLP-A algorithm is provided below.

The FOLP-A algorithm

Required signal pre-processing: Blind carrier frequency and timing synchronization.
Input: The observed symbols $r(k)$, $k = 0, 1, ..., K-1$, and frequency and timing information.
- Compute the fourth-order lag product $y(k) = r^2(k)r^2(k+1)$.
- Compute $Y(n)$ using (2.17).
- $n_1 = \arg\max_n |Y(n)|, \qquad n = 0, 1, ..., K-1.$
if $n_1 \in \{0, K/2\}$ **then**
    - AL-STBC is declared present ($\mathcal{H}_1$ true).
else
    - SM is declared present ($\mathcal{H}_0$ true).
end if

2.5.2 FOLP-B classification algorithm

The FOLP-B classification algorithm exploits the statistical properties of $|Y(n)|$, $n = 0, \cdots, K-1$, to decide whether $|Y(n)|$ exhibits a peak either at $n = 0$ or $n = K/2$. Note that $\mathcal{E}$ depends on the modulation format and the channel coefficients, which are unknown at the receiver; as such, the statistics of $Y(n = 0)$ and $Y(n = K/2)$ for the Alamouti code are unknown, as well. The basic idea behind this algorithm is to set a threshold, ϵ, to achieve a given probability of false alarm[4], P_{fa}. As a consequence, if either $|Y(n = 0)|$ or $|Y(n = K/2)|$ is greater than ϵ, the AL-STBC is declared present ($\mathcal{H}_1$ true); if not, SM is declared present ($\mathcal{H}_0$ true). The problem is to set this threshold to yield the desired value of P_{fa}. Since the distributions of $Y(n = 0)$ and $Y(n = K/2)$ for the SM are Gaussian with zero mean, the distributions of $|Y(n = 0)|$ and $|Y(n = K/2)|$ are Rayleigh. Accordingly, the probability of false alarm, P_{fa}, can be expressed as

$$P_{fa} = \int_{\varepsilon}^{\infty} \frac{2x}{\Omega} e^{\frac{-x^2}{\Omega}} dx, \tag{2.21}$$

where Ω represents the second-order moment which characterizes the Rayleigh distribution. Hence, ε can be calculated as

[4]The probability of false alarm is defined as the probability of incorrectly deciding that a statistically significant peak is present.

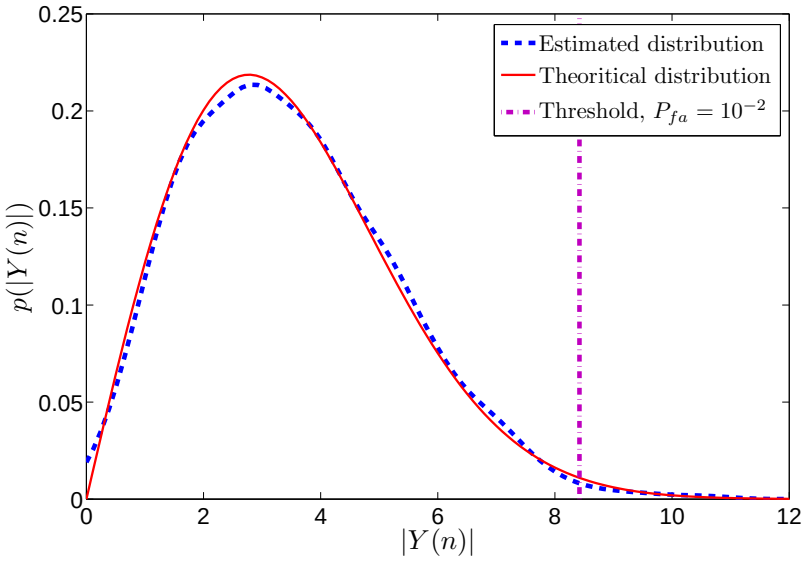

Fig. 2.2: Distribution of $|Y(n)|$, $n \neq 0, K/2$, for the AL-STBC with QPSK modulation and $K = 2048$, at SNR=20 dB over Nakagami-m channel, $m = 3$.

$$\varepsilon = \sqrt{-\Omega \ln (P_{fa})}. \tag{2.22}$$

In practice, an estimate of Ω is employed, which is obtained as

$$\hat{\Omega} = \frac{1}{K-2} \left[\sum_{n=0, n\neq 0, K/2}^{K-1} |Y(n)|^2 \right]. \tag{2.23}$$

Note that $|Y(0)|$ and $|Y(K/2)|$ are excluded, as these have a different distribution if the AL-STBC is present (hypothesis $\mathcal{H}_1$).

Fig. 2.2 presents the distribution of $|Y(n)|$ with $n \neq 0, K/2$ for the AL-STBC with quadrature PSK (QPSK) modulation, $K = 2048$, and 20 dB signal-to-noise ratio (SNR). We also show the theoretical Rayleigh distribution with $\Omega = \hat{\Omega}$. Since the simulation and theoretical results are in reasonable agreement, the assumption that $|Y(n)|$ with $n \neq 0, K/2$ has a Rayleigh distribution is validated. Similar results are obtained for $\left|Y^{\mathrm{SM}}(n)\right|$, but are not shown due to space considerations. Furthermore, Fig. 2.3 depicts

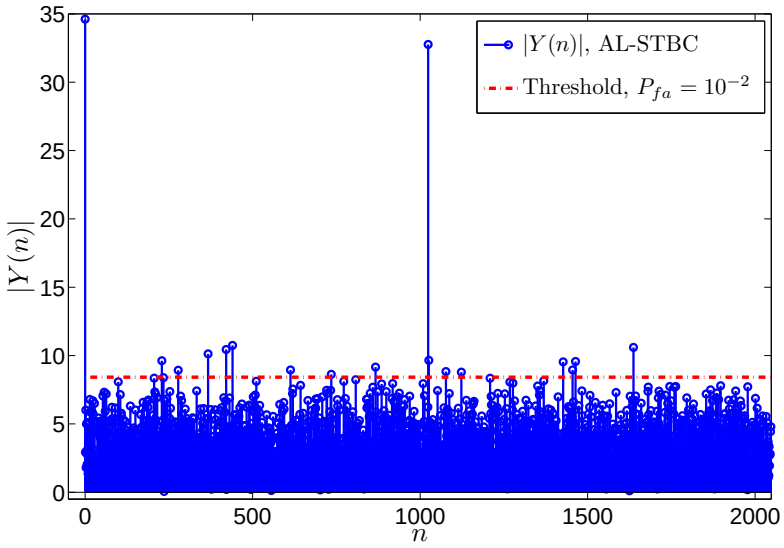

Fig. 2.3: $|Y(n)|$ for the AL-STBC with QPSK modulation and $K = 2048$, at SNR = 20 dB over Nakagami-m channel, $m = 3$.

$|Y(n)|$ for the AL-STBC as a function of n, along with the threshold ε associated to the probability of false alarm $P_{fa} = 10^{-2}$. Note that the value of $|Y(n)|$ is greater than ε for $n = 0, K/2$, as expected. A summary of the proposed FOLP-B is provided below.

The FOLP-B algorithm

Required signal pre-processing: Blind carrier frequency and timing synchronization.
Input: The observed symbols $r(k)$, $k = 0, 1, ..., K-1$, and frequency and timing information.
- Compute the fourth-order lag product $y(k) = r^2(k)r^2(k+1)$.
- Compute $Y(n)$ using (2.17).
- Estimate Ω using (2.23).
- Compute ε using (2.22) based on the target P_{fa}.

if $|Y(0)|$ or $|Y(K/2)| \geq \varepsilon$ **then**
    - AL-STBC is declared present ($\mathcal{H}_1$ true).
else
    - SM is declared present ($\mathcal{H}_0$ true).
end if

2.5.3 FOLP-C classification algorithm

The basic idea of the FOLP-C classification algorithm is to measure the distance between the positions of the two most prominent peaks in $|Y(n)|$; this equals $K/2$ for the AL-STBC, whereas it does not for SM. We define n_1 as in (2.20), and n_2 as

$$n_2 = \arg\max_n |Y(n)|, \qquad n = 0, 1, ..., K-1, n \neq n_1. \tag{2.24}$$

If $|n_1 - n_2| = K/2$, then the AL-STBC is declared present ($\mathcal{H}_1$ true); otherwise, SM is declared present ($\mathcal{H}_0$ true).

A summary of the proposed FOLP-C algorithm is provided below.

The FOLP-C algorithm

Required signal pre-processing: Timing synchronization.
Input: The observed symbols $r(k)$, $k = 0, 1, ..., K-1$ and timing information.
- Compute the fourth-order lag product $y(k) = r^2(k)r^2(k+1)$.
- Compute $Y(n)$ using (2.17).
- $n_1 = \arg\max_n |Y(n)|, \qquad n = 0, 1, ..., K-1.$
- $n_2 = \arg\max_n |Y(n)|, \qquad n = 0, 1, ..., K-1, n \neq n_1.$

if $|n_1 - n_2| = K/2$ **then**
    - AL-STBC is declared present ($\mathcal{H}_1$ true).
else
    - SM is declared present ($\mathcal{H}_0$ true).
end if

2.6 Simulation Results

2.6.1 Simulation setup

The performance of the proposed algorithms was evaluated using Monte Carlo simulations with 1000 trials employed for each scenario. Unless otherwise indicated, QPSK modulation was used, $K = 1024$, $P_{fa} = 10^{-2}$ for the FOLP-B classification algorithm, and the received signal was affected by AWGN with variance σ_w^2 and a frequency-flat Nakagami-m

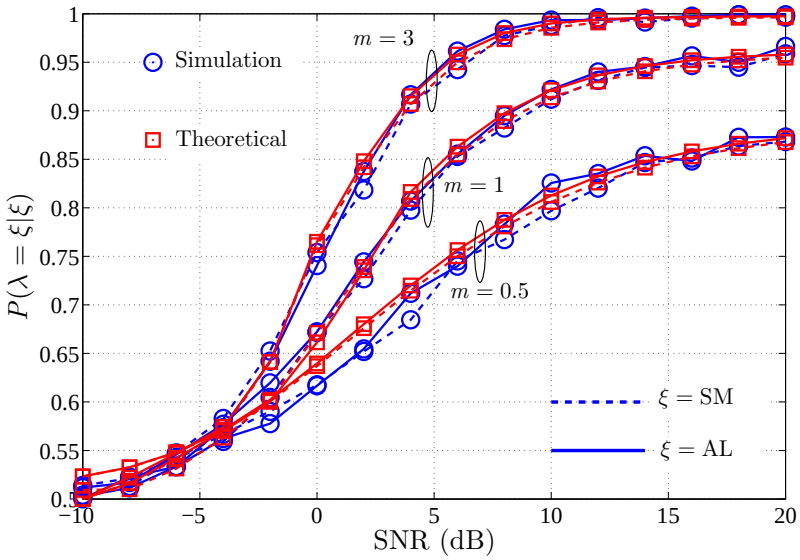

Fig. 2.4: Probability of correct classification, $P(\lambda = \xi|\xi)$, $\xi \in \{\text{SM, AL}\}$, versus SNR for different Nakagami-m fading channels, for the FOM-based classification algorithm with QPSK modulation and $K = 1024$.

fading channel [36], with $m = 3$, and $\mathrm{E}\{|h_i^2|\} = 1$, $i = 0, 1$. Under the assumption of unit variance constellations, the SNR was defined as $10\log_{10}(N_t/\sigma_w^2)$. Two performance measures, the probability of correct classification, $P(\lambda = \xi|\xi)$, $\xi \in \{\text{SM, AL}\}$, and the average probability of correct classification, given in (2.14), were used.

2.6.2 Performance evaluation

Fig. 2.4 shows the analytical and simulation results for the probability of correct classification achieved with the FOM-based classification algorithm over Nakagami-m fading channel for $m = 3$ and 1. Note that the simulation and theoretical results are in very good agreement. The performance deteriorates as the effect of the channel increases. The explanation is that the increase in the variance of h_0 and h_1 with decreasing m leads to an increase in the variance of $\hat{m}_{r,4,0}$ and contributes to erroneous decisions.

The probability of correct classification for the three proposed FOLP-based classifi-

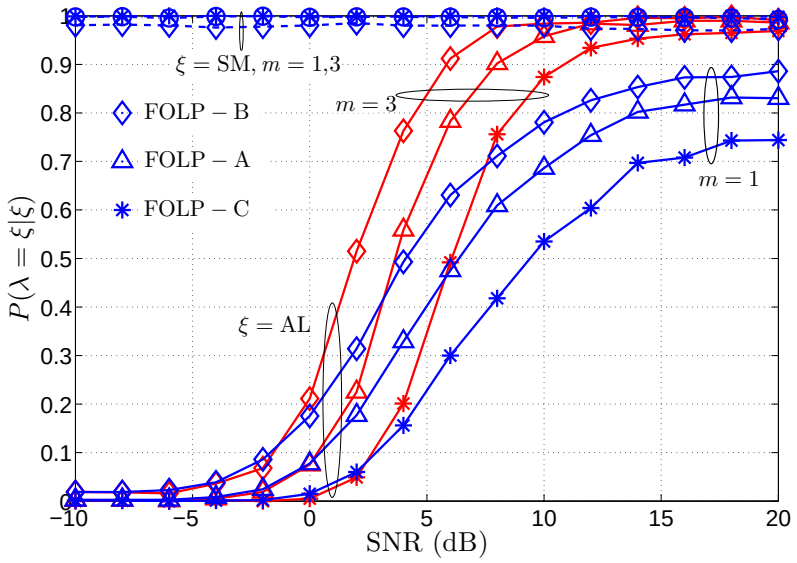

Fig. 2.5: Probability of correct classification, $P(\lambda = \xi|\xi)$, $\xi \in \{\text{SM, AL}\}$, versus SNR for different Nakagami-m fading channels, for the FOLP-based classification algorithms with QPSK modulation and $K = 1024$. $P_{fa} = 10^{-2}$ for the FOLP-B classification algorithm. Solid lines are used for $P(\lambda = \text{AL}|\text{AL})$ and dashed lines for $P(\lambda = \text{SM}|\text{SM})$.

cation algorithms over Nakagami-m fading channel, $m = 3$ and 1, is presented in Fig. 2.5. Note that for all FOLP-based algorithms, the channel parameter m and SNR affect the probability of correct classification for the AL-STBC, $P(\lambda = \text{AL}|\text{AL})$, but do not for SM. In general, the noise components and the channel coefficients control the peaks that appear in $|Y^{\text{AL}}(n)|$ at $n = 0, K/2$, as can be seen from (2.19). For the SM, $Y^{\text{SM}}(n), n = 0, 1, ..., K-1$, can be shown to be statistically independent and identically distributed. Accordingly, the peak of $|Y^{\text{SM}}(n)|$ can occur at any position n with the same probability, i.e., $P(|Y(0)| = \max|Y(n)|) = P(|Y(K/2)| = \max|Y(n)|) = 1/K$, regardless of the channel parameter m and noise power. Recall that, for the FOLP-A algorithm, SM is not declared present if the maximum occurs either at $n = 0$ or $K/2$. Hence, $P(\lambda = \text{SM}|\text{SM}) = 1 - 2/K$ and this approaches one for large K. For the FOLP-C algorithm, SM is not declared present if $|n_1 - n_2| = K/2$, with n_1 and n_2 defined by (2.20) and (2.24), respectively. In this case, $P(\lambda = \text{SM}|\text{SM}) = (K-2)/(K-1)$, which

Table 2.2: Computational cost of the proposed algorithms and those in [21] and [26].

Classification algorithm	Computational cost (flops)	Number of flops for $K = 1024$, $M = 4$, $\rho = 4$, and $\mathcal{W} = 100$
Optimal likelihood [21]	$240KM^2$	3,932,160
Cyclostionarity [26]	$18\rho K + 5\rho K \log_2 \rho K + 27\mathcal{W}$	322,188
FOM	$20K + 233$	20,713
FOLP-A	$22K + 5K \log_2 K$	73,728
FOLP-B	$22K + 5K \log_2 K$	73,728
FOLP-C	$23K + 5K \log_2 K$	74,752

also approaches one for large K. On the other hand, for the FOLP-B classification algorithm, the probability of correctly classifying SM is predetermined by the probability of false alarm, i.e., $P(\lambda = \text{SM}|\text{SM}) = 1 - 2P_{fa}$, which is independent of SNR and m. It is noteworthy that the results of this analysis agree with simulation findings shown in Fig. 2.5.

2.6.3 Performance comparison

Fig. 2.6 compares the average probability of correct classification, P_c, achieved by the proposed algorithms, the optimal likelihood-based algorithm in [21], and the cyclostionarity-based algorithm in [26]. An oversampling factor $\rho = 4$ and a window size $\mathcal{W} = 100$ are used with the algorithm in [26]. $P_{fa} = 10^{-2}$ for both FOLP-B classification algorithm and the algorithm in [26]. As expected, the algorithm in [21] provides the best performance, as it exploits the full probability density function of the received signal[5]. Furthermore, the FOM-based classification algorithm outperforms the FOLP-based algorithms, since it uses the LRT to make the decision. On the other hand, the algorithm in [26] has the lowest performance, as accurate estimation of the fourth-order cyclic cumulant requires a relatively large observation period. For example, we observed that the values obtained for

[5]However, it is well known that this approach heavily relies on pre-processing, is sensitive to model mismatches, and is computationally complex.

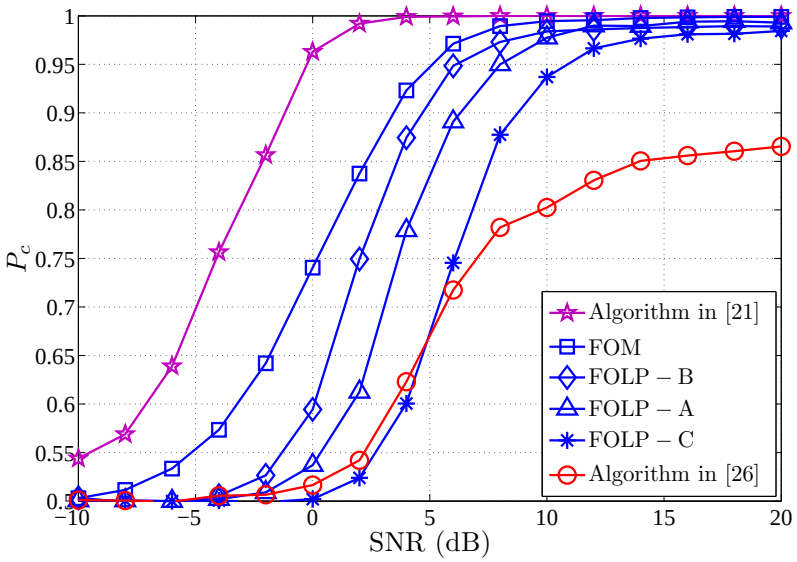

Fig. 2.6: Performance comparison of the proposed algorithms and the ones in [21] and [26] over Nakagami-m fading channel, $m = 3$, with QPSK modulation, $K = 1024$.

P_c showed a strong dependence on K, ranging from $P_c = 0.96$ for $K = 4096$ to $P_c = 0.86$ for $K = 1024$ at SNR= 20 dB.

Additionally, the computational cost measured by the required number of floating point operations (flops) [37] is provided in Table 2.2 for the proposed algorithms and those described in [21] and [26]. As can be seen, the FOM-based algorithm has the lowest computational cost followed by the FOLP-based algorithms. The computational cost of the algorithms in [21] and [26] is considerably higher.

2.6.4 Effect of the number of observed samples

Fig. 2.7 illustrates the effect of the number of received samples, K, on the average probability of correct classification, P_c, for the proposed classification algorithms at SNR=10 dB. Note that the performance improves with increasing K. This can be explained as follows. For the FOM-based classification algorithm, the estimate of the fourth-order moment improves as K increases, thus improving the probability of correct classification.

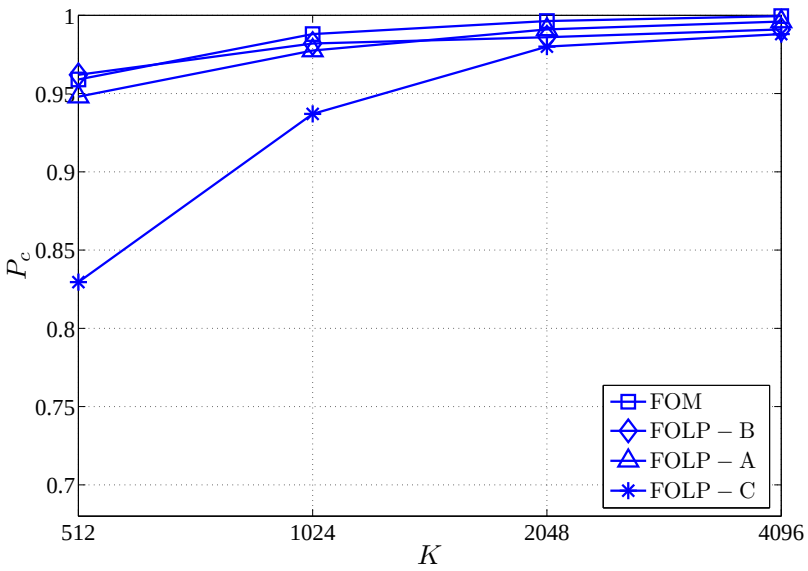

Fig. 2.7: The effect of K on the average probability of correct classification, P_c, for the proposed algorithms over Nakagami-m channel, $m = 3$, with QPSK modulation at SNR = 10 dB. $P_{fa} = 10^{-2}$ for the FOLP-B classification algorithm.

On the other hand, for the FOLP-based classification algorithms, the noise contributions that affect the peaks in $|Y^{\mathrm{AL}}(n)|$ at $n = 0, K/2$ decrease with increasing K, thus improving the classification performance for the AL-STBC. The SM classification performance approaches unity for sufficiently large K for the FOLP-A and FOLP-C algorithms, but is relatively insensitive to K for the FOLP-B algorithm. Overall, the classification performance improves with increasing K. Furthermore, Fig. 2.7 indicates that low values of K have a particularly adverse effect on the FOLP-C algorithm. The explanation is that the FOLP-C algorithm requires the detection of two peaks (see (2.20) and (2.24)) to classify the AL-STBC with, whereas the detection of either of the two peaks is sufficient for the FOLP-A and FOLP-B algorithms.

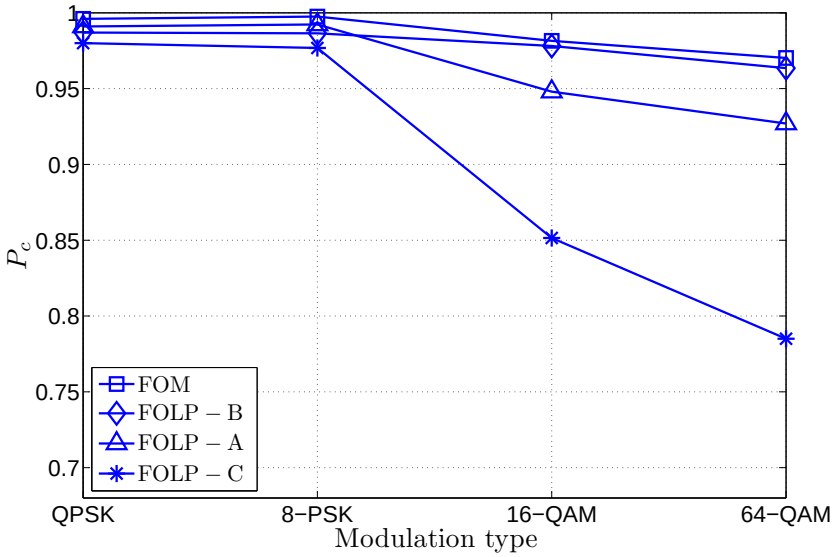

Fig. 2.8: The effect of the modulation type on the average probability of correct classification, P_c, for the proposed algorithms over the Nakagami-m channel, $m = 3$, with $K = 2048$ at SNR = 10 dB. $P_{fa} = 10^{-2}$ for the FOLP-B classification algorithm.

2.6.5 Effect of the modulation type

Fig. 2.8 depicts the effect of the modulation type on the average probability of correct classification, P_c, for the proposed algorithms at SNR=10 dB, and $K = 2048$. The explanation for the dependence of the classification performance on the modulation type is as follows. According to Section 2.4, the performance of the FOM-based algorithm is determined by the Euclidean distance between zero and $h_0^2 h_1^2 c_{x,4,2}$, with the classification performance improving as the distance increases. This distance does not depend on the M-PSK constellation, i.e., $c_{x,4,2}$ is independent of M, whereas for the M-QAM constellations, it decreases as M increases. For the FOLP-based algorithms, classification of SM is not affected by the modulation type (this can be seen from the previous discussion on $P(\lambda = \text{SM}|\text{SM})$). On the other hand, classification of the AL-STBC is independent of M for the M-PSK constellations, whereas this depends on M for M-QAM constellations. This is because the peaks in $|Y^{\text{AL}}(n)|$ at $n = 0, K/2$ depend on $c_{x,4,2}$.

2.6.6 Effect of the frequency offset

Fig. 2.9 presents the effect of the frequency offset normalized with respect to the data rate, Δf, on the average probability of correct classification, P_c, for the proposed algorithms at SNR=10 dB and $K = 2048$. These results show that the FOM-based classification algorithm is sensitive to Δf. This behavior is consistent with the analysis in the Appendix, where it is shown that a frequency offset affects the FOM of the AL-STBC signal. The performance of the FOLP-A and FOLP-B algorithms is also affected by Δf. The explanation is that Δf introduces a shift in the peaks in $\left|Y^{\mathrm{AL}}(n)\right|$, $n = 0, K/2$, except for the cases where Δf is an integer multiple of 1/8 (see Appendix for the proof), and the decision criteria rely on the presence of a peak either at $n = 0$ or $n = K/2$. On the other hand, the performance of the FOLP-C algorithm is relatively insensitive to the frequency offset. This is because the decision criterion depends on the distance between the peak positions, which is unaffected by Δf (see Appendix for the proof). Nevertheless, some performance degradation results when the shifted positions are misaligned with the DFT bins, since the peak values are attenuated (see Appendix for the proof).

2.6.7 Effect of the timing offset

The previous analysis assumed perfect timing synchronization. Here we evaluate the performance of the proposed algorithms in the presence of a timing offset, $0 \leq \mu < 1$. For the case of rectangular pulse shaping, after the matched filtering, the timing offset, μ, translates into a two path channel $[1 - \mu, \mu]$ [11]. Fig. 2.10 shows the performance of the proposed algorithms as a function of μ at SNR=10 dB and $K = 2048$. The FOLP-based algorithms display much less sensitivity to timing offsets than the FOM-based algorithm.

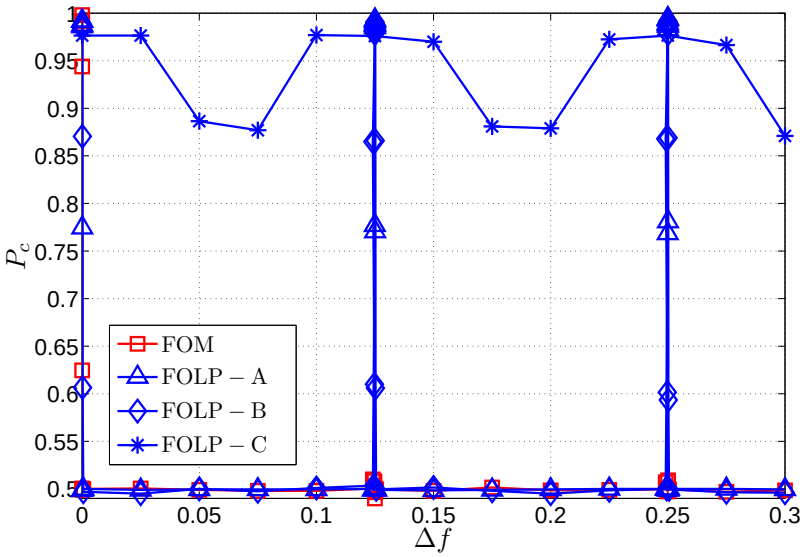

Fig. 2.9: The effect of the frequency offset on the average probability of correct classification, P_c, for the proposed algorithms over Nakagami-m channel, $m = 3$, with QPSK modulation and $K = 2048$ at SNR = 10 dB. $P_{fa} = 10^{-2}$ for the FOLP-B classification algorithm.

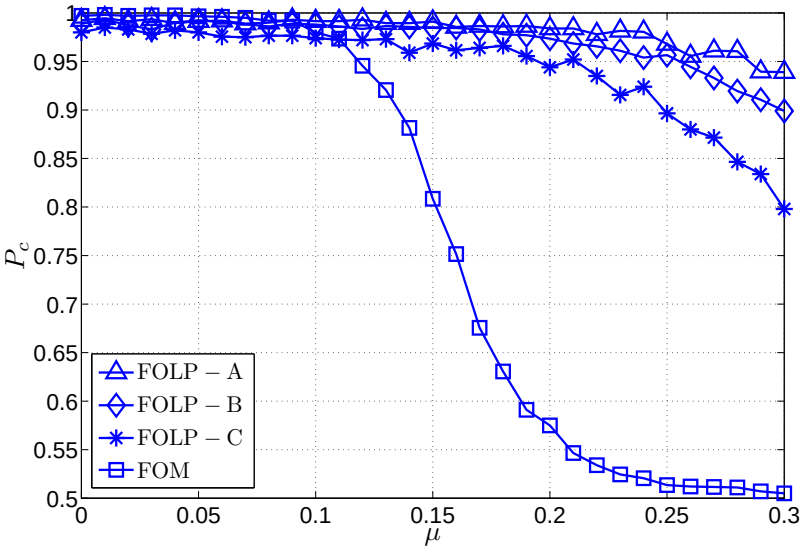

Fig. 2.10: The effect of the timing offset on the average probability of correct classification, P_c, over Nakagami-m channel, $m = 3$, with QPSK modulation and $K = 2048$ at SNR = 10 dB. $P_{fa} = 10^{-2}$ for the FOLP-B classification algorithm.

2.6.8 Effect of the spatially correlated fading

Independent fading was considered in the previous analysis. Here we show the effect of correlated fading on the classification performance. Correlated Nakagami-m fading was generated using correlated complex-valued Gaussian variables ([38], p. 25), the inverse cumulative distribution function (cdf) method [36], and an approximation of the Nakagami-m inverse cdf [36]. Fig. 2.11 shows the average probability of correct classification, P_c, of the FOM-based and FOLP-C algorithms versus the correlation coefficient between h_0 and h_1, ν, over Nakagami-m fading with $m = 3$ and 1, for the QPSK modulation at SNR=10 dB and $K = 2048$. Note that the performance improves as ν increases, especially at lower values of m [6]. This can be explained as follows. We recall that, for the AL-STBC, $|m_{r,4,0}|$, which controls the performance of the FOM-based algorithm, and the absolute value of the DFT peak, $|\mathcal{E}|$, which controls the performance of the FOLP-based algorithms, are proportional to $|h_0^2 h_1^2|$ (as shown in (2.5) and Section IV). For SM, these two parameters are zero valued if the noise contributions are neglected. The question arises how the spatial correlation between the two channels affects $|h_0^2 h_1^2|$. Fig. 2.12, which shows $\mathrm{E}\{|h_0|^2|h_1|^2\}$ as a function of ν for different values of m, helps us to answer this question. Note that since h_0 and h_1 change their values randomly from one realization to another, we resort to the statistical mean value, $\mathrm{E}\{|h_0|^2|h_1|^2\}$, instead of the instantaneous value, $|h_0^2 h_1^2|$. It is obvious from Fig. 2.12 that $\mathrm{E}\{|h_0|^2|h_1|^2\}$ is an increasing function of ν. This explains why the classification performance improves with ν for $m = 1$, as shown in Fig. 2.11. However, for $m = 3$, there is not much improvement in the classification performance. This is because the classification performance at $\nu = 0$ is high enough and $\mathrm{E}\{|h_0|^2|h_1|^2\}$ increases slowly with ν. This agrees with the fact that in the case of no fading (m tends to infinity), $\mathrm{E}\{|h_0|^2|h_1|^2\}$ is essentially independent of ν.

[6] Similar results are obtained for the FOLP-A and FOLP-B algorithms; however, these results were omitted due to space considerations.

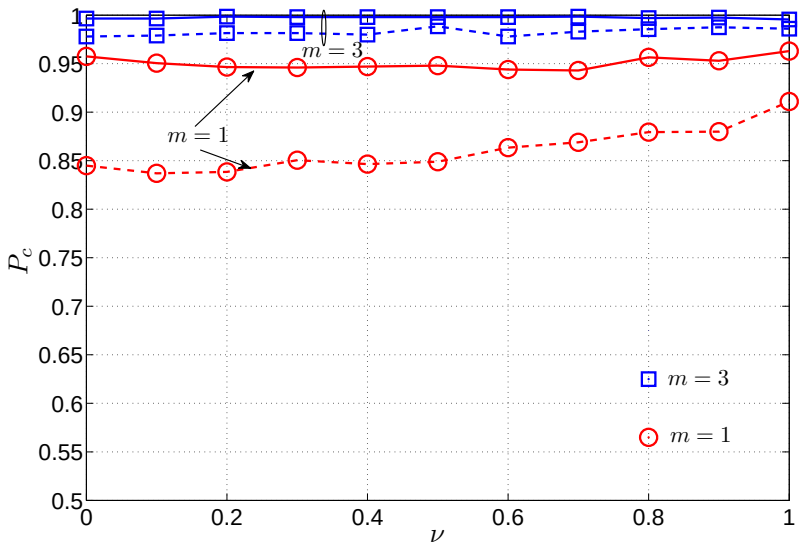

Fig. 2.11: The effect of the spatial correlation between transmitted antennas on the average probability of correct classification, P_c, for the FOM and FOLP-C classification algorithms over Nakagami-m fading channel, $m = 3$ and 1, with QPSK modulation and $K = 2048$ at SNR=10 dB. Solid lines are used for the FOM-based algorithm and dashed lines for the FOLP-C algorithm.

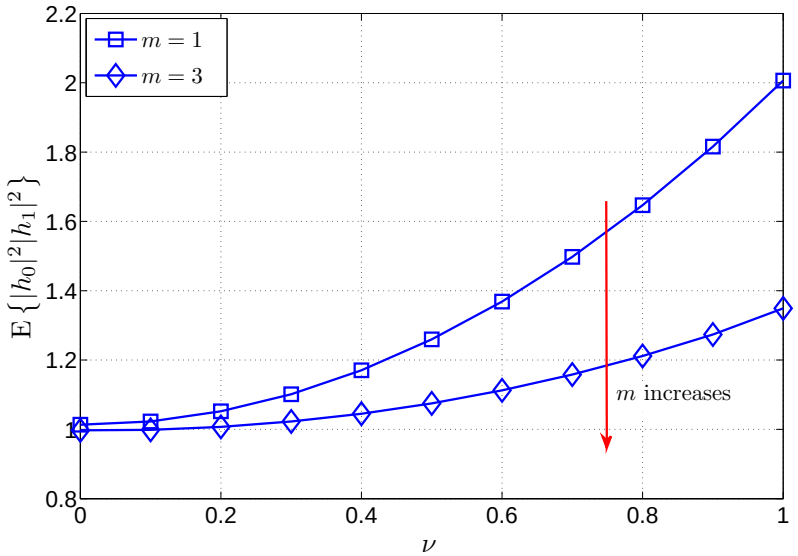

Fig. 2.12: $\mathrm{E}\{|h_0|^2|h_1|^2\}$ versus the correlation coefficient, ν, for Nakagami-m fading channel, $m = 3$ and 1.

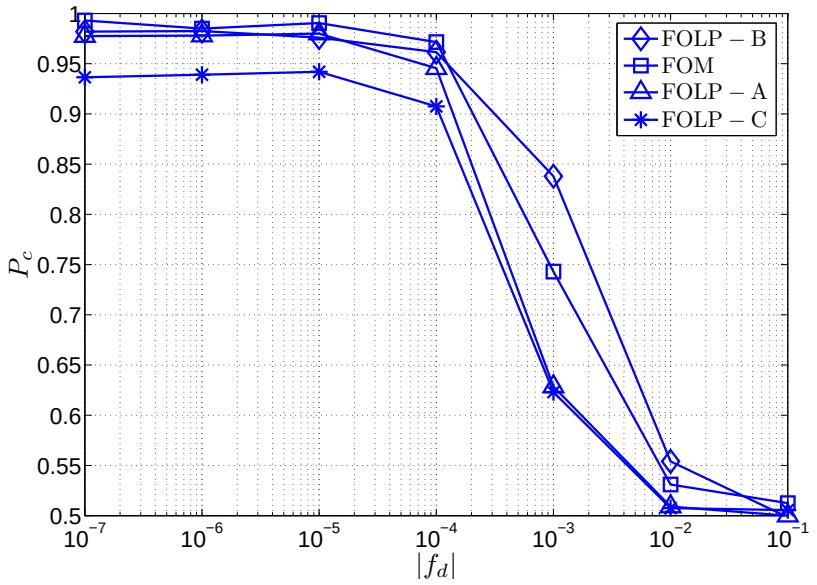

Fig. 2.13: The effect of the Doppler frequency on the average probability of correct identification, P_c, for the proposed identification algorithms over Nakagami-m fading channel, $m = 3$, with QPSK modulation and $K = 1024$ at SNR=10 dB.

2.6.9 Effect of the Doppler frequency

The previous analysis assumed constant channel coefficients over the observation period. Here we consider the effect of the Doppler frequency on the performance of the proposed algorithms. Fig. 2.13 shows the average probability of correct classification, P_c, for the FOM- and FOLP-based algorithms versus the Doppler frequency magnitude normalized to the data rate, $|f_d|$, at SNR= 10 dB and $K = 1024$. These results show good robustness for $|f_d| < 10^{-4}$.

2.6.10 Effect of the probability of false alarm

Fig. 2.14 presents the effect of the probability of false alarm, P_{fa}, on the probability of correct classification, $P(\lambda = \xi|\xi)$, $\xi \in \{\text{SM, AL}\}$, for the FOLP-B classification algorithm. It is noted that the AL-STBC classification performance improves as P_{fa} increases. An increase in the P_{fa} leads to a reduction in the threshold value, and, hence, $|Y(0)|$ or

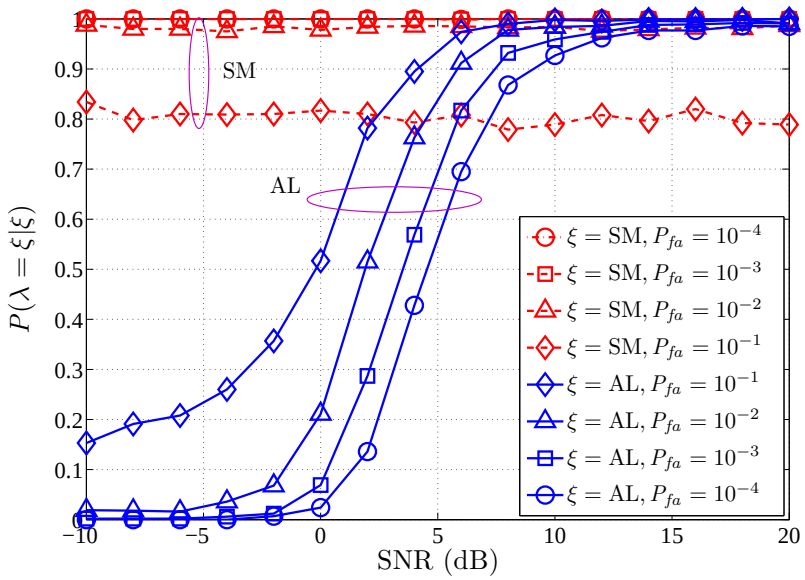

Fig. 2.14: The effect of P_{fa} on the probability of correct classification, $P(\lambda = \xi|\xi)$, $\xi \in \{\text{SM, AL}\}$, for the FOLP-B classification algorithm over Nakagami-m channel, $m = 3$, with QPSK modulation and $K = 1024$.

$|Y(K/2)| \geq \varepsilon$ are more easily satisfied, thus leading to a better performance. On the other hand, the SM classification performance decreases with an increase in P_{fa}, as $P(\lambda = \text{SM}|\text{SM}) = 1 - 2P_{fa}$. Therefore, the value of P_{fa} is chosen as a trade-off between the SM and AL-STBC classification performances.

2.7 Conclusion

The classification of spatial multiplexing (SM) and Alamouti space-time block code (AL-STBC) signals was investigated in this paper. It was shown that a fourth-order moment (FOM) and the discrete Fourier transform (DFT) of a fourth-order lag product (FOLP) can be used as discriminating signal features. Based on these results, four novel classification algorithms were proposed. The first algorithm employs the FOM of the received signal as a discriminating feature and the likelihood ratio test (LRT) to make a decision. Analytical results for the algorithm classification performance were derived. However, the

practical implementation of this algorithm is complicated by the need for channel estimation, modulation classification, and noise power estimation. To relax these requirements, we proposed three algorithms based on the DFT of the received signal FOLP, namely FOLP-A, FOLP-B, and FOLP-C. The influence of model mismatches (e.g., frequency and timing offsets, Doppler frequency, and spatially correlated fading) on the performance of the proposed algorithms was also investigated. Unlike the FOM-based, FOLP-A, and FOLP-B algorithms, FOLP-C is robust with respect to frequency offsets. Furthermore, the FOLP-based algorithms have lower sensitivity to the timing offset when compared to the FOM-based algorithm. The proposed algorithms are tolerant to a Doppler frequency whose magnitude, normalized with respect to the data rate, is lower than 10^{-4}. Also, their performance can benefit from spatially correlated fading. As part of future work, we plan to extend the proposed classification algorithms to a larger pool of STBCs.

Appendix

Effect of the frequency offset on the discriminating signal features

The effects of a frequency offset on the proposed discriminating signal features have been determined. In the presence of such an offset, the received signal, $r'(k)$ is

$$r'(k) = r(k)e^{-j(2\pi\Delta f k)}, \qquad k = 0, 1, ..., K-1, \tag{2.25}$$

where $r(k)$ is given in (3) and Δf represents the frequency offset normalized to the data rate.

Effect on the FOM-based feature

In the presence of a frequency offset, the estimated fourth-order moment, $\hat{m}_{r',4,0}$, is given by

$$\begin{aligned}\hat{m}_{r',4,0} &= \frac{1}{K}\sum_{k=0}^{K-1} r'^2(k)r'^2(k+1) \\ &= e^{-j(4\pi\Delta f)}\left[\frac{1}{K}\sum_{k=0}^{K-1} r^2(k)r^2(k+1)e^{-j(8\pi\Delta f k)}\right]. \end{aligned} \tag{2.26}$$

The discrete-time Fourier transform of the sequence $y(k) = r^2(k)r^2(k+1), k = 0, 1, ..., K-1$, can be computed as,

$$\mathcal{Y}(f) = \sum_{k=0}^{K-1} r^2(k)r^2(k+1)e^{-j(2\pi f k)}, \quad 0 \leq f \leq 1. \tag{2.27}$$

From (2.26) and (2.27), it is clear that $\hat{m}_{r',4,0} = e^{-j(4\pi\Delta f)}\left[\frac{1}{K}\mathcal{Y}(4\Delta f)\right]$. If $K \to \infty$, the noise components $\psi^{\mathrm{SM}}(k)$ and $\psi^{\mathrm{AL}}(k)$ in (2.15) and (2.16) vanish, with the result that $\mathcal{Y}(f) = K(h_0^2 h_1^2 c_{x,4,2})[\delta(f) + \delta(f-1/2)]$ for the AL STBC, while $\mathcal{Y}(f) = 0$ for the SM. Under such conditions, it follows that, for the AL STBC, $\hat{m}_{r',4,0} = m_{r',4,0} = m_{r,4,0} = h_0^2 h_1^2 c_{x,4,2}$ if $\Delta f = 0$, $\hat{m}_{r',4,0} = m_{r',4,0} = -jh_0^2 h_1^2 c_{x,4,2}$ if $\Delta f = 0.125$, and $\hat{m}_{r',4,0} = 0$ otherwise, whereas for the SM $\hat{m}_{r',4,0} = m_{r',4,0} = m_{r,4,0} = 0$ regardless of Δf. As such, the classification of AL STBC is affected by Δf.

Effect on the FOLP-based feature

The FOLP in the presence of the frequency offset can be calculated as,

$$
\begin{aligned}
y'(k) &= r'^2(k) r'^2(k+1) \\
&= e^{-j(4\pi\Delta f)} r^2(k) r^2(k+1) e^{-j(8\pi\Delta f k)}, \quad k = 0, 1, ..., K-1.
\end{aligned}
\tag{2.28}
$$

Taking the K-point DFT of (2.28) yields

$$
\begin{aligned}
Y'(n) &= \frac{1}{\sqrt{K}} \sum_{k=0}^{K-1} y'(k) e^{-j(2\pi k n/K)} \\
&= e^{-j(4\pi\Delta f)} \left[\frac{1}{K} \sum_{k=0}^{K-1} r^2(k) r^2(k+1) e^{-j2\pi k(n+4K\Delta f)/K} \right].
\end{aligned}
\tag{2.29}
$$

Since the decision is taken according to $|Y'(n)|$, the term $e^{-j(4\pi\Delta f)}$ has no effect. By using the shift property of the DFT, we obtain

$$
|Y'(n)| = \mathcal{A}(n) |Y(n + \lceil 4K\Delta f \rfloor)|, \tag{2.30}
$$

where $\lceil . \rfloor$ denotes the rounding function and $\mathcal{A}(n)$ represents an attenuation factor, which can be calculated as,

$$
\mathcal{A}(n) = \frac{1}{|Y(n)|} \left| \frac{1}{\sqrt{K}} \sum_{k=0}^{K-1} y(k) e^{-j2\pi k(n + [\lceil 4K\,\Delta f \rfloor - 4K\Delta f])/K} \right|. \tag{2.31}
$$

Examination of (2.30) shows that the peaks $|Y(0)|$ and $|Y(K/2)|$ for the AL STBC are shifted by $\lceil 4K\Delta f \rfloor$ and their magnitudes are scaled by $\mathcal{A}(0)$ and $\mathcal{A}(K/2)$, respectively. If Δf is an integer multiple of $1/8$, it is straightforward to show that the peaks are circularly shifted by $K/2$, with the result that their positions are unchanged. Furthermore, note

that $\mathcal{A}(n)$ equals one if Δf is an integer multiple of $1/4K$; otherwise, $\mathcal{A}(n)$ is less than one.

References

[1] B. Wang and K. Liu, "Advances in cognitive radio networks: A survey," *IEEE J. Sel. Topics Signal Process.*, vol. 5, pp. 5–23, Feb. 2011.

[2] A. B. MacKenzie et al. , "Cognitive radio and networking research at Virginia Tech," *Proc. of the IEEE, invited paper*, vol. 97, pp. 660–688, Apr. 2009.

[3] D. Cabric, "Cognitive Radios: System Design Perspective," Ph.D. dissertation, University of California, Berkeley, USA, 2007.

[4] D. Cabric, S. Mishra, and R. Brodersen, "Implementation issues in spectrum sensing for cognitive radios," in *Proc. IEEE ASILOMAR*, 2004, pp. 772–776.

[5] T. Yucek and H. Arslan, "A survey of spectrum sensing algorithms for cognitive radio applications," *IEEE Commun. Surveys Tuts.*, vol. 11, pp. 116–130, Mar. 2009.

[6] Y. Zheng, Y.-C. Liang, A. T. Hoang, and R. Zhang, "A review on spectrum sensing for cognitive radio: Challenges and solutions," *EURASIP J. Adv. Sig. Proc.,* DOI:10.1155/2010/381465, 2010.

[7] E. Axell, G. Leus, E. G. Larsson, and H. Poor, "Spectrum sensing for cognitive radio: State-of-the-art and recent advances," *IEEE Signal Process. Mag.*, vol. 29, pp. 101–116, May 2012.

[8] O. A. Dobre, A. Abdi, Y. Bar-Ness, and W. Su, "Survey of automatic modulation classification techniques: Classical approaches and new trends," *IET Commun.*, vol. 1, pp. 137–156, Apr. 2007.

[9] H.-C. Wu, M. Saquib, and Z. Yun, "Novel automatic modulation classification using cumulant features for communications via multipath channels," *IEEE Trans. Wireless Commun.*, vol. 7, pp. 3098–3105, Aug. 2008.

[10] M. Oner and F. Jondral, "On the extraction of the channel allocation information in spectrum pooling systems," *IEEE J. Sel. Areas Commun.*, vol. 25, pp. 558–565, Apr. 2007.

[11] A. Swami and B. M. Sadler, "Hierarchical digital modulation classification using cumulants," *IEEE Trans. Commun.*, vol. 48, pp. 416–429, Mar. 2000.

[12] A. Punchihewa, Q. Zhang, O. Dobre, C. Spooner, S. Rajan, and R. Inkol, "On the cyclostationarity of OFDM and single carrier linearly digitally modulated signals in time dispersive channels: theoretical developments and application," *IEEE Trans. Wireless Commun.*, vol. 9, pp. 2588–2599, Aug. 2010.

[13] F. Hameed, O. Dobre, and D. Popescu, "On the likelihood-based approach to modulation classification," *IEEE Trans. Wireless Commun.*, vol. 8, pp. 5884–5892, Dec. 2009.

[14] V. Chavali and C. R. da Silva, "Maximum-likelihood classification of digital amplitude-phase modulated signals in flat fading non-gaussian channels," *IEEE Trans. Commun.*, vol. 59, pp. 2051–2056, Aug. 2011.

[15] W. C. Headley and C. R. da Silva, "Asynchronous classification of digital amplitude-phase modulated signals in flat-fading channels," *IEEE Trans. Commun.*, vol. 59, pp. 7–12, Jan. 2011.

[16] A. Al-Habashna, O. A. Dobre, R. Venkatesan, and D. C. Popescu, "Second-order cyclostationarity of mobile WiMAX and LTE OFDM signals and application to spectrum awareness in cognitive radio systems," *IEEE J. Sel. Topics Signal Process.*, vol. 6, pp. 26–42, Feb. 2012.

[17] M. Shi, Y. Bar-Ness, and W. Su, "Adaptive estimation of the number of transmit antennas," in *Proc. IEEE MILCOM*, 2007, pp. 1–5.

[18] O. Somekh, O. Simeone, Y. Bar-Ness, and W. Su, "Detecting the number of transmit antennas with unauthorized or cognitive receivers in MIMO systems," in *Proc. IEEE MILCOM*, 2007, pp. 1–5.

[19] V. Choqueuse, S. Azou, K. Yao, and G. Burel, " Blind modulation recognition for MIMO systems," *J. Military Technical Academy Review*, vol. XIX, pp. 183–196, Jun. 2009.

[20] K. Hassan, I. Dayoub, W. Hamouda, C. N. Nzeza, and M. Berbineau, "Blind digital modulation identification for spatially-correlated MIMO systems," *IEEE Trans. Wireless Commun.*, vol. 11, pp. 683–693, Feb. 2012.

[21] V. Choqueuse, M. Marazin, L. Collin, K. C. Yao, and G. Burel, "Blind recognition of linear space–time block codes: A likelihood-based approach," *IEEE Trans. Signal Process.*, vol. 58, pp. 1290–1299, Mar. 2010.

[22] V. Choqueuse, K. Yao, L. Collin, and G. Burel, "Hierarchical space-time block code recognition using correlation matrices," *IEEE Trans. Wireless Commun.*, vol. 7, pp. 3526–3534, Sep. 2008.

[23] V. Choqueuse, K. Yao, L. Collin, and G. Burel, "Blind recognition of linear space time block codes," in *Proc. IEEE ICASSP*, 2008, pp. 2833–2836.

[24] M. Shi, Y. Bar-Ness, and W. Su, "STC and BLAST MIMO modulation recognition," in *Proc. IEEE GLOBECOM*, 2007, pp. 3034–3039.

[25] M. Marey, O. A. Dobre, and R. Inkol, "Classification of space-time block codes based on second-order cyclostationarity with transmission impairments," *IEEE Trans. Wireless Commun.*, vol. 11, pp. 2574–2584, Jul. 2012.

[26] M. DeYoung, R. Heath, and B. Evans, "Using higher order cyclostationarity to identify space-time block codes," in *Proc. IEEE GLOBECOM*, 2008, pp. 1–5.

[27] M. Jankiraman, *Space-Time Codes and MIMO Systems.* Artech House, 2004.

[28] V. Tarokh, H. Jafarkhani, and A. R. Calderbank, "Space-time block codes from orthogonal designs," *IEEE Trans. Inf. Theory*, vol. 45, pp. 1456–1467, Jul. 1999.

[29] S. M. Alamouti, "A simple transmit diversity technique for wireless communications," *IEEE J. Sel. Areas Commun.*, vol. 16, pp. 1451–1458, Oct. 1998.

[30] J. Mendel, "Tutorial on higher-order statistics (spectra) in signal processing and system theory: Theoretical results and some applications," *Proceedings of the IEEE*, vol. 79, pp. 278–305, Mar. 1991.

[31] D. R. Brillinger, *Time Series: Data Analysis and Theory.* Society for Industrial and Applied Mathematics, 2001.

[32] J. G. Proakis and M. Salehi, *Communication Systems Engineering.* Prentice Hall, 2002.

[33] P. J. Davis, and P. Rabinowitz, *Methods of Numerical Integration.* Academic Press, 1975, vol. 1.

[34] H. Van Trees, *Detection, Estimation, and Modulation Theory: Detection, Estimation, and Linear Modulation Theory.* Wiley, 2001.

[35] A. Papoulis and S. Pillai, *Probability, Random Variables and Stochastic Processes*. McGraw-Hill, 2001.

[36] N. C. Beaulieu and C. Cheng, "Efficient Nakagami-m fading channel simulation," *IEEE Trans. Veh. Technol.*, vol. 54, pp. 413–424, Mar. 2005.

[37] D. Watkins, *Fundamentals of Matrix Computations*. Wiley, 2002.

[38] M. E. Johnson, *Multivariate Statistical Simulation*. Wiley, 1987.

Chapter 3

An Efficient Algorithm for Space-Time Block Code Classification

3.1 Abstract

This paper proposes a novel and efficient algorithm for space-time block code (STBC) classification, when a single antenna is employed at the receiver. The algorithm exploits the discriminating features provided by the discrete Fourier transform (DFT) of the fourth-order lag products (FOLPs) of the received signal. It does not require estimation of the channel, signal-to-noise ratio (SNR), and modulation of the transmitted signal. Computer simulations are conducted to evaluate the performance of the proposed algorithm. The results show the validity of the algorithm, its robustness to carrier frequency offset, and low sensitivity to timing offset.

3.2 Introduction

Blind classification of communication signals plays a pivotal role in both civilian and military applications, e.g., parameter configuration in software-defined radio, spectrum awareness in cognitive radio, and spectrum monitoring and surveillance [1–3].

A large number of studies have been carried out for developing blind signal classification algorithms in single-input single-output scenarios (see the comprehensive survey [3] and references therein). Regarding multiple-input multiple-output (MIMO) technology, which has been recently included in wireless standards such as IEEE 802.11n, IEEE 802.16e, and 3GPP LTE [4], new and challenging signal classification problems have arisen. These relate to the estimation of the number of transmit antennas, as well as space-time code and modulation classification. The research on signal classification for MIMO scenarios is at an incipient stage. Blind estimation of the number of transmit antennas is investigated in [5, 6], and modulation classification for spatial multiplexing (SM) in [7–10], while blind classification of linear space-time block codes (STBCs) has been recently explored in [11–17]. Classification algorithms can be mainly divided into two categories: likelihood-based [11] and feature-based algorithms [12–17]. Likelihood-based algorithms calculate the likelihood function of the received signal, and employ the maximum likelihood criterion for decision making [11]. However, these algorithms require channel estimation, time, block, and frequency synchronization, and knowledge of the modulation format. Furthermore, they suffer from high computational complexity. Second-order statistics are exploited in [12,13], while fourth-order statistics are considered in [14]. In [15–17], signal cyclostationarity-based features are used. Most of these investigations assume perfect timing and frequency synchronization [11–16]. Some of these papers study the classification of SM and Alamouti (AL)-STBC [14–16], whereas others consider a larger pool of STBCs [11–13,17]. Furthermore, most employ multiple antennas at the receiver [12,13,16,17]. Since this requirement can not always be met, solutions for

STBC blind classification when a single receive antenna is available are of interest.

This paper proposes an efficient algorithm for the linear STBC classification, which exploits features based on the discrete Fourier transform (DFT) of the fourth-order lag products (FOLPs) of the received signal. The proposed algorithm does not require information about channel, modulation, and signal-to-noise ratio (SNR). Moreover, it is robust to carrier frequency offset and requires only a rough estimate of clock timing.

The rest of this paper is organized as follows: Section 3.3 introduces the signal model. Section 3.4 describes the proposed STBC classification algorithm. Simulation results are presented in Section 3.5. Finally, concluding remarks are drawn in Section 3.6.

3.3 Signal Model

We consider a wireless communication system which employs linear STBCs with multiple transmit antennas. In such a case, a block of N_s modulated symbols is encoded to generate N_t parallel signal sequences of length L, to be transmitted simultaneously with N_t antennas in L consecutive time periods [18]. We denote the bth block of N_s complex symbols to be transmitted by the column vector $\mathbf{X}_b = [x_{b,0}, ..., x_{b,N_s-1}]^T$, with the superscript T denoting transposition. The symbols are zero-mean independent and identically distributed (i.i.d) random variables, with values drawn from an alphabet corresponding to an M-PSK or M-QAM, $M \geq 4$, signal constellation. Without loss of generality, we consider unit variance constellations, i.e., $\mathrm{E}\{|x|^2\}$ =1, with $\mathrm{E}\{.\}$ as the statistical expectation. Further, we denote the $N_t \times L$ space-time coding matrix and the $(l+1)$th column of this matrix by $\mathbb{G}(\mathbf{X}_b)$ and $\mathbb{G}_l(\mathbf{X}_b)$, $0 \leq l < L$, respectively.

The received signal is assumed to be encoded by one of the following STBCs[1]: SM [18] with $N_t = 2$ and $L = 1$, AL code [18] with $N_t = 2$ and $L = 2$ (orthogonal with rate 1),

[1]We choose AL and SM as they are the most commonly used in wireless standards [4], and STBC3 and STBC4, as being commonly referred codes [18, 19].

STBC3 [18] with $N_t = 3$ and $L = 4$ (orthogonal with rate $\frac{3}{4}$), or STBC4 [19] with $N_t = 3$ and $L = 8$ (orthogonal with rate $\frac{1}{2}$).

For example, the transpose coding matrix of STBC4 is defined as [19]

$$(\mathbb{G}^{\text{STBC4}}(\mathbf{X}_b))^T = \begin{bmatrix} x_{b,0} & x_{b,1} & x_{b,2} \\ -x_{b,1} & x_{b,0} & -x_{b,3} \\ -x_{b,2} & x_{b,3} & x_{b,0} \\ -x_{b,3} & -x_{b,2} & x_{b,1} \\ x^*_{b,0} & x^*_{b,1} & x^*_{b,2} \\ -x^*_{b,1} & x^*_{b,0} & -x^*_{b,3} \\ -x^*_{b,2} & x^*_{b,3} & x^*_{b,0} \\ -x^*_{b,3} & -x^*_{b,2} & x^*_{b,1} \end{bmatrix}, \tag{3.1}$$

where the rows and columns correspond to the time periods and transmit antennas, respectively.

We consider a receiver equipped with a single antenna, and assume that the STBC time alignment and length are unknown, whereas symbol and carrier synchronization are performed. Later in the paper, we will study the effect of timing and carrier frequency offsets. Without loss of generality, we assume that the first received symbol, denoted by $r(0)$, intercepts the $(k_1 + 1)$th column, $0 \leq k_1 < L$, of the bth transmitted block, denoted by $\mathbb{G}_{k_1}(\mathbf{X}_b)$. Under these assumptions, the kth received symbol, $r(k)$, $k \geq 0$, is expressed as [12]

$$r(k) = \mathbf{H}\mathbf{S}(k) + w(k), \tag{3.2}$$

where $\mathbf{S}(k) = \mathbb{G}_p(\mathbf{X}_q)$, with $p = (k + k_1) \bmod L$, $q = b + (k + k_1) \operatorname{div} L$, and $z \bmod L$ and $z \operatorname{div} L$ denoting respectively the remainder and the quotient of the division z/L, $\mathbf{H} = [h_0, ..., h_{N_t-1}]$ represents the vector of the channel coefficients, which characterize the

paths between the transmit and receive ends, and $w(k)$ represents the complex additive white Gaussian noise (AWGN) with zero mean and variance σ_w^2.

3.4 An efficient classification algorithm

In this section, we show how the DFT of the FOLP of the received signal can be exploited to blindly classify the STBCs under consideration based on K received symbols, $r(k)$, $0 \leq k \leq K-1$, when a single receive antenna is employed.

3.4.1 Discriminating features

The FOLP of the received sequence, $\{r(k)\}_{k=0}^{K-1}$, at delay vector [0,0,τ,τ] is defined as

$$y(k,\tau) = r^2(k)r^2(k+\tau), \quad k = 0, 1, ..., K-1. \tag{3.3}$$

Based on the structure of the code matrices, we first consider $\tau = 4$ due to its discriminating property for STBC4, as it is subsequently explained.

Without loss of generality, we assume that the first received symbol, $r(0)$, corresponds to the start of the STBC block. Later we will show that this assumption will not affect the performance of the proposed algorithm.

By substituting (3.2) in (3.3) of the FOLP, one can express the FOLPs corresponding to the considered STBCs as

$$y^{\text{STBC4}}(k,4) = \begin{cases} a(k) + \psi_1(k) & \text{under event } \Im_1 \\ \\ \psi_2(k) & \text{under event } \Im_2 \end{cases} \tag{3.4}$$

and

$$y^{\xi}(k,4) = \psi_3^{\xi}(k), \qquad \xi \in \{\text{SM}, \text{AL}, \text{STBC3}\}, \tag{3.5}$$

where $\Im_1$ is the event that $r(k)$ and $r(k+4)$ belong to the same transmitted data block, $\Im_2$ is the event that they do not, and $a(k) = [\mathbf{HS}(k)]^2 [\mathbf{HS}(k+4)]^2$. Furthermore, $\psi_1(k)$, $\psi_2(k)$, and $\psi_3(k)$ represent the remaining signal and AWGN components.

Note that $a(k)$ depends on the channel coefficients and the transmitted data symbols corresponding to $r(k)$ and $r(k+4)$ under event $\Im_1$. For example, one can show that $a(k = bL)$ is given by

$$\begin{aligned} a(bL) = \; & 4(|x_{b,0}|^2|x_{b,1}|^2h_0^2h_1^2 + |x_{b,0}|^2|x_{b,2}|^2h_0^2h_2^2 \\ & +|x_{b,1}|^2|x_{b,2}|^2h_1^2h_2^2) + |x_{b,0}|^4h_0^4 \\ & +|x_{b,1}|^4h_1^4 + |x_{b,2}|^4h_2^4, \end{aligned} \tag{3.6}$$

where $x_{b,0}$, $x_{b,1}$, and $x_{b,2}$ are the data symbols transmitted in the first time period of the bth STBC4 block. Similar expressions can be also obtained for $a(k)$, $k \neq bL$. It is noteworthy that $a(k)$ is constant for the M-PSK signals, i.e., it does not depend on the transmitted symbols, as PSK is a constant envelope modulation. For M-QAM signals, $a(k)$ can be expressed as a constant, $A_{\text{QAM}} = \text{E}\{a(k)\}$, plus a variable $\psi_4(k)$, which represents the deviation from the mean[2]. For the convenience of notation, subsequently we use the constant $A \in \{A_{\text{PSK}}, A_{\text{QAM}}\}$, which is given by

$$A = m_{x,4,2}(h_0^4 + h_1^4 + h_2^4) + 4(m_{x,2,1})^2(h_0^2h_1^2 + h_0^2h_2^2 + h_1^2h_2^2), \tag{3.7}$$

with $m_{x,\alpha,\beta} = \text{E}\{x^{\alpha-\beta}(x^*)^\beta\}$ as the (α, β) moment of the points in the signal constellation. Examples of $m_{x,4,2}$ values are provided in Table 3.1 for various unit variance signal constellations [3].

In the absence of the noisy components, i.e., $\psi_1(k) + \psi_4(k) = \psi_2(k) = \psi_3(k) = 0$, the FOLP sequence is

[2]Generally speaking, a random variable x can be expressed as $x = \text{E}\{x\} + \nu$, where ν is a zero-mean random variable which represents the deviation from the mean $\text{E}\{x\}$ [20].

Table 3.1: Moment values for various signal constellations.

	QPSK	8-PSK	16-QAM	64-QAM
$m_{x,2,1}$	1	1	1	1
$m_{x,4,2}$	1	1	1.32	1.38

- STBC4: [A A A A 0 0 0 0 A A A A 0 0 0 0 ...]

  and

- STBC3, AL, and SM: [0 0 0 ....].

Thus STBC4 can be recognized by detecting the periodicity of its FOLP at $\tau = 4$, for which we employ the DFT. Let $\mathbf{Y} = [Y(0,\tau), Y(1,\tau), ..., Y(K-1,\tau)]$ denote the K-point DFT of $\mathbf{y}$, with

$$Y(n,\tau) = \frac{1}{\sqrt{K}} \sum_{k=0}^{K-1} y(k,\tau) e^{-j2\pi kn/K}, \qquad n = 0, 1, ..., K-1. \tag{3.8}$$

By replacing (3.4) and (3.5) in (3.8), it follows that

$$Y^{\text{STBC4}}(n,4) = \begin{cases} \mathcal{A}(n) + \Psi_1(n) & n = 0, \frac{K}{8}, \frac{3K}{8}, \frac{5K}{8}, \frac{7K}{8}, \\ \\ \Psi_1(n) & \text{otherwise}, \end{cases} \tag{3.9}$$

and

$$Y^{\xi}(n,4) = \Psi_2(n), \quad \xi \in \{\text{SM, AL, STBC3}\}, \tag{3.10}$$

where $\Psi_1(n)$ and $\Psi_2(n)$ represent the DFT of the noisy components, and $\mathcal{A}(n)$ represents the peak values at $n = 0, \frac{K}{8}, \frac{3K}{8}, \frac{5K}{8}, \frac{7K}{8}$, which depend on A and K. One can easily show that $\mathcal{A}(0) = \frac{\sqrt{K}}{2}A$, $\mathcal{A}(\frac{K}{8}) = \mathcal{A}(\frac{7K}{8}) = \frac{\sqrt{K}}{8}A\left(1 - i\left(1 + \sqrt{2}\right)\right)$, and $\mathcal{A}(\frac{3K}{8}) = \mathcal{A}(\frac{5K}{8}) = \frac{\sqrt{K}}{8}A\left(1 + i\left(1 - \sqrt{2}\right)\right)$.

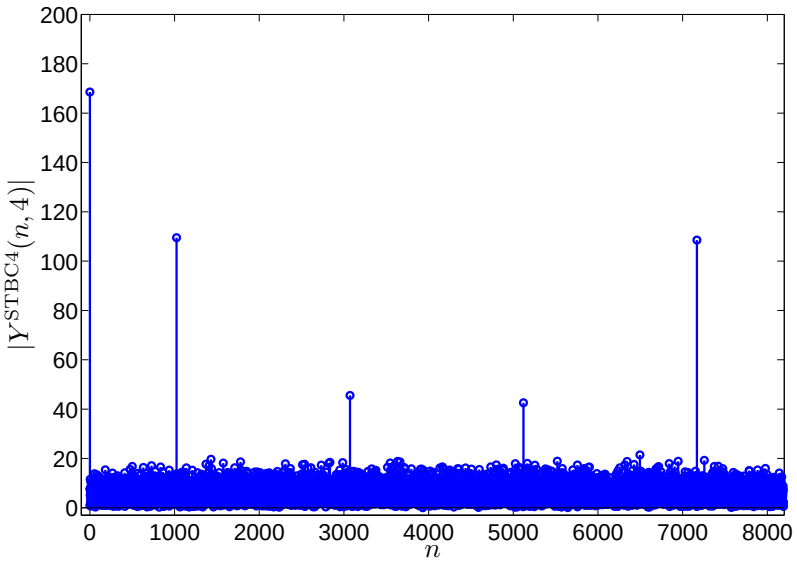

Fig. 3.1: $|Y^{\mathrm{STBC4}}(n,4)|$ with QPSK modulation and $K = 8192$, at SNR=20 dB over Nakagami-m fading channel, $m = 3$.

The inspection of (3.9) and (3.10) indicates that $|Y(n,4)|$ exhibits 5 peaks at $n = 0, \frac{K}{8}, \frac{3K}{8}, \frac{5K}{8}, \frac{7K}{8}$ for STBC4, while it does not for the other codes; thus, this discriminating feature can be exploited to recognize STBC4[3]. $|Y^{\mathrm{STBC4}}(n,4)|$ is shown as a function of n in Fig. 3.1. Based on the vector $Y(n,4)$, we define the vector $Z(u,4)$,

$$Z(u,4) = \sum_{l=0}^{3} \left| Y(\frac{lK}{4} + u, 4) \right|^2, \quad u = 0, 1, ..., \frac{K}{4} - 1. \tag{3.11}$$

For STBC4, $Z^{\mathrm{STBC4}}(u,4)$ exhibits two peaks at $u = 0, \frac{K}{8}$, where

$$Z^{\mathrm{STBC4}}(0,4) = |Y^{\mathrm{STBC4}}(0,4)|^2, \tag{3.12}$$

and

[3]Note that timing misalignment will introduce a cyclic shift in the FOLP sequence [A A A A 0 0 0 0 A A A A ...], which will affect neither the positions nor the magnitudes of the DFT peaks.

$$Z^{\mathrm{STBC4}}(\tfrac{K}{8},4) = |Y^{\mathrm{STBC4}}(\tfrac{K}{8},4)|^2 + |Y^{\mathrm{STBC4}}(\tfrac{3K}{8},4)|^2 + |Y^{\mathrm{STBC4}}(\tfrac{5K}{8},4)|^2 + |Y^{\mathrm{STBC4}}(\tfrac{7K}{8},4)|^2. \tag{3.13}$$

Note that this operation reduces the number of peaks to two for STBC4, while it strengthens the second peak value. Furthermore, we should note that $Z(u,4)$ has no peaks for STBC3, AL, and SM.

Similarly, one can show that for $\tau = 1$ and in the absence of the noisy components, the FOLP sequence is

- STBC3: [0 B1 B2 0 0 B1 B2 0 ...], with

$$B_1 = 2(m_{x,4,2} - 2(m_{x,2,1})^2)h_1^2 h_2^2,$$

and

$$B_2 = 2(m_{x,4,2} - 2(m_{x,2,1})^2)h_0^2 h_1^2.$$

- AL: [C 0 C 0 C 0...], with

$$C = 2(m_{x,4,2} - 2(m_{x,2,1})^2)h_0^2 h_1^2.$$

- SM: [0 0 0 ...].

In this case, $|Y(n,1)|$ exhibits four peaks at $n = 0,\ \frac{K}{4},\ \frac{K}{2}, \frac{3K}{4}$ for STBC3, and two peaks at $n = 0,\ \frac{K}{2}$ for AL.

We further define the vector $Z(u,1)$ as,

$$Z(u,1) = \sum_{l=0}^{1} \left| Y(\frac{lK}{2} + u, 1) \right|^2, \quad u = 0, 1, ..., \frac{K}{2} - 1. \tag{3.14}$$

One can show that $Z(u,1)$ has two peaks at $u = 0, \frac{K}{4}$ for STBC3, where

$$Z^{\text{STBC3}}(0,1) = |Y^{\text{STBC3}}(0,1)|^2 + |Y^{\text{STBC3}}(\frac{K}{2},1)|^2, \tag{3.15}$$

and

$$Z^{\text{STBC3}}(\frac{K}{4},1) = |Y^{\text{STBC3}}(\frac{K}{4},1)|^2 + |Y^{\text{STBC3}}(\frac{3K}{4},1)|^2. \tag{3.16}$$

Note that this operation reduces the number of peaks to two for STBC3, and strengthens the peak values. Furthermore, it can be easily shown that $Z(u,1)$ has only one peak at $u=0$ for AL, while it has no peaks for SM.

3.4.2 Decision tree algorithm for STBC classification

STBC classification is formulated as a hypothesis testing problem, i.e., under hypothesis $\mathcal{H}_\xi$, the STBC $\xi \in \{\text{SM, AL, STBC3, STBC4}\}$ is selected. The discriminating features previously described are used with a decision tree classification algorithm, which is presented in Fig. 3.2.

At node 1, $Z(u,4)$ is used to discriminate between STBC4 and {SM, AL, STBC3} based on the existence of the two peaks in $Z(u,4)$, whose difference in location is $\frac{K}{8}$,

$$|u_1 - u_2| = \frac{K}{8}, \tag{3.17}$$

where

$$u_1 = \arg\max_u Z(u,4), \tag{3.18}$$

and

$$u_2 = \arg\max_{u,u\neq u_1} Z(u,4). \tag{3.19}$$

At node 2, $Z(u,1)$ is used to discriminate between STBC3 and {SM, AL} based on the existence of the two peaks in $Z(u,1)$, whose difference in location is $\frac{K}{4}$. In other words, if u_1 and u_2 are the positions of the two maximum values in $Z(u,1)$, STBC3 is

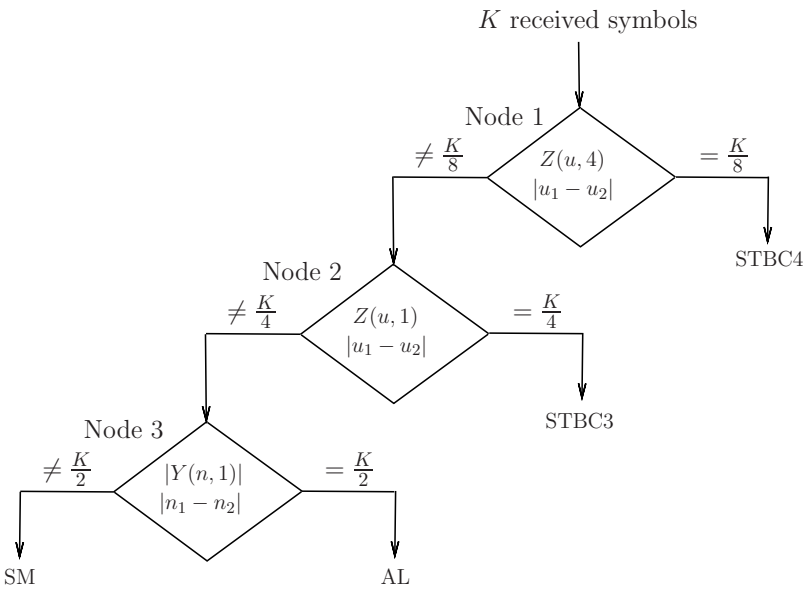

Fig. 3.2: Decision tree algorithm for STBC classification.

declared present if

$$|u_1 - u_2| = \frac{K}{4}. \tag{3.20}$$

Finally, at node 3, discrimination between AL and SM is performed based on the peak positions in $|Y(n,1)|$ [14]. If n_1 and n_2 are the positions of the maximum values in $|Y(n,1)|$, AL is recognized if

$$|n_1 - n_2| = \frac{K}{2}. \tag{3.21}$$

Otherwise, SM is declared present.

3.5 Simulation results

3.5.1 Simulation setup

Unless otherwise mentioned, the number of observed samples, K, was set to 8192 and quadrature phase-shift-keying (QPSK) modulation was used. The average probability of correct classification, i.e, $P_c = 4^{-1} \sum_{\xi \in \{\text{SM, AL, STBC3, STBC4}\}} P(\xi|\xi)$, was employed as a performance measure. $P(\xi|\xi)$ was estimated from 1000 Monte Carlo trials for each $\xi \in \{\text{SM, AL, STBC3, STBC4}\}$. The received signal was affected by a frequency-flat Nakagami-m fading channel [21] with $m = 3$, unless otherwise mentioned. Furthermore, AWGN with variance σ_w^2 was considered. Given a unit variance constellation, the SNR is defined as $10 \log_{10}(N_t/\sigma_w^2)$.

3.5.2 Performance evaluation

Fig. 3.3 shows P_c achieved with the proposed algorithm over Nakagami-m fading channel with $m = 1, 3, 10$ and ∞. As expected, the performance improves as m increases. For example, at SNR=10 dB, $P_c = 0.9, 0.97$, and 0.986 for $m = 1, 3$, and 10, respectively, while it reaches 1 for $m = \infty$. This can be easily explained, as the variance of the channel coefficients increases for lower m values, which strongly affects the value of the discriminating peaks; thus, leading to erroneous decisions.

3.5.3 Effect of the number of observed samples

Fig. 3.4 illustrates the effect of the number of received samples on P_c. The performance enhances by increasing K, as the peak values are proportional to $\sqrt{K}$. Moreover, increasing K leads to a reduction of the effect of the noisy components. Note that, as the proposed algorithm depends on fourth-order statistics, a large number of observed samples is required for accurate estimation of the discriminating feature.

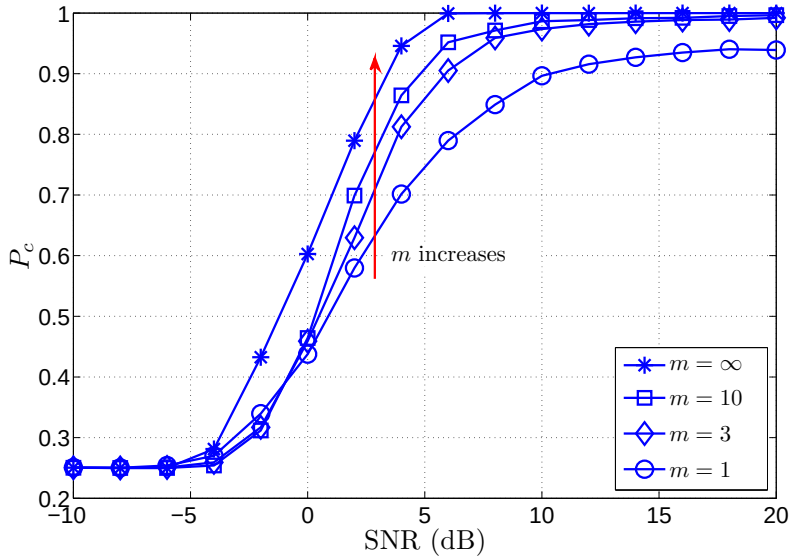

Fig. 3.3: Average probability of correct classification, P_c, versus SNR with QPSK modulation and $K = 8192$ for diverse Nakagami-m fading channels.

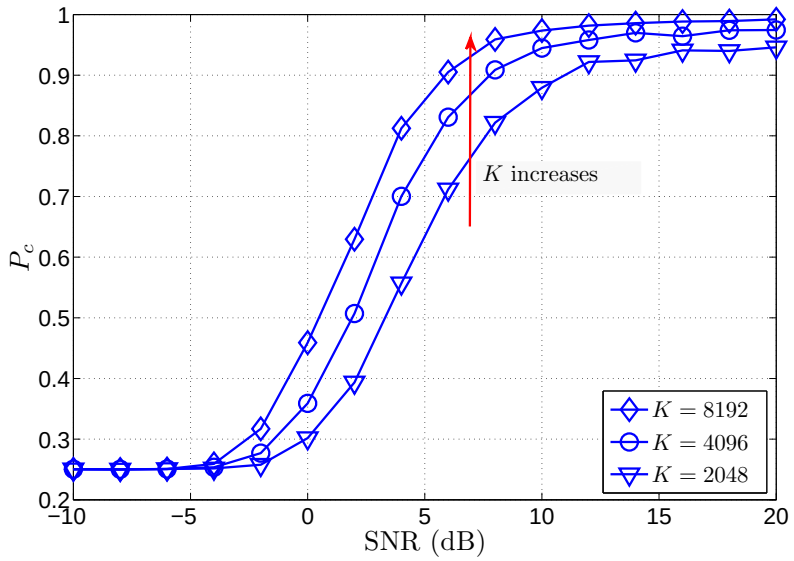

Fig. 3.4: Effect of the number of received samples, K, on P_c with QPSK modulation over Nakagami-m fading channel, $m = 3$.

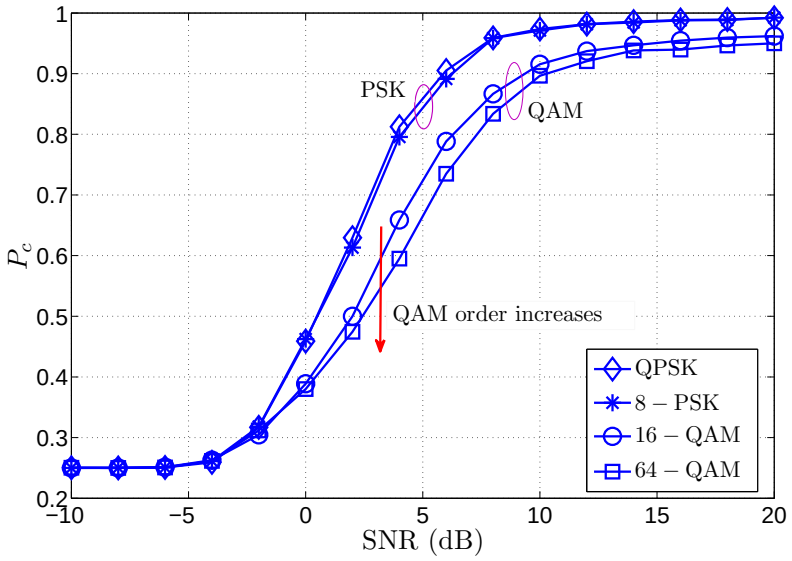

Fig. 3.5: Effect of the modulation type on P_c with $K = 8192$ over Nakagami-m fading channel, $m = 3$.

3.5.4 Effect of modulation type

Fig. 3.5 shows the effect of the modulation type on P_c; a better performance is achieved for M-PSK signals when compared with M-QAM signals. The explanation is that $a(k)$ is constant for M-PSK, whereas it is not for M-QAM. This yields an increase in the variance of the noisy components as M increases, leading to performance degradation.

3.5.5 Effect of frequency offset

The previous analysis assumed carrier frequency synchronization. Here we evaluate the performance of the proposed algorithm in the presence of a carrier frequency offset. Fig. 3.6 presents the effect of the frequency offset normalized to the data rate, Δf, on P_c. It can be noticed that the performance does not depend on Δf. This is because Δf introduces a shift in the position of the peaks, and thus, it has no effect on the decision made on the difference between these positions. Hence, the algorithm is robust to carrier frequency offset.

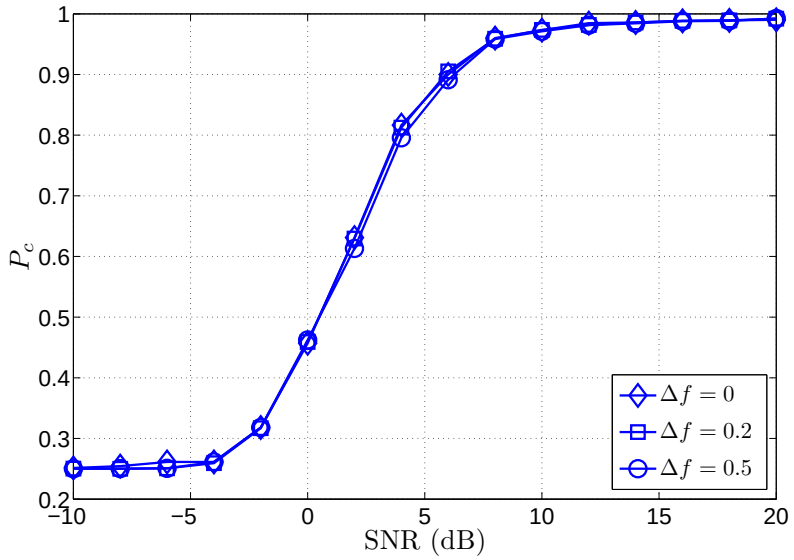

Fig. 3.6: Effect of the frequency offset on P_c with QPSK modulation and $K = 8192$ over Nakagami-m fading channel, $m = 3$.

3.5.6 Effect of timing offset

The previous analysis additionally assumed perfect timing synchronization. Here we show the performance of the proposed algorithm in the presence of a timing offset normalized to the sampling period, $0 \leq \mu < 1$. For the case of rectangular pulse shaping, after the matched filtering, the timing offset μ translates into a two path channel $[1 - \mu, \mu]$ [12]. Fig. 3.7 shows P_c for $\mu = 0, 0.2, 0.3$ and 0.4. The performance slightly decreases for $\mu = 0.2$ and 0.3, while it reduces more for $\mu = 0.4$.

3.5.7 Effect of the spatially correlated fading

Independent fading was considered in the previous analysis. Here we evaluate the classification performance under spatial correlation fading environment. Spatially correlated Nakagami-m fading with correlation coefficient ρ, $0 \leq \rho \leq 1$, is generated using correlated complex-valued Gaussian variables ([22], p. 25), the inverse cumulative distribution

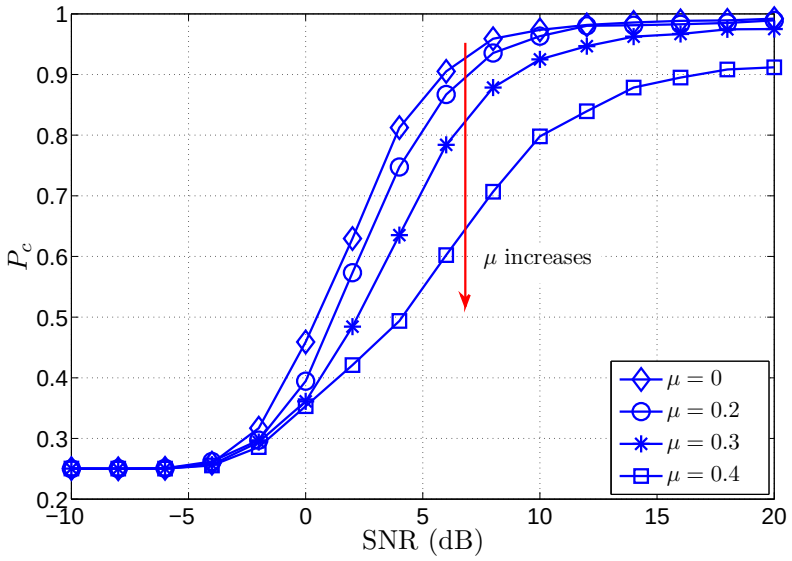

Fig. 3.7: Effect of the timing offset on P_c with QPSK modulation and $K = 8192$ over Nakagami-m fading channel, $m = 3$.

function (cdf) method [21], and an approximation of the Nakagami-m inverse cdf [21]. Fig. 3.8 shows the effect of the spatial correlation between transmitted antennas on the P_c for $\rho = 0, 0.5$, and 1. Note that a similar performance is obtained for $\rho = 0$ and 0.5, while the performance slightly improves for $\rho = 1$. This is because the performance is basically controlled by the absolute values of the DFT peaks, which are proportional to $(|h_i|^2|h_j|^2)$, $i, j = 0, 1, 2$, $i \neq j$, and $\mathrm{E}\{|h_i|^2|h_j|^2\}$ is a slowly increasing function of ρ [14].

3.5.8 Performance comparison

Fig. 3.9 compares P_c obtained with the proposed algorithm, the optimal likelihood-based algorithm in [11], and the second-order correlation-based algorithm in [12]. Note that the former requires estimation of the channel coefficients, noise power, and modulation type, and results are shown for perfect estimates of these parameters. As expected, under such a scenario, it provides the best performance. On the other hand, the proposed algorithm has no such requirements, which makes it suitable for practical applications. Moreover,

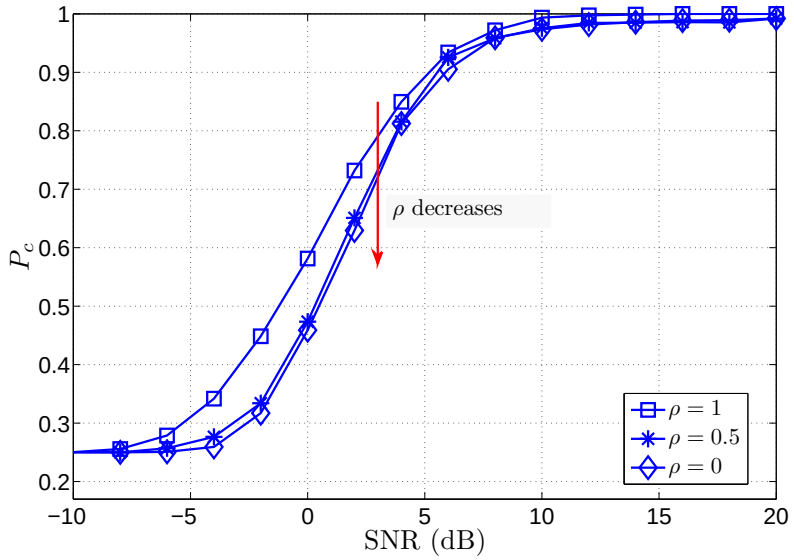

Fig. 3.8: Effect of the spatial correlation between transmitted antennas on P_c with QPSK modulation and $K = 8192$ over Nakagami-m fading channel, $m = 3$.

the computational cost measured by the required number of floating point operations (flops) [23] for the proposed algorithm is $47K + 10K \log_2 K$, which is significantly lower than $K(240M^2 + 640M^3 + 1652M^4)$ for the likelihood-based algorithm. For example, with QPSK modulation and $K = 8192$, the proposed algorithm needs only 1.45×10^6 flops, whereas the likelihood-based algorithm requires 3.83×10^9 flops. Furthermore, the proposed algorithm greatly outperforms the algorithm in [12], which achieves a $P_c = 0.5$ even for high SNR. This can be explained as the second-order correlation provides a discriminating feature for SM and STBC4 only. For AL and STBC3, it equals zero, leading to the mis-classification of these codes as they are considered as SM.

3.6 Conclusion

This paper proposed an algorithm for blind classification of space-time block codes (STBCs) using a single receive antenna. It was shown that the discrete Fourier transform (DFT)

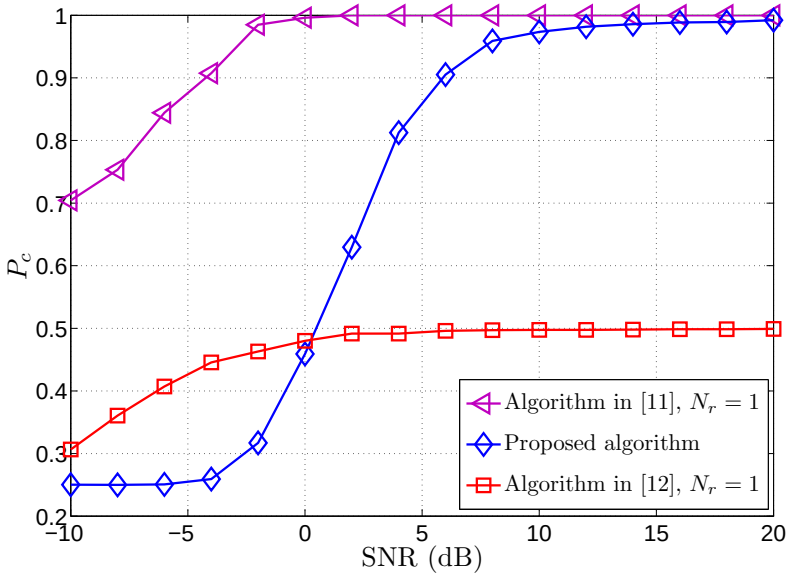

Fig. 3.9: Performance comparison of the proposed algorithm, the optimal likelihood-based algorithm in [11], and the second-order correlation-based algorithm in [12] with QPSK modulation and $K = 8192$ over Nakagami-m fading channel, $m = 3$.

of the fourth-order lag products (FOLPs) of the received signal provides a discriminating signal feature; a decision tree classification algorithm was developed based on this feature. The algorithm performance was evaluated through simulations in terms of average probability of correct classification. The results indicated the validity of the algorithm, with the advantages that it does not require channel estimation, is robust to carrier frequency offset, and exhibits a low sensitivity to timing offset. Moreover, it can benefit from spatially correlated fading.

References

[1] J. L. Xu, W. Su, and M. Zhou, "Software-defined radio equipped with rapid modulation recognition," *IEEE Trans. Veh. Technol.*, vol. 59, pp. 1659–1667, May 2010.

[2] T. Yucek and H. Arslan, "A survey of spectrum sensing algorithms for cognitive radio applications," *IEEE Commun. Surveys Tuts.*, vol. 11, pp. 116–130, Mar. 2009.

[3] O. A. Dobre, A. Abdi, Y. Bar-Ness, and W. Su, "Survey of automatic modulation classification techniques: Classical approaches and new trends," *IET Commun.*, vol. 1, pp. 137–156, Apr. 2007.

[4] L. Korowajczuk, *LTE, WiMAX and WLAN Network Design, Optimization and Performance Analysis.* Wiley, 2011.

[5] M. Shi, Y. Bar-Ness, and W. Su, "Adaptive estimation of the number of transmit antennas," in *Proc. IEEE MILCOM*, 2007, pp. 1–5.

[6] O. Somekh, O. Simeone, Y. Bar-Ness, and W. Su, "Detecting the number of transmit antennas with unauthorized or cognitive receivers in MIMO systems," in *Proc. IEEE MILCOM*, 2007, pp. 1–5.

[7] V. Choqueuse, S. Azou, K. Yao, and G. Burel, " Blind modulation recognition for MIMO systems," *J. Military Technical Academy Review*, vol. XIX, pp. 183–196, Jun. 2009.

[8] K. Hassan, I. Dayoub, W. Hamouda, C. N. Nzeza, and M. Berbineau, "Blind digital modulation identification for spatially-correlated MIMO systems," *IEEE Trans. Wireless Commun.*, vol. 11, pp. 683–693, Feb. 2012.

[9] M. S. Mühlhaus, M. Öner, O. A. Dobre, H. U. Jäkel, and F. K. Jondral, "Automatic modulation classification for MIMO systems using fourth-order cumulants," in *Proc. IEEE VTC(Fall)*, 2012, pp. 1–5.

[10] M. Muhlhaus, M. Oner, O. A. Dobre, H. Jakel, and F. K. Jondral, "A novel algorithm for mimo signal classification using higher-order cumulants," in *Proc. IEEE RWS*, 2013, pp. 7–9.

[11] V. Choqueuse, M. Marazin, L. Collin, K. C. Yao, and G. Burel, "Blind recognition of linear space–time block codes: A likelihood-based approach," *IEEE Trans. Signal Process.*, vol. 58, pp. 1290–1299, Mar. 2010.

[12] V. Choqueuse, K. Yao, L. Collin, and G. Burel, "Hierarchical space-time block code recognition using correlation matrices," *IEEE Trans. Wireless Commun.*, vol. 7, pp. 3526–3534, Sep. 2008.

[13] V. Choqueuse, K. Yao, L. Collin, and G. Burel, "Blind recognition of linear space time block codes," in *Proc. IEEE ICASSP*, 2008, pp. 2833–2836.

[14] Y. A. Eldemerdash, M. Marey, O. A. Dobre, G. Karagiannidis, and R. Inkol, "Fourth-order statistics for blind classification of spatial multiplexing and Alamouti space-time block code signals," *IEEE Trans. Commun.*, vol. 61, pp. 2420–2431, Jun. 2013.

[15] M. DeYoung, R. Heath, and B. Evans, "Using higher order cyclostationarity to identify space-time block codes," in *Proc. IEEE GLOBECOM*, 2008, pp. 1–5.

[16] M. Shi, Y. Bar-Ness, and W. Su, "STC and BLAST MIMO modulation recognition," in *Proc. IEEE GLOBECOM*, 2007, pp. 3034–3039.

[17] M. Marey, O. A. Dobre, and R. Inkol, "Classification of space-time block codes based on second-order cyclostationarity with transmission impairments," *IEEE Trans. Wireless Commun.*, vol. 11, pp. 2574–2584, Jul. 2012.

[18] E. Larsson and P. Stoica, *Space-Time Block Coding for Wireless Communication*. Cambridge Press, 2003.

[19] V. Tarokh, H. Jafarkhani, and A. R. Calderbank, "Space-time block codes from orthogonal designs," *IEEE Trans. Inf. Theory*, vol. 45, pp. 1456–1467, Jul. 1999.

[20] A. Papoulis and S. Pillai, *Probability, Random Variables and Stochastic Processes*. McGraw-Hill, 2001.

[21] N. C. Beaulieu and C. Cheng, "Efficient Nakagami-m fading channel simulation," *IEEE Trans. Veh. Technol.*, vol. 54, pp. 413–424, Mar. 2005.

[22] M. E. Johnson, *Multivariate Statistical Simulation*. Wiley, 1987.

[23] D. Watkins, *Fundamentals of Matrix Computations*. Wiley, 2002.

Chapter 4

Blind Identification of SM and Alamouti STBC-OFDM Signals

4.1 Abstract

This paper proposes an efficient identification algorithm for spatial multiplexing (SM) and Alamouti (AL) coded orthogonal frequency division multiplexing (OFDM) signals. The cross-correlation between the received signals from different antennas is exploited to provide a discriminating feature to identify SM-OFDM and AL-OFDM signals. The proposed algorithm requires neither estimation of the channel coefficients and noise power, nor the modulation of the transmitted signal. Moreover, it does not need space-time block code (STBC) or OFDM block synchronization. The effectiveness of the proposed algorithm is demonstrated through extensive simulation experiments in the presence of diverse transmission impairments, such as time and frequency offsets, Doppler frequency, and spatially correlated fading.

4.2 Introduction

Blind signal identification plays an important role in various military and commercial applications, including electronic warfare, radio surveillance, software defined radio, and spectrum awareness in cognitive radio [1–3]. For example, in software defined radio the transmitter provides a flexible architecture, in which the same hardware can be used for different transmission parameters, e.g., modulation format, coding rate, and antenna configuration. Accordingly, algorithms are required at the receive-side to blindly estimate these signal parameters [3].

Numerous studies have addressed the problem of blind signal identification in single-input single-output scenarios. These include identification of the modulation format [4–8], single- versus multi-carrier transmissions [9], the type of multi-carrier technique [10, 11], and channel encoders [12–14], as well as blind parameter estimation [9, 15]. Recently, multiple-input multiple-output (MIMO) technology has been adopted by different wireless standards, such as IEEE 802.11n, IEEE 802.16e, and 3GPP LTE [16]. However, the study of MIMO signal identification is at an early stage. For example, estimation of the number of transmit antennas has been investigated in [17, 18], modulation identification in [19–21], and space-time block code (STBC) identification in [22–27]. All these studies considered single-carrier transmission over frequency-flat fading. However, in practice high data rate applications necessitate transmissions over frequency-selective channels; hence, the assumption of frequency-flat fading is not practically accepted. Additionally, the orthogonal frequency division multiplexing (OFDM) technique has been adopted as the main transmission scheme over frequency-selective fading channels [16]. Therefore, investigating the problem of MIMO-OFDM signal identification becomes a practically required challenge. Recently, this problem has been explored in [28–31]: modulation identification for spatial multiplexing (SM)-OFDM was studied in [28] and STBC-OFDM signal identification was considered in [29–31], with the latter being relevant for our work.

The identification algorithm proposed in [29, 30] requires a large observation period to achieve a good identification performance and suffers from high sensitivity to frequency offset. In addition to these drawbacks, the algorithm in [31] is applicable only for a reduced number of OFDM subcarriers.

In this paper, we propose an efficient algorithm to blindly identify Alamouti (AL)-OFDM and SM-OFDM signals[1]. A novel cross-correlation is defined for the received sequences with re-arranged blocks, which provides a powerful discriminating feature. Additionally, a novel criterion of decision is developed based on the statistical properties of the feature estimate. The proposed algorithm does not require information about the channel, modulation format, noise power, or timing synchronization. Moreover, it has the advantage of providing a good identification performance with a short observation period and for various numbers of OFDM subcarriers, as well as of being relatively robust to the frequency offset.

The rest of this paper is organized as follows. Section 4.3 introduces the system model. Section 4.4 describes the proposed identification algorithm. Simulation results are presented in Section 4.5. Finally, concluding remarks are drawn in Section 4.6.

4.3 System Model

We consider a MIMO-OFDM system with two transmit antennas, which employs either an AL or SM encoder, as shown in Fig. 4.1 [32]. The data symbols, which are randomly and independently drawn from an M-point constellation, $M \geq 4$, are considered as blocks of length N. These are fed to the encoder, whose output is $[\ \boldsymbol{c}_{2b+0}^{(0)} \quad \boldsymbol{c}_{2b+1}^{(0)};\quad \boldsymbol{c}_{2b+0}^{(1)} \quad \boldsymbol{c}_{2b+1}^{(1)}\ ]$ for AL-OFDM and $[\ \boldsymbol{c}_{b+0}^{(0)};\quad \boldsymbol{c}_{b+0}^{(1)}\ ]$ for SM-OFDM. The notation $\boldsymbol{c}_{Ub+u}^{(f)} = [c_{Ub+u}^{(f)}(0), ..., c_{Ub+u}^{(f)}(N-$

[1]Note that we assume that the received signal is either AL-OFDM or SM-OFDM. The AL and SM STBCs are considered, as they are commonly used in various wireless standards, such as IEEE 802.11n, IEEE 802.16e, and 3GPP LTE [16].

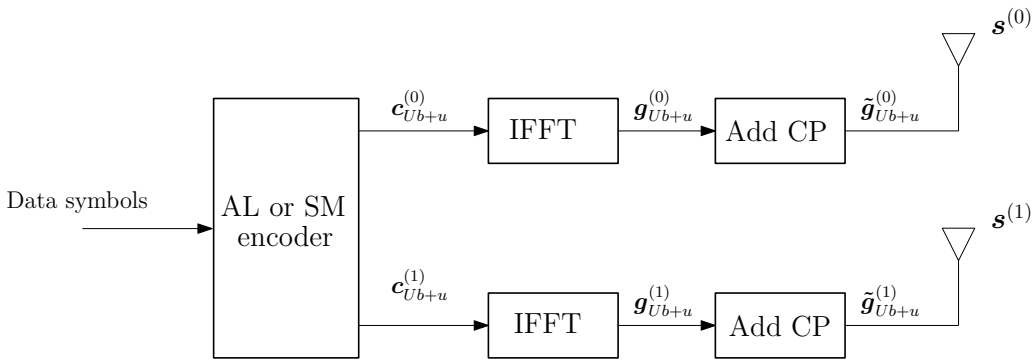

Fig. 4.1: Block diagram of a MIMO-OFDM transmitter [32].

1)] is used to represent the $(Ub+u)$th data block of N symbols from the fth antenna, $f = 0, 1$, with b as the STBC block index, U as the length of the STBC block ($U = 2$ for AL and $U = 1$ for SM), and u as the slot index within an STBC block, $u = 0, 1, ..., U-1$. For AL-OFDM, the data blocks have the property that [29]: $\boldsymbol{c}^{(1)}_{2b+1} = (\boldsymbol{c}^{(0)}_{2b+0})^*$ and $\boldsymbol{c}^{(0)}_{2b+1} = -(\boldsymbol{c}^{(1)}_{2b+0})^*$, where $*$ denotes complex conjugate.

Each block $\boldsymbol{c}^{(f)}_{Ub+u}$ is input to an N-point inverse fast Fourier transform (N-IFFT), leading to the time-domain block $\boldsymbol{g}^{(f)}_{Ub+u} = [g^{(f)}_{Ub+u}(0),\ g^{(f)}_{Ub+u}(1), ..., g^{(f)}_{Ub+u}(N-1)]$. Then, a cyclic prefix of length ν is added, with the resulting OFDM block written as $\tilde{\boldsymbol{g}}^{(f)}_{Ub+u} = [\tilde{g}^{(f)}_{Ub+u}(0), ..., \tilde{g}^{(f)}_{Ub+u}(\nu), \tilde{g}^{(f)}_{Ub+u}(\nu+1), ..., \tilde{g}^{(f)}_{Ub+u}(N+\nu-1)] = [g^{(f)}_{Ub+u}(N-\nu), ..., g^{(f)}_{Ub+u}(0),\ g^{(f)}_{Ub+u}(1), ..., g^{(f)}_{Ub+u}(N-1)]$. Accordingly, the time-domain samples of the OFDM block can be expressed as

$$\tilde{g}^{(f)}_{Ub+u}(n) = \frac{1}{\sqrt{N}} \sum_{p=0}^{N-1} c^{(f)}_{Ub+u}(p) e^{\frac{j2\pi p(n-\nu)}{N}}, \quad n = 0, 1, .., N+\nu-1. \tag{4.1}$$

With the transmit sequence from the fth antenna as $\boldsymbol{s}^{(f)} = \left[...\tilde{\boldsymbol{g}}^{(f)}_{-1}, \tilde{\boldsymbol{g}}^{(f)}_{0}, \tilde{\boldsymbol{g}}^{(f)}_{1}, \tilde{\boldsymbol{g}}^{(f)}_{2}, ...\right]$, whose kth element is denoted by $s^{(f)}(k)$, the kth received sample at the ith receive antenna, $i = 0, 1, ..., N_r - 1$, can be expressed as [29]

$$r^{(i)}(k) = \sum_{f=0}^{1} \sum_{l=0}^{L_h-1} h_{fi}(l) s^{(f)}(k-l) + w^{(i)}(k), \tag{4.2}$$

where L_h is the number of propagation paths, $h_{fi}(l)$ is the channel coefficient corresponding to the lth path between the transmit antenna f and the receive antenna i, and $w^{(i)}(k)$ represents the complex additive white Gaussian noise (AWGN) at the ith receive antenna, with zero mean and variance σ_w^2.

4.4 Proposed algorithm

In this section, we investigate the second-order cross-correlation as a discriminating feature for AL-OFDM and SM-OFDM signal identification. Initially, we consider the $N_r = 2$ case, for which we explore the cross-correlation between $\{r^{(0)}(k)\}$ and $\{r^{(1)}(k)\}$ and develop a new decision criterion based on the statistical properties of the feature estimate. Then, we extend the analysis to the case of $N_r > 2$.

4.4.1 Cross-correlation properties ($N_r = 2$)

First, the cross-correlation properties for AL-OFDM and SM-OFDM signals are analyzed at the transmit-side, and then the analysis is extended to the receive-side.

Transmit-side

Let us form the sequence $\boldsymbol{s}^{(f,\tau)}$, whose components are given by $s^{(f,\tau)}(k) = s^{(f)}(k+\tau)$, $\tau = 0, 1, ..., N+\nu-1$. This is further divided into consecutive $(N+\nu)$-length blocks, i.e., $\boldsymbol{s}^{(f,\tau)} = [...\tilde{\boldsymbol{g}}_{-1}^{(f,\tau)}, \tilde{\boldsymbol{g}}_{0}^{(f,\tau)}, \tilde{\boldsymbol{g}}_{1}^{(f,\tau)}, ..., \tilde{\boldsymbol{g}}_{q-1}^{(f,\tau)}, \tilde{\boldsymbol{g}}_{q}^{(f,\tau)}, \tilde{\boldsymbol{g}}_{q+1}^{(f,\tau)}, ...]$, as it is graphically illustrated in Fig. 4.2.

Proposition 1. *For the AL-OFDM signal, the samples of the $(N+\nu)$-length blocks of the newly formed sequence $\boldsymbol{s}^{(f,\tau)}$ exhibits the following properties:*

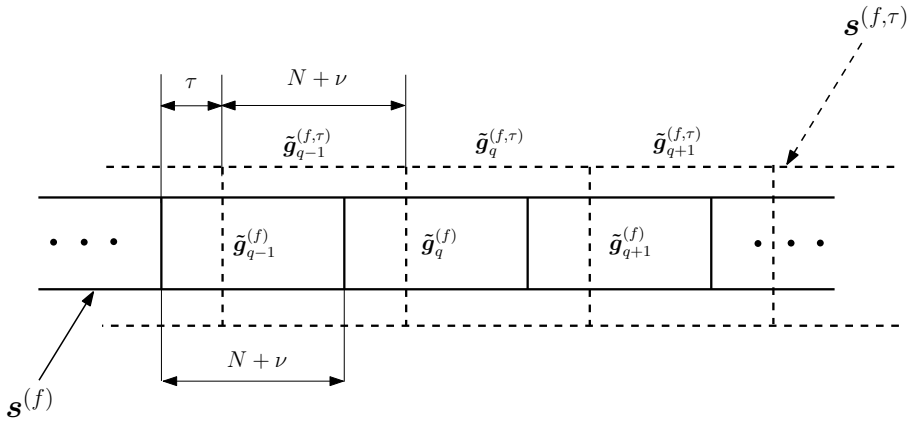

Fig. 4.2: Illustration of the relation between the $\boldsymbol{s}^{(f)}$ and $\boldsymbol{s}^{(f,\tau)}$ sequences. Solid lines are used to delimitate the OFDM blocks of $\boldsymbol{s}^{(f)}$, while dashed lines show the $(N+\nu)$-length blocks of $\boldsymbol{s}^{(f,\tau)}$.

- $\tau = 0$:

$$\tilde{g}_{2b+0}^{(0,0)}(n) = \tilde{g}_{2b+1}^{(1,0)^*}(mod(-(n-\nu), N) + \nu), \tag{4.3a}$$
$$n = 0, 1, ..., N+\nu-1,$$

- $\tau = N/2$:

$$\tilde{g}_{2b+0}^{(0,\frac{N}{2})}(n) = \tilde{g}_{2b+1}^{(1,\frac{N}{2})^*}(mod(-(n-\nu), N) + \nu), \tag{4.3b}$$
$$n = 0, 1, ..., \nu,$$

- $\tau = N/2 + \nu$:

$$\tilde{g}_{2b-1}^{(0,\frac{N}{2}+\nu)}(n) = \tilde{g}_{2b+0}^{(1,\frac{N}{2}+\nu)^*}(mod(-(n-\nu), N) + \nu), \tag{4.3c}$$
$$n = \tfrac{N}{2}, \tfrac{N}{2}+1, ..., \tfrac{N}{2}+2\nu.$$

Such properties do not hold for any other values of τ and n. Additionally, these are not valid for the SM-OFDM signal.

Proof: See Appendix. ■

Illustrative examples for *Proposition 1* are provided in Fig. 4.3 for the AL-OFDM signal with $N = 4$, $\nu = \frac{N}{4} = 1$, $\tau = 0$, $\tau = 2$ $(= \frac{N}{2})$, and $\tau = 3$ $(= \frac{N}{2} + \nu)$. Note that

n	$mod(-(n-\nu), N)+\nu$
0	2
1	1
2	4
3	3
4	2

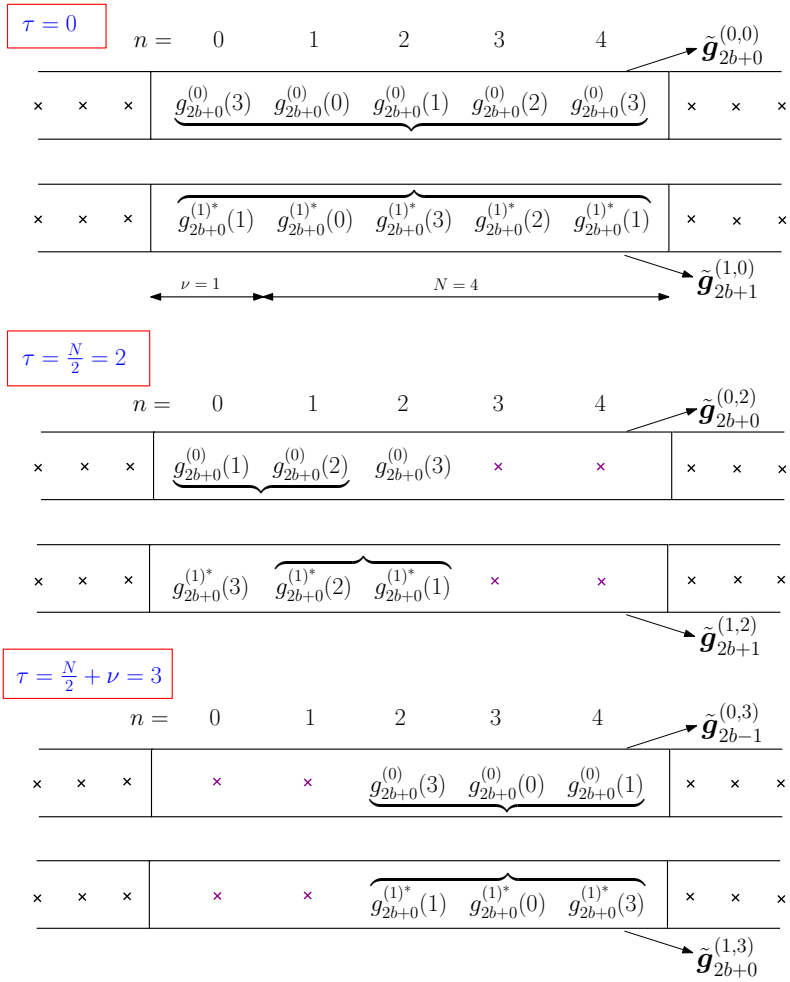

Fig. 4.3: Illustration of the cross-correlation between the $(N+\nu)$-length blocks, with $N = 4$ and $\nu = 1$, and for $\tau = 0, \frac{N}{2}, \frac{N}{2} + \nu$.

the vector components are written based on (4.23)-(4.29), given in the appendix, and by taking into account the relationship between $\tilde{\boldsymbol{g}}_{2b+u}^{(f)}$ and $\boldsymbol{g}_{2b+u}^{(f)}$. The uncorrelated and correlated samples are indicated by using '$\times$' and braces, respectively.

Based on results of *Proposition 1*, we define the following cross-correlation

$$\begin{aligned} R_g(\tau) = & \ \mathrm{E}\left\{\tilde{\boldsymbol{g}}_q^{(0,\tau)}\left[\bar{\boldsymbol{g}}_{q+1}^{(1,\tau)}\right]^T\right\} \\ & \triangleq \lim_{N_B\to\infty}\frac{1}{N_B}\sum_{q=0}^{N_B-1}\tilde{\boldsymbol{g}}_q^{(0,\tau)}\left[\bar{\boldsymbol{g}}_{q+1}^{(1,\tau)}\right]^T, \end{aligned} \tag{4.4}$$

where $\mathrm{E}\{.\}$ indicates the statistical expectation over the block, $\bar{\boldsymbol{g}}_{q+1}^{(1,\tau)}$ is an $(N+\nu)$-length block with components $\bar{g}_{q+1}^{(1,\tau)}(p) = \tilde{g}_{q+1}^{(1,\tau)}(mod(-(p-\nu), N)+\nu)$, $p = 0, 1, ..., N+\nu-1$, the superscript T denotes matrix transpose, and N_B is the number of blocks.

By using *Proposition 1*, one can easily see that for $\tau = 0, 1, ..., N+\nu-1$, the cross-correlation for AL-OFDM and SM-OFDM signals is respectively given by

$$R_g^{\mathrm{AL}}(\tau) = \begin{cases} \frac{1}{2}(N+\nu)\sigma_d^2, & \tau = 0, \\ \frac{1}{2}(\nu+1)\sigma_d^2, & \tau = \frac{N}{2}, \\ \frac{1}{2}(2\nu+1)\sigma_d^2, & \tau = \frac{N}{2}+\nu, \\ 0, & \text{otherwise}, \end{cases} \tag{4.5}$$

and

$$R_g^{\mathrm{SM}}(\tau) = 0, \tag{4.6}$$

where σ_d^2 is the variance of the modulated symbols[2]. Note that the factor $\frac{1}{2}$ in (4.5) is due to the fact that correlation exists only between the $(N+\nu)$-length blocks which belong to the same AL block. According to (4.5) and (4.6), $R_g(\tau)$ provides a feature for the identification of the AL-OFDM and SM-OFDM signals.

[2]Note that based on the Parseval's theorem, the variance of the modulated symbols is equal to the variance of the samples in the block $\boldsymbol{g}_{Ub+u}^{(f)}$ at the output of the IFFT.

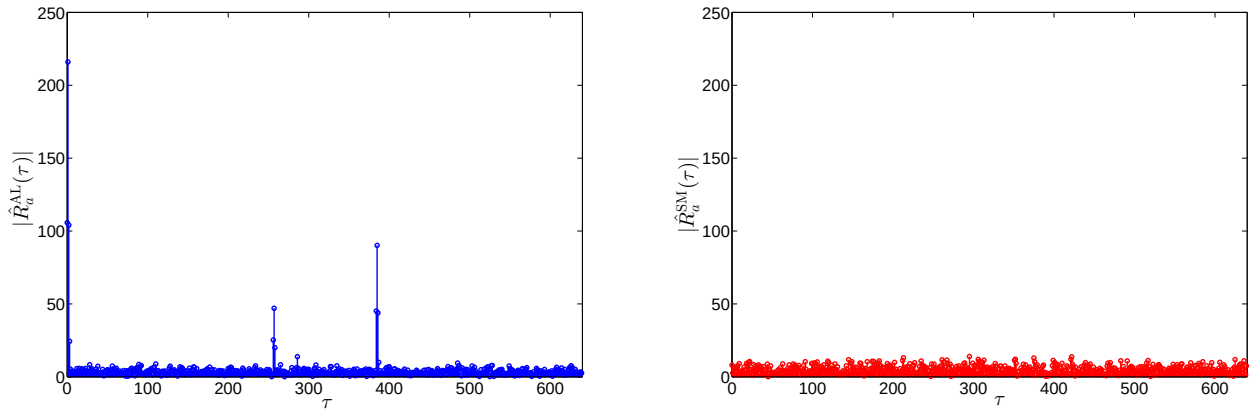

(a) (b)

Fig. 4.4: $|\hat{R}_a(\tau)|$ with QPSK modulation, $N = 512$, $\nu = N/4$, and $N_B = 100$, at SNR = 10 dB over multipath Rayleigh fading channel, $L_h = 4$, for (a) AL-OFDM and (b) SM-OFDM signals.

Receive-side

Without loss of generality, we assume that the first intercepted sample corresponds to the start of an OFDM block; later in the paper, we will relax this assumption. Let us define the sequence $\boldsymbol{r}^{(i,\tau)}$, whose components are given by $r^{(i,\tau)}(k) = r^{(i)}(k+\tau)$, $\tau = 0, 1, ..., N+\nu-1$, and further divide it into $(N+\nu)$-length[3] blocks, i.e., $\boldsymbol{r}^{(i,\tau)} = [..., \boldsymbol{a}_{-1}^{(i,\tau)}, \boldsymbol{a}_0^{(i,\tau)}, \boldsymbol{a}_1^{(i,\tau)}, ...]$, where $\boldsymbol{a}_q^{(i,\tau)} = [a_q^{(i,\tau)}(0), ..., a_q^{(i,\tau)}(N+\nu-1)]$, with $a_q^{(i,\tau)}(p) = r^{(i,\tau)}(q(N+\nu)+p)$, $p = 0, 1, ..., N+\nu-1$.

By using (4.2), the definition of the correlation in (4.4), (4.5), and (4.6), and taking into account the independence between the transmitted data symbols, noise, and channel coefficients, for $\tau = 0, 1, ..., N+\nu-1$ it is straightforward to show that

[3]We assume that the OFDM block length is known. Different algorithms in the literature, e.g., [33], can be combined with the proposed algorithm to blindly estimate the OFDM block length.

$$R_a^{\mathrm{AL}}(\tau) = \mathrm{E}\left\{\tilde{\boldsymbol{a}}_q^{(0,\tau)}\left[\bar{\boldsymbol{a}}_{q+1}^{(1,\tau)}\right]^T\right\}$$

$$= \begin{cases} \frac{\sigma_d^2}{2}(N+\nu)\Xi(\tau), & \tau = 0,1,...,L_h-1, \\ \frac{\sigma_d^2}{2}(\nu+1)\Xi(\tau-\frac{N}{2}), & \tau = \frac{N}{2}, \frac{N}{2}+1, ..., \\ & \frac{N}{2}+L_h-1, \\ \frac{\sigma_d^2}{2}(2\nu+1)\Xi(\tau-\frac{N}{2}-\nu), & \tau = \frac{N}{2}+\nu, \frac{N}{2}+\nu+1, \\ & ..., \frac{N}{2}+\nu+L_h-1, \\ 0, & \text{otherwise}, \end{cases} \tag{4.7}$$

and

$$R_a^{\mathrm{SM}}(\tau) = 0, \tag{4.8}$$

where $\Xi(\tau) = \sum_{l,l'=0}^{L_h-1}(h_{00}(l)h_{11}(l') - h_{10}(l)h_{01}(l'))\delta(2\tau - l - l')$.

Fig. 4.4 shows the absolute value of the estimated cross-correlation, $|\hat{R}_a(\tau)|$, $\tau = 0, 1, ..., N+\nu-1$, for both AL-OFDM and SM-OFDM signals with QPSK modulation, $N = 512$, $\nu = N/4$, and $N_B = 100$ over multipath Rayleigh fading channel with $L_h = 4$ at SNR=10 dB. Note that the limited observation period results in non-zero, but statistically non-significant values for $|R_a^{\mathrm{AL}}(\tau)|$ and $|R_a^{\mathrm{SM}}(\tau)|$ at the null positions. The existence of the statistically significant peaks in $|R_a^{\mathrm{AL}}(\tau)|$ will be used as a discriminating feature to identify AL-OFDM and SM-OFDM signals. It is worthy to mention that the first received sample does not have to correspond to the start of an OFDM block. In such a case, the peaks in Fig. 4.4 (a) will be cyclically shifted by the number of samples corresponding to the delay between the first received sample and the start of the first received OFDM block, which does not affect the discriminating feature.

4.4.2 Discriminating feature and decision criterion ($N_r = 2$ case)

The identification of AL-OFDM and SM-OFDM signals relies on detecting whether statistically significant peaks are present or not in $|\hat{R}_a(\tau)|$, $\tau = 0, 1, ..., N + \nu - 1$. This can be formulated as a binary hypothesis testing problem, where under hypothesis $\mathcal{H}_0$ (no peaks are detected) SM-OFDM is decided to be the received signal, whereas AL-OFDM signal is selected under hypothesis $\mathcal{H}_1$ (peaks are detected). Here we propose a statistical test to detect the peak presence.

Without loss of generality, we assume that the number of observed samples, K, corresponds to an integer number of OFDM blocks, $N_B = \frac{K}{N+\nu}$ [4]. In this case, $R_a(\tau)$ can be estimated as

$$\hat{R}_a(\tau) = \frac{1}{N_B} \sum_{q=0}^{N_B-1} \boldsymbol{a}_q^{(0,\tau)} \left[\bar{\boldsymbol{a}}_{q+1}^{(1,\tau)}\right]^T. \tag{4.9}$$

Following [34], $\hat{R}_a(\tau)$ can be represented as

$$\hat{R}_a(\tau) = R_a(\tau) + \psi(\tau), \tag{4.10}$$

where $\psi(\tau)$ is a zero-mean random variable representing the estimation error, which vanishes asymptotically ($N_B \to \infty$). As shown in (4.7), under the assumption that the first received sample corresponds to the start of an OFDM block, $R_a^{\mathrm{AL}}(\tau)$ exhibits L_h peaks around $\tau = 0, \frac{N}{2}$, and $\frac{N}{2} + \nu$. In general, if the first received sample corresponds to the τ_0th point in the OFDM block, the peaks in $R_a^{\mathrm{AL}}(\tau)$ will be around $\tau = \tau_0$, $\tau = \tau_1 = mod(\tau_0 + \frac{N}{2}, N + \nu)$, and $\tau = \tau_2 = mod(\tau_0 + \frac{N}{2} + \nu, N + \nu)$.

[4] If this not the case, zeros can be added after the observed samples to ensure this relation. Additionally, it is worth noting that the number of received blocks used for signal identification, N_B, is finite.

Based on (4.7), (4.10) can be written for the AL-OFDM signal as

$$\hat{R}_a^{\mathrm{AL}}(\tau) = R_a^{\mathrm{AL}}(\tau) + \psi^{\mathrm{AL}}(\tau), \tag{4.11}$$

where $R_a^{\mathrm{AL}}(\tau)$ is non-zero for $\tau \in \Omega_0$, $\Omega_0 = \{\tau_0, \tau_0+1, ..., \tau_0+L_h-1\} \cup \{\tau_1, \tau_1+1, ..., \tau_1+L_h-1\} \cup \{\tau_2, \tau_2+1, ..., \tau_2+L_h-1\}$.

Furthermore, based on (4.8), (4.10) can be written for the SM-OFDM signal as

$$\hat{R}_a^{\mathrm{SM}}(\tau) = \psi^{\mathrm{SM}}(\tau), \ \forall \tau = 0, 1, ..., N+\nu-1. \tag{4.12}$$

As such, if $R_a(\tau) \neq 0$ [5] for at least one value of τ, the AL-OFDM signal is declared present ($\mathcal{H}_1$ is true); otherwise, the SM-OFDM signal is declared present ($\mathcal{H}_0$ is true). The proposed statistical test detects the presence of the non-zero value of $R_a(\tau)$ as follows. For $\tau = 0, 1, ..., N+\nu-1$, we define τ_p as the value of τ that maximizes $|\hat{R}_a(\tau)|$,

$$\tau_p = \arg\max_{\tau} |\hat{R}_a(\tau)|. \tag{4.13}$$

Based on the results provided in (4.7), one can notice that for the AL-OFDM signal, τ_p will take values in the set $\{\tau_0, \tau_0+1, ..., \tau_0+L_h-1\}$. Depending on the τ_p value within this range, in order to eliminate all possible peak positions, we consider the set $\Omega_p = \{\tau_p - L_h + 1, ..., \tau_p, ..., \tau_p + L_h - 1\} \cup \{\tau_{p1} - L_h + 1, ..., \tau_{p1}, ..., \tau_{p1} + L_h - 1\} \cup \{\tau_{p2} - L_h + 1, ..., \tau_{p2}, ..., \tau_{p2} + L_h - 1\}$, with $\tau_{p1} = mod(\tau_p + \frac{N}{2}, N+\nu)$ and $\tau_{p2} = mod(\tau_p + \frac{N}{2} + \nu, N+\nu)$. As such, $R_a(\tau) = 0$ for both AL-OFDM and SM-OFDM signals for the delay range $\tau \notin \Omega_p$, $\tau = 0, 1, ..., N+\nu-1$. This result will be used in the definition of the test statistic to avoid the statistically significant peaks.

When the SM-OFDM signal is received (under hypothesis $\mathcal{H}_0$), $\hat{R}_a(\tau) = \psi(\tau)$ has an asymptotic complex Gaussian distribution with zero-mean and variance σ^2 [34, 35].

[5] Henceforth, the superscript AL or SM is dropped in the cross-correlation, as this is not known at the receive-side.

Therefore, the normalized cross-correlation, $\sqrt{\frac{2}{\sigma^2}}\hat{R}_a(\tau)$, asymptotically follows a complex Gaussian distribution with zero-mean and variance equal to 2. Based on that, we define the function $\mathcal{F}(\tau)$ as

$$\mathcal{F}(\tau) = \frac{2|\hat{R}_a(\tau)|^2}{\frac{1}{N+\nu-\overline{\overline{\Omega}}_p}\sum_{\tau' \notin \Omega_p} |\hat{R}_a(\tau')|^2}, \tag{4.14}$$

where $\overline{\overline{\Omega}}_p$ is the cardinality of the set Ω_p.[6] Note that the denominator in (4.14) is an estimate of the variance of $\hat{R}_a(\tau)$ under hypothesis $\mathcal{H}_0$, which converges to σ^2 when N goes to infinity. As such, $\mathcal{F}(\tau)$ has an asymptotic chi-square distribution with two degrees of freedom under hypothesis $\mathcal{H}_0$ [36]. Accordingly, we define the test statistic Υ as

$$\Upsilon = \max \mathcal{F}(\tau), \quad \tau = 0, 1, ..., N+\nu-1. \tag{4.15}$$

Then we set a threshold, η, to yield a desired probability of false alarm, P_{fa}, i.e., $P_{fa} = P(\mathcal{H}_1|\mathcal{H}_0) = P(\Upsilon \geq \eta)$. Using the expression of the cumulative distribution function (CDF) of the chi-square distribution with two degrees of freedom [36], we can find that

$$P(\Upsilon < \eta) = (1 - e^{\frac{-\eta}{2}})^{(N+\nu)}. \tag{4.16}$$

Since $P_{fa} = 1 - P(\Upsilon < \eta)$, the threshold, η, can be calculated for a given P_{fa} as

$$\eta = -2\ln(1 - (1 - P_{fa})^{\frac{1}{N+\nu}}). \tag{4.17}$$

Finally, if $\Upsilon \geq \eta$, the AL-OFDM signal is decided to be received; otherwise, the SM-OFDM signal is selected. A summary of the proposed identification algorithm is given below.

[6]Note that in a practical implementation of the algorithm, knowledge of L_h is not required; a reasonably large value is considered. However, this is significantly low when compared to $N + \nu$ and does not affect the algorithm performance.

Summary of the proposed identification algorithm ($N_r = 2$)

Required signal pre-processing: Estimation of the OFDM block length ($N + \nu$).
Input: The observed K samples from two receive antennas $\left\{r^{(0)}(k)\right\}_{k=0}^{K-1}$ and $\left\{r^{(1)}(k)\right\}_{k=0}^{K-1}$.
- Estimate the cross-correlation $R_a(\tau)$, $\tau = 0, 1, ..., N + \nu - 1$, using (4.9).
- Compute Υ using (4.14) and (4.15).
- Compute η using (4.17) based on the target P_{fa}.
if $\Upsilon \geq \eta$ **then**
- the AL-OFDM signal is declared present ($\mathcal{H}_1$ true).
else
- the SM-OFDM signal is declared present ($\mathcal{H}_0$ true).
end if

4.4.3 Discriminating feature and decision criterion ($N_r > 2$ case)

In the previous section we considered two receive antennas ($N_r = 2$); here, we generalize the proposed identification algorithm to $N_r > 2$. Basically, the cross-correlations between each pair of the receive antennas will be combined to improve the discriminating feature. Similar to (4.9), the cross-correlation between the ith and jth receive antennas, $\hat{R}_{a,i,j}(\tau), i = 0, 1, ..., N_r - 2$, $j = i + 1, i + 2, ..., N_r - 1$, can be estimated as

$$\hat{R}_{a,i,j}(\tau) = \frac{1}{N_B} \sum_{q=0}^{N_B-1} \boldsymbol{a}_q^{(i,\tau)} \left[\bar{\boldsymbol{a}}_{q+1}^{(j,\tau)}\right]^T. \tag{4.18}$$

For each pair of receive antennas, the function $\mathcal{F}_{i,j}(\tau)$, $\tau = 0, 1, ..., N + \nu - 1$, is calculated as

$$\mathcal{F}_{i,j}(\tau) = \frac{2|\hat{R}_{a,i,j}(\tau)|^2}{\frac{1}{N+\nu-\overline{\overline{\Omega}}_{p,i,j}} \sum\limits_{\tau \notin \Omega_{p,i,j}} |\hat{R}_{a,i,j}(\tau)|^2}, \tag{4.19}$$

and the functions for all pairs of receive antennas are combined as

$$\mathcal{F}_c(\tau) = \sum_{i=0}^{N_r-2} \sum_{j=i+1}^{N_r-1} \mathcal{F}_{i,j}(\tau). \tag{4.20}$$

Accordingly, the test statistic is defined as

$$\Upsilon = \max \mathcal{F}_c(\tau). \tag{4.21}$$

As $\mathcal{F}_{i,j}(\tau)$ has an asymptotic chi-square distribution with two degrees of freedom under hypothesis $\mathcal{H}_0$, $\mathcal{F}_c(\tau)$ asymptotically follows the chi-square distribution with $2N_c$ degrees of freedom, where $N_c = \frac{N_r(N_r-1)}{2}$ is the number of pairs of the receive antennas. Hence, for a certain $P_{fa} = P(\mathcal{H}_1|\mathcal{H}_0) = P(\Upsilon \geq \eta)$ we set the threshold based on the CDF of this chi-square distribution, i.e.,

$$(1 - P_{fa})^{\frac{1}{N+\nu}} = \frac{\gamma(N_c, \eta/2)}{(N_c - 1)!}, \tag{4.22}$$

where $\gamma(\centerdot, \centerdot)$ is the lower incomplete Gamma function [37]. Note that for $N_r = 2$, the threshold, η, in (4.22) can be expressed as in (4.17). On the other hand, for $N_r > 2$, the threshold η cannot be expressed in a closed form; in such cases, this is numerically calculated for a certain P_{fa} using the bisection method [38].

4.4.4 Computational complexity

The computational complexity of the proposed algorithm is measured by the required number of floating point operations (flops) [39], which can be easily found to be equal to $N_c(6N_B(N+\nu)^2 + (2N_B+4)(N+\nu))$. For example, with $N = 256$, $\nu = \frac{N}{4}$, $N_r = 2$, and $N_B = 100$, the proposed algorithm requires 61,505,280 flops. Practically speaking, a microprocessor with 79.992 Giga-flops[7] can perform the calculations needed for the proposed algorithm in approximately 769 μsec.

[7][online], available: http://download.intel.com/support/processors/corei7/sb/core_i7-900_d.pdf

4.5 Simulation results

4.5.1 Simulation setup

The identification performance of the proposed algorithm was evaluated using Monte Carlo simulations with 1000 trials for each signal type. The OFDM signals are generated based on the IEEE 802.11e standard, with a useful OFDM block duration of 91.4 μsec and a subcarrier spacing of 10.94 kHz. Unless otherwise mentioned, the modulation was QPSK, the number of OFDM subcarriers $N = 256$ (2.5 MHz double-sided bandwidth), the cyclic prefix $\nu = N/4$, the number of observed OFDM blocks $N_B = 100$, the number of receive antennas $N_r = 2$, and the probability of false alarm $P_{fa} = 10^{-3}$. Furthermore, the received signal was affected by a frequency selective Rayleigh fading channel[8] consisting of $L_h = 4$ statistically independent taps, with an exponential power delay profile [40], $\sigma^2(l) = \exp(-l/5)$, where $l = 0, ..., L_h - 1$. A Butterworth filter was used at the receive-side to remove the out-of-band noise, and the SNR was considered at the output of this filter. The average probability of correct identification, $P_c = 0.5(P(\lambda = \text{AL}|\text{AL}) + P(\lambda = \text{SM}|\text{SM}))$, was employed as a performance measure, where λ is the estimated signal type.

4.5.2 Performance evaluation

Fig. 4.5 shows the performance of the proposed algorithm in comparison with that in [29] for different numbers of OFDM subcarriers, N. Apparently, the proposed algorithm outperforms the algorithm in [29], which basically fails; the reason is that the latter requires a large number of OFDM blocks to estimate the discriminating feature, e.g., simulation results show that $N_B = 10,000$ is needed to reach $P_c \approx 1$ at SNR = -4 dB.

In terms of computational complexity, the algorithm in [29] requires $(N+\nu)(8N_B+4)$

[8]While a Rayleigh fading channel is considered here, it is worth noting that a similar performance is achieved under multipath Nakagami-m fading conditions, as the distribution of the test statistic is similar under diverse channel conditions, as shown by simulations.

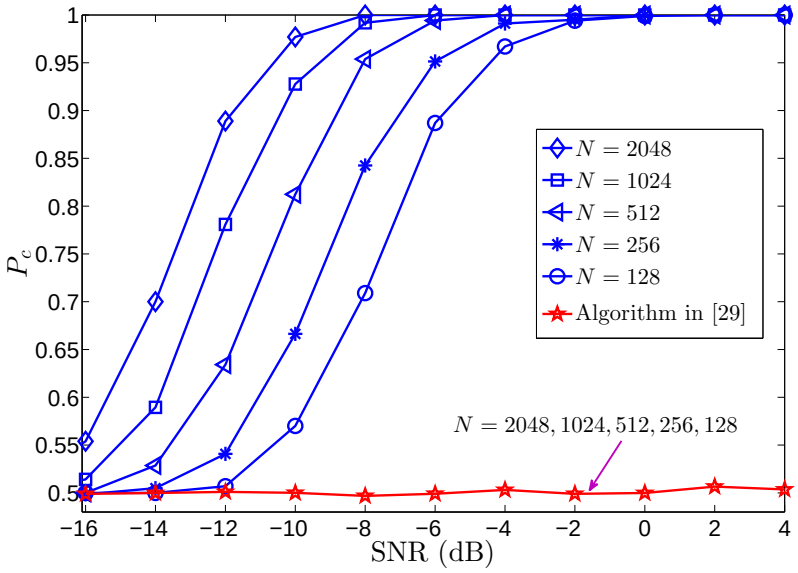

Fig. 4.5: Performance comparison between the proposed algorithm and the one in [29] for various numbers of OFDM subcarriers, N, with $N_B = 100$.

flops. If we compare the complexity of this algorithm and the proposed algorithm for given values of N_B, N, ν, and N_r, the algorithm in [29] is less computationally demanding. For example, for $N_B = 100$, $N = 256$, $\nu = N/4$, and $N_r = 2$, the former requires 257,280 flops, while the latter needs 61,505,280 flops. However, such a complexity comparison is not fair due to the difference in performance (as discussed above, based on results in Fig. 4.5). If we consider the N_B values for which the algorithms reach $P_c \approx 1$ at a given SNR, along with the fact that the time to make a decision consists of both observation and computing times, then it can be easily found that the algorithm in [29] requires a longer time for decision. For example, when a microprocessor with 79.992 Giga-flops is employed for computation, the algorithm in [29] needs 1.1428 sec to make a decision with $P_c \approx 1$ at SNR= -4 dB ($N_B = 10,000$), whereas the proposed algorithm requires only 12.194 $m$sec ($N_B = 100$).

Furthermore, it can be observed from Fig. 4.5 that the identification performance of the proposed algorithm significantly improves by increasing N. This is because the peak

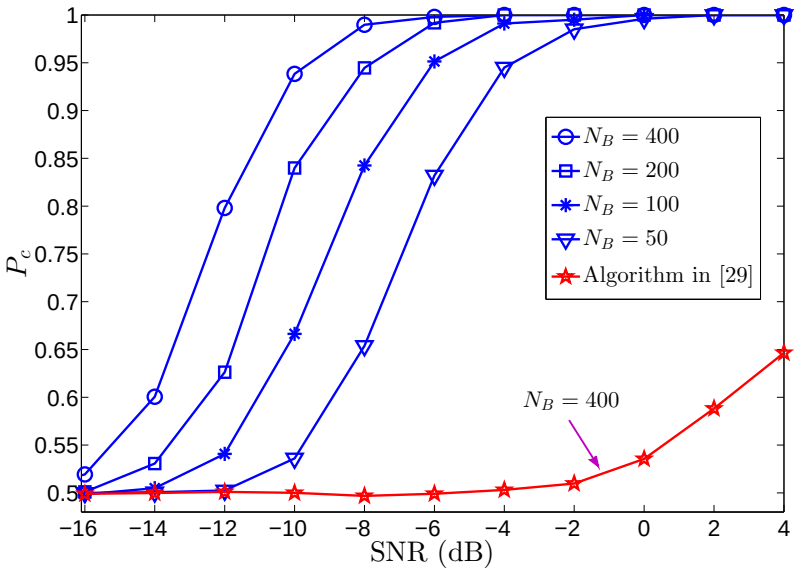

Fig. 4.6: The effect of the number of OFDM blocks, N_B, on the average probability of correct identification, P_c.

values in $|R_a^{\mathrm{AL}}(\tau)|$ are significantly enhanced, i.e., $|R_a^{\mathrm{AL}}(\tau)|$ is proportional to $(N+\nu)$ as can be noticed from (4.7). This reflects on the discriminating feature and leads to identification performance improvement.

4.5.3 Effect of the number of OFDM blocks

Fig. 4.6 shows the effect of the number of OFDM blocks, N_B, on the average probability of correct identification, P_c. A comparison with the algorithm in [29] for $N_B = 400$ is also included. As expected, increasing N_B enhances the performance of the proposed algorithm, as it leads to a better estimate of the cross-correlation, $\hat{R}_a(\tau)$. Note that the proposed algorithm provides an excellent performance ($P_c \approx 1$) at SNR = 0 dB and with a small number of blocks, $N_B = 50$, whereas the algorithm in [29] does not achieve a good performance even for $N_B = 400$.

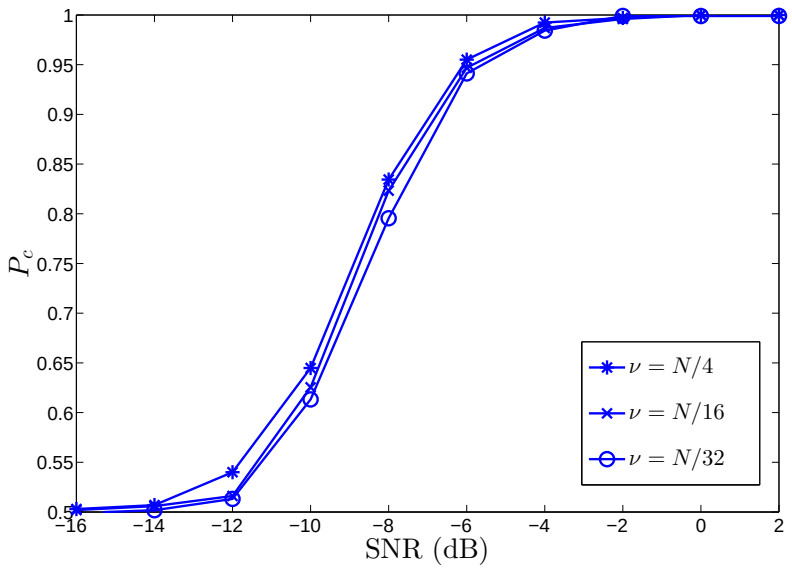

Fig. 4.7: The effect of the cyclic prefix length, ν, on the average probability of correct identification, P_c.

4.5.4 Effect of the cyclic prefix length

Fig. 4.7 shows the average probability of correct identification, P_c, for $\nu = N/4$, $N/16$, and $N/32$. One can notice that the performance slightly improves by increasing ν; this is because under the $\mathcal{H}_1$ hypothesis (the AL-OFDM signal), the peak values in $|\hat{R}_a^{\mathrm{AL}}(\tau)|$ slightly increase with ν. It is worth noting that the improvement obtained by increasing N is more significant, as was seen in Fig. 4.5.

4.5.5 Effect of the number of receive antennas

Fig. 4.8 illustrates the effect of the number of receive antennas, N_r, on the average probability of correct identification, P_c. It can be seen that the identification performance is improved by increasing N_r. For example, with $N_r = 5$, an excellent performance is obtained at SNR $= -10$ dB, when compared with SNR $= -2$ dB for $N_r = 2$. However, the computational complexity increases by a factor of 10, according to results presented in Section 4.4.4.

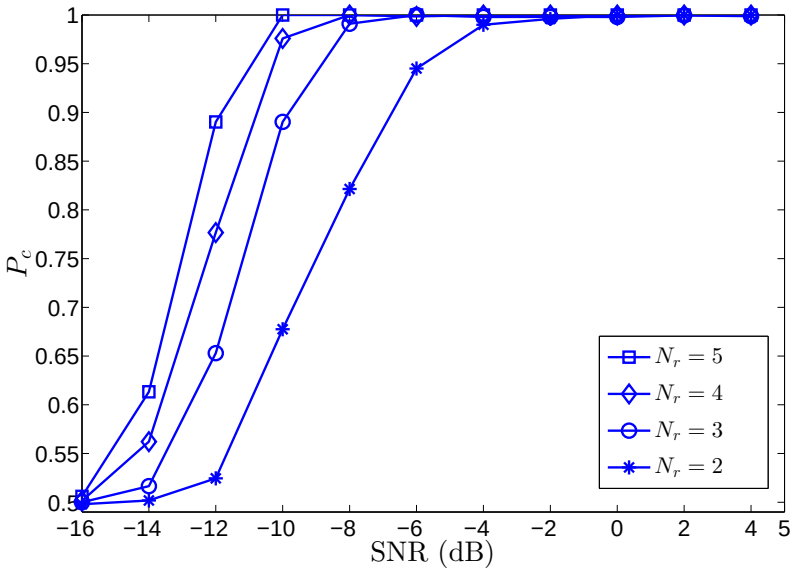

Fig. 4.8: The effect of the number of receive antennas, N_r, on the average probability of correct identification, P_c.

4.5.6 Effect of the modulation format

Fig. 4.9 presents the effect of the modulation format on the average probability of correct identification, P_c. Clearly, it does not affect the performance of the proposed algorithm, as the peak values in $|R_a^{\mathrm{AL}}(\tau)|$ do not depend on the modulation format, according to (4.7).

4.5.7 Effect of the timing offset

Perfect timing synchronization was assumed in the previous study. Here we evaluate the performance of the proposed algorithm in the presence of a timing offset. As mentioned in Section 4.4, a timing offset equal to a multiple integer of the sampling period leads to a shift in the positions of the $|R_a^{\mathrm{AL}}(\tau)|$ peaks by an amount corresponding to that offset; consequently, this does not affect the discriminating feature. On the other hand, when the timing offset is a fraction of the sampling period, its effect is modeled as a two path channel $[1-\mu, \mu]$, where $0 \leq \mu < 1$ is the normalized timing offset [22]. Fig. 4.10 shows

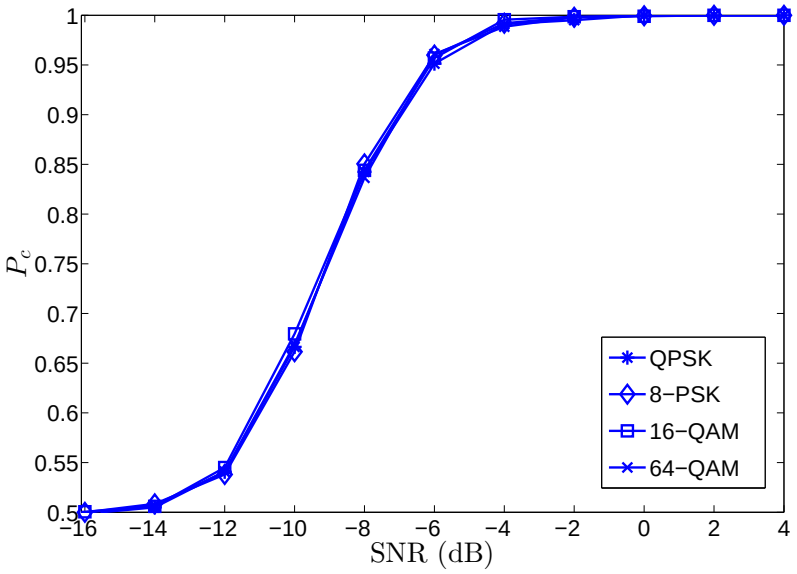

Fig. 4.9: The effect of the modulation format on the average probability of correct identification, P_c.

the average probability of correct identification, P_c, for $\mu = 0, 0.2$, and 0.5. The results indicate that while the performance slightly decreases at lower SNRs, it is not affected at higher SNRs. This can be explained, as the effect of μ can be considered as an additional noise component that affects the discriminating peaks in $|R_a^{\mathrm{AL}}(m)|$. At higher SNRs, the discriminating peaks are strong enough, and the effect of such noise component is negligible.

4.5.8 Effect of the frequency offset

Fig. 4.11 presents the effect of the frequency offset normalized to the subcarrier spacing, Δf, on the average probability of correct identification, P_c, at SNR = 0 dB and for different values of N and N_B. Note that as the OFDM block duration is constant regardless of N (see Section 1.5.1), the observation period increases with N_B, which leads to an increased effect of the frequency offset on the performance. It is worth noting that a reduced number of OFDM blocks is required to achieve a good performance for a larger

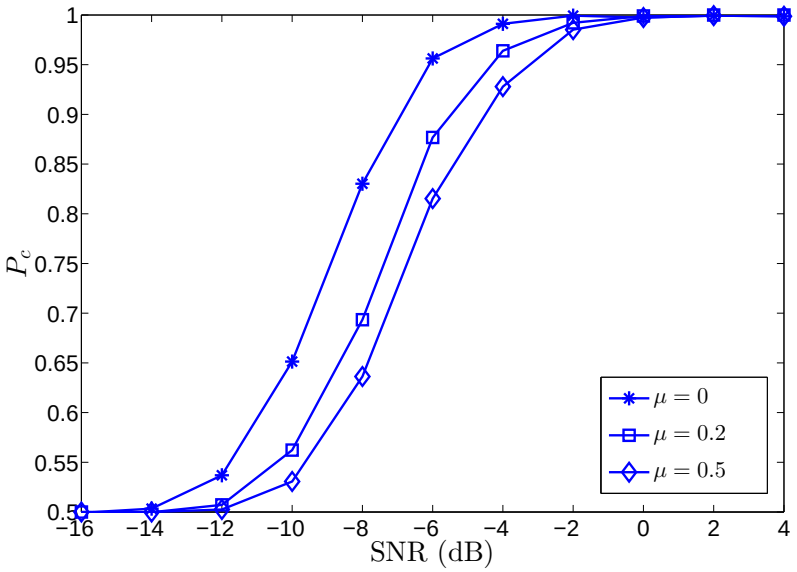

Fig. 4.10: The effect of the timing offset on the average probability of correct identification, P_c.

number of subcarriers, which results in a lower sensitivity to the frequency offset. Results in Fig. 4.11 show a good robustness for $\Delta f < 10^{-2}$ when $N = 2048$ and $N_B = 6$.

4.5.9 Effect of the Doppler frequency

The previous analysis assumed constant channel coefficients over the observation period. Here, we consider the effect of the Doppler frequency on the performance of the proposed algorithm. Fig. 4.12 shows the average probability of correct identification, P_c, versus the absolute value of the Doppler frequency normalized to the sampling rate, $|f_d|$, at SNR = 0 dB and $N_B = 50$ and 100. The results show a good robustness for $|f_d| < 10^{-4}$.

4.5.10 Effect of the spatially correlated fading

In the previous study, independent fading was considered. Here, we show the effect of the spatially correlated fading on the performance of the proposed algorithm. Fig. 4.13 shows the average probability of correct identification of the proposed algorithm, P_c, versus the

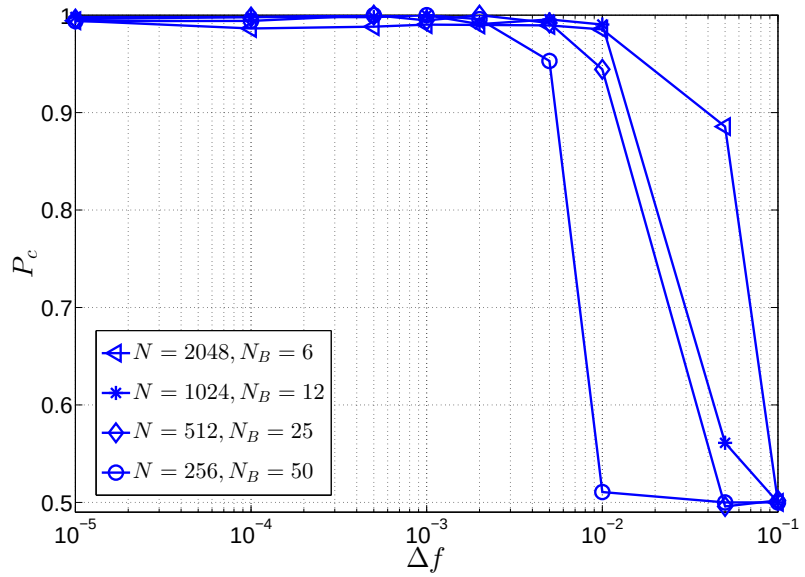

Fig. 4.11: The effect of the frequency offset on the average probability of correct identification, P_c, for different values of N and N_B at SNR = 0 dB.

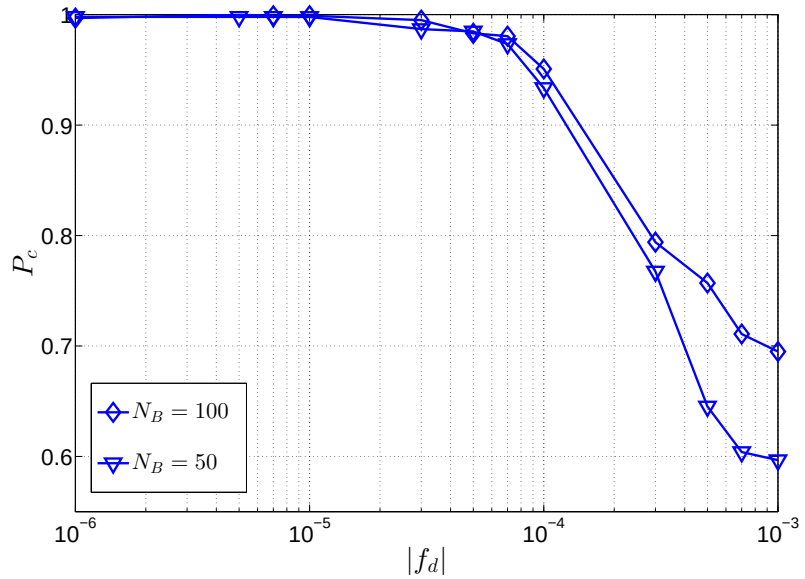

Fig. 4.12: The effect of the Doppler frequency on the average probability of correct identification, P_c, for $N_B = 50, 100$ at SNR = 0 dB.

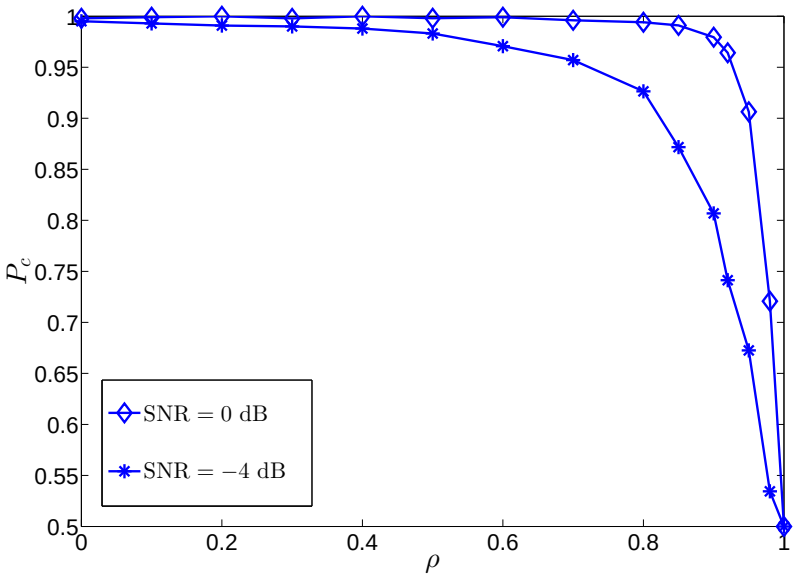

Fig. 4.13: The effect of the spatially correlated fading on the average probability of correct identification, P_c, at SNR=-4 dB and 0 dB.

spatial correlation coefficient, ρ, at SNR $= -4$ dB and 0 dB. As shown in (4.7), the channel coefficients affect the peak values in $|\hat{R}_a^{\mathrm{AL}}(\tau)|$ by the factor $|\sum_{l,l'=0}^{L_h-1}(h_{00}(l)h_{11}(l') - h_{10}(l)h_{01}(l'))|$. At high values of ρ, $h_{00}(l) \approx h_{01}(l)$ and $h_{11}(l') \approx h_{10}(l')$, $l, l' = 0, 1, ..., L_h - 1$. As such, the discriminating peaks vanish and the identification performance degrades[9]. As expected, the performance is more affected by spatially correlated fading at lower SNR.

4.6 Conclusion

The identification of the AL-OFDM and SM-OFDM signals has been investigated in this paper. A new cross-correlation was developed, which provides an efficient feature for signal identification. Based on the statistical properties of the feature estimate, a

[9]It is worth noting that the same performance is obtained if the spatially correlated fading occurs at the transmit-side; in this case $h_{00}(l) \approx h_{10}(l)$ and $h_{11}(l') \approx h_{01}(l')$, $l, l' = 0, 1, ..., L_h - 1$, at high values of the correlation coefficient.

novel criterion of decision was introduced. The proposed identification algorithm, which employs the aforementioned discriminating feature and decision criterion, provides an improved performance when compared with the previous work in the literature, at lower SNR and with reduced observation period. The algorithm has the advantages that it does not require channel and noise power estimation, modulation identification or timing synchronization. Furthermore, it exhibits a relatively low sensitivity to spatially correlated fading and frequency offset.

Appendix

Proof of *Proposition 1*

For the AL-OFDM signal, by using the definition of the $(N+\nu)$-length blocks in the $\boldsymbol{s}^{(f,\tau)}$ sequence (see Fig. 4.2 for the graphical illustration), one can easily express the samples of $\tilde{\boldsymbol{g}}_{2b+0}^{(0,\tau)}$ and $\tilde{\boldsymbol{g}}_{2b+1}^{(1,\tau)}$ respectively as

$$\tilde{g}_{2b+0}^{(0,\tau)}(n) = \begin{cases} \tilde{g}_{2b+0}^{(0)}(n+\tau), & n = 0, 1, ..., \\ & N+\nu-\tau-1, \\ & \\ \tilde{g}_{2b+1}^{(0)}(n+\tau-N-\nu), & n = N+\nu-\tau, \\ & ..., N+\nu-1, \end{cases} \tag{4.23}$$

and

$$\tilde{g}_{2b+1}^{(1,\tau)}(n') = \begin{cases} \tilde{g}_{2b+1}^{(1)}(n'+\tau), & n' = 0, 1, ..., \\ & N+\nu-\tau-1, \\ & \\ \tilde{g}_{2(b+1)}^{(1)}(n'+\tau-N-\nu), & n' = N+\nu-\tau, \\ & ..., N+\nu-1. \end{cases} \tag{4.24}$$

Based on (4.1), for the case of $\tau = 0$, it can be written that

$$\tilde{g}_{2b+0}^{(0,0)}(n) = \tilde{g}_{2b+0}^{(0)}(n) = \frac{1}{\sqrt{N}} \sum_{p=0}^{N-1} c_{2b+0}^{(0)}(p) e^{\frac{j2\pi p(n-\nu)}{N}}, \quad n = 0, 1, .., N + \nu - 1, \tag{4.25}$$

and

$$\tilde{g}_{2b+1}^{(1,0)}(n') = \tilde{g}_{2b+1}^{(1)}(n') = \frac{1}{\sqrt{N}} \sum_{p=0}^{N-1} c_{2b+1}^{(1)}(p) e^{\frac{j2\pi p(n'-\nu)}{N}}, \quad n' = 0, 1, .., N + \nu - 1. \tag{4.26}$$

For AL-OFDM signal, one can show that $c_{2b+1}^{(1)}(p) = (c_{2b+0}^{(0)}(p))^*$, $p = 0, 1, ..., N-1$. By taking the complex conjugate of (4.26), it is straightforward that

$$\tilde{g}_{2b+1}^{(1,0)^*}(n') = \frac{1}{\sqrt{N}} \sum_{p=0}^{N-1} c_{2b+0}^{(0)}(p) e^{\frac{-j2\pi p(n'-\nu)}{N}}, \quad n' = 0, 1, .., N + \nu - 1. \tag{4.27}$$

It is easy to see that $\tilde{g}_{2b+0}^{(0,0)}(n) = \tilde{g}_{2b+1}^{(1,0)^*}(n')$, $n, n' = 0, 1, ..., N + \nu - 1$ only when $n' - \nu = mod(-(n-\nu), N)$. A few examples are given as follows: $n = 0, n' = 2\nu$; $n = \nu, n' = \nu$; $n = \nu + 1, n' = N + \nu - 1$; and $n = N + \nu - 1, n' = \nu + 1$. Hence, one can notice that $n + n' = 2\nu$ for $n = 0, 1, ..., \nu$, and $n + n' = N + 2\nu$ for $n = \nu + 1, ..., N + \nu - 1$. This leads to the result shown in (4.3a).

For $\tau > 0$, it is straightforward that $\tilde{\boldsymbol{g}}_{2b+0}^{(0,\tau)}$ and $\tilde{\boldsymbol{g}}_{2b+1}^{(1,\tau)}$ belong to the (same) bth AL block for $n, n' = 0, 1, ..., N + \nu - \tau - 1$. Moreover, based on the aforementioned results regarding n and n', one can see that $\tilde{g}_{2b+0}^{(0,\tau)}(n) = \tilde{g}_{2b+1}^{(1,\tau)^*}(n' = mod(-(n-\nu), N) + \nu)$ if n and τ satisfy $n + n' = 2\nu, N + 2\nu$ and $n + n' + 2\tau = 2\nu, N + 2\nu$. If $n + n' = 2\nu$ and $n + n' + 2\tau = N + 2\nu$, then $\tau = N/2$, $n = 0, 1, ..., \nu$. This directly leads to the result in (4.3b). On the other hand, if $n + n' = n + n' + 2\tau$ (either equal to 2ν or $N + 2\nu$), then $\tau = 0$, $n = 0, 1, ..., N + \nu - 1$; this leads to the case of $\tau = 0$ discussed above. Furthermore, if $n + n' = N + 2\nu$ and $n + n' + 2\tau = 2\nu$, then $\tau = -N/2$, which is out of range ($0 \leq \tau < N + \nu$).

Moreover, also for the AL-OFDM signal, one can similarly express the samples of $\tilde{\boldsymbol{g}}_{2b-1}^{(0,\tau)}$ and $\tilde{\boldsymbol{g}}_{2b+0}^{(1,\tau)}$ respectively as

$$\tilde{g}_{2b-1}^{(0,\tau)}(n) = \begin{cases} \tilde{g}_{2b-1}^{(0)}(n+\tau), & n = 0, 1, ..., \\ & N+\nu-\tau-1, \\ & \\ \tilde{g}_{2b+0}^{(0)}(n+\tau-N-\nu), & n = N+\nu-\tau, \\ & ..., N+\nu-1, \end{cases} \tag{4.28}$$

and

$$\tilde{g}_{2b}^{(1,\tau)}(n') = \begin{cases} \tilde{g}_{2b+0}^{(1)}(n'+\tau), & n' = 0, 1, ..., \\ & N+\nu-\tau-1, \\ & \\ \tilde{g}_{2b+1}^{(1)}(n'+\tau-N-\nu), & n' = N+\nu-\tau, \\ & ..., N+\nu-1. \end{cases} \tag{4.29}$$

Accordingly, $\tilde{g}_{2b-1}^{(0,\tau)}(n)$ and $\tilde{g}_{2b+0}^{(1,\tau)}(n')$ belong to the (same) bth AL block for $n, n' = N+\nu-\tau, ..., N+\nu-1$. Following the same aforementioned analysis, one can prove results given in (4.3c).

References

[1] O. A. Dobre, A. Abdi, Y. Bar-Ness, and W. Su, "Survey of automatic modulation classification techniques: Classical approaches and new trends," *IET Commun.*, vol. 1, pp. 137–156, Apr. 2007.

[2] D. Cabric, "Addressing feasibility of cognitive radios," *IEEE Signal Process. Mag.*, vol. 25, pp. 85–93, Nov. 2008.

[3] J. L. Xu, W. Su, and M. Zhou, "Software-defined radio equipped with rapid modulation recognition," *IEEE Trans. Veh. Technol.*, vol. 59, pp. 1659–1667, May 2010.

[4] H.-C. Wu, M. Saquib, and Z. Yun, "Novel automatic modulation classification using cumulant features for communications via multipath channels," *IEEE Trans. Wireless Commun.*, vol. 7, pp. 3098–3105, Aug. 2008.

[5] W. Su, "Feature space analysis of modulation classification using very high-order statistics," *IEEE Commun. Lett.*, vol. 17, pp. 1688–1691, Sep. 2013.

[6] W. Su, J. L. Xu, and M. Zhou, "Real-time modulation classification based on maximum likelihood," *IEEE Commun. Lett.*, vol. 12, pp. 801–803, Nov. 2008.

[7] O. A. Dobre, M. Oner, S. Rajan, and R. Inkol, "Cyclostationarity-based robust algorithms for QAM signal identification," *IEEE Commun. Lett.*, vol. 16, pp. 12–15, Jan. 2012.

[8] D. Grimaldi, S. Rapuano, and L. De Vito, "An automatic digital modulation classifier for measurement on telecommunication networks," *IEEE Trans. Instrum. Meas.*, vol. 56, pp. 1711–1720, Oct. 2007.

[9] Q. Zhang, O. A. Dobre, Y. A. Eldemerdash, S. Rajan, and R. Inkol, "Second-order cyclostationarity of BT-SCLD signals: Theoretical developments and applications to signal classification and blind parameter estimation," *IEEE Trans. Wireless Commun.*, vol. 12, pp. 1501–1511, Apr. 2013.

[10] A. Bouzegzi, P. Ciblat, and P. Jallon, "New algorithms for blind recognition of OFDM based systems," *Elsevier Signal Processing*, vol. 90, pp. 900–913, Mar. 2010.

[11] A. Al-Habashna, O. A. Dobre, R. Venkatesan, and D. C. Popescu, "Second-order cyclostationarity of mobile WiMAX and LTE OFDM signals and application to spectrum awareness in cognitive radio systems," *IEEE J. Sel. Topics Signal Process.*, vol. 6, pp. 26–42, Feb. 2012.

[12] T. Xia and H.-C. Wu , "Blind identification of nonbinary LDPC codes using average LLR of syndrome a posteriori probability," *IEEE Commun. Lett.*, vol. 17, pp. 1301–1304, Jul. 2013.

[13] ——, "Novel blind identification of LDPC codes using average LLR of syndrome a posteriori probability," *IEEE Trans. Signal Process.*, vol. 62, pp. 632–640, Feb. 2014.

[14] ——, "Joint blind frame synchronization and encoder identification for low-density parity-check codes," *IEEE Commun. Lett.*, vol. 18, pp. 352–355, Feb. 2014.

[15] H.-C. Wu, X. Huang, and D. Xu, "Pilot-free dynamic phase and amplitude estimations for wireless ICI self-cancellation coded OFDM systems," *IEEE Trans. Broadcast.*, vol. 51, pp. 94–105, Mar. 2005.

[16] L. Korowajczuk, *LTE, WiMAX and WLAN Network Design, Optimization and Performance Analysis*. Wiley, 2011.

[17] M. Shi, Y. Bar-Ness, and W. Su, "Adaptive estimation of the number of transmit antennas," in *Proc. IEEE MILCOM*, 2007, pp. 1–5.

[18] O. Somekh, O. Simeone, Y. Bar-Ness, and W. Su, "Detecting the number of transmit antennas with unauthorized or cognitive receivers in MIMO systems," in *Proc. IEEE MILCOM*, 2007, pp. 1–5.

[19] K. Hassan, I. Dayoub, W. Hamouda, C. N. Nzeza, and M. Berbineau, "Blind digital modulation identification for spatially-correlated MIMO systems," *IEEE Trans. Wireless Commun.*, vol. 11, pp. 683–693, Feb. 2012.

[20] V. Choqueuse, S. Azou, K. Yao, and G. Burel, " Blind modulation recognition for MIMO systems," *J. Military Technical Academy Review*, vol. XIX, pp. 183–196, Jun. 2009.

[21] M. S. Mühlhaus, M. Öner, O. A. Dobre, and F. K. Jondral, "A low complexity modulation classification algorithm for MIMO systems," *IEEE Commun. Lett.*, vol. 17, pp. 1881–1884, Oct. 2013.

[22] V. Choqueuse, K. Yao, L. Collin, and G. Burel, "Hierarchical space-time block code recognition using correlation matrices," *IEEE Trans. Wireless Commun.*, vol. 7, pp. 3526–3534, Sep. 2008.

[23] V. Choqueuse, M. Marazin, L. Collin, K. C. Yao, and G. Burel, "Blind recognition of linear space–time block codes: A likelihood-based approach," *IEEE Trans. Signal Process.*, vol. 58, pp. 1290–1299, Mar. 2010.

[24] M. Marey, O. A. Dobre, and R. Inkol, "Classification of space-time block codes based on second-order cyclostationarity with transmission impairments," *IEEE Trans. Wireless Commun.*, vol. 11, pp. 2574–2584, Jul. 2012.

[25] M. Luo, L. Gan, and L. Li, "Blind recognition of space-time block code using correlation matrices in a high dimensional feature space," *J. Inf. Comput. Sci*, vol. 9, pp. 1469–1476, Jun. 2012.

[26] G. Qian, L. Li, M. Luo, H. Liao, and H. Zhang, "Blind recognition of space-time block code in MISO system," *EURASIP JWCN*, vol. 1, pp. 164–176, Jun. 2013.

[27] Y. A. Eldemerdash, M. Marey, O. A. Dobre, G. Karagiannidis, and R. Inkol, "Fourth-order statistics for blind classification of spatial multiplexing and Alamouti space-time block code signals," *IEEE Trans. Commun.*, vol. 61, pp. 2420–2431, Jun. 2013.

[28] H. Agirman-Tosun, Y. Liu, A. M. Haimovich, O. Simeone, W. Su, J. Dabin, and E. Kanterakis, "Modulation classification of MIMO-OFDM signals by independent component analysis and support vector machines," in *Proc. IEEE ASILOMAR*, 2011, pp. 1903–1907.

[29] M. Marey, O. A. Dobre, and R. Inkol, "Novel algorithm for stbc-ofdm identification in cognitive radios," in *Proc. IEEE ICC*. IEEE, 2013, pp. 2770–2774.

[30] ——, "Blind STBC identification for multiple-antenna OFDM systems," *IEEE Trans. Commun.*, vol. 62, pp. 1554–1567, May 2014.

[31] E. Karami and O. A. Dobre, "Identification of SM-OFDM and AL-OFDM signals based on their second-order cyclostationarity," *IEEE Trans. Veh. Technol.*, vol. 64, pp. 942–953, Mar. 2015.

[32] Y. G. Li, J. H. Winters, and N. R. Sollenberger, "MIMO-OFDM for wireless communications: signal detection with enhanced channel estimation," *IEEE Trans. Commun.*, vol. 50, pp. 1471–1477, Sep. 2002.

[33] A. Punchihewa, V. K. Bhargava, and C. Despins, "Blind estimation of OFDM parameters in cognitive radio networks," *IEEE Trans. Wireless Commun.*, vol. 10, pp. 733–738, Mar. 2011.

[34] S. M. Kay, *Fundamentals of Statistical Signal Processing: Estimation Theory* . Prentice Hall, 1993.

[35] D. R. Brillinger, *Time Series: Data Analysis and Theory.* Society for Industrial and Applied Mathematics, 2001.

[36] A. Papoulis and S. Pillai, *Probability, Random Variables and Stochastic Processes.* McGraw-Hill, 2001.

[37] M. K. Simon, *Probability Distributions Involving Gaussian Random Variables: A Handbook for Engineers and Scientists.* Springer, 2007.

[38] J. Stoer and R. Bulirsch, *Introduction to Numerical Analysis.* Springer, 2002.

[39] D. Watkins, *Fundamentals of Matrix Computations.* Wiley, 2002.

[40] M. Patzold, A. Szczepanski, and N. Youssef, "Methods for modeling of specified and measured multipath power-delay profiles," *IEEE Trans. Veh. Technol.*, vol. 51, pp. 978–988, Sep. 2002.

Chapter 5

On The Identification of SM and Alamouti Coded SC-FDMA Signals: A Statistical-Based Approach

5.1 Abstract

In this paper, we investigate the identification of spatial multiplexing (SM) and Alamouti (AL) space-time block code (STBC) with single carrier frequency division multiple access (SC-FDMA) signals. A discriminating feature is provided based on a fourth-order statistic of the received signal. A constant false alarm decision criterion is developed based on the statistical properties of the feature estimate. Furthermore, the theoretical performance analysis of the proposed identification algorithm is presented. The algorithm does not require channel or noise power estimation, modulation classification, and block synchronization. Extensive simulation results show the validity of the proposed algorithm, as well as a very good agreement with the theoretical analysis.

5.2 Introduction

With the extensive growth in wireless communication services, the available spectrum has become increasingly crowded, and limiting the interference as well as maximizing the capacity in wireless networks represents a challenge for network designers. In this context, intelligent radios appear as a promising solution for managing the interference and capacity problems in crowded wireless networks. Such radios have the capability of adapting the transmission parameters according to the existing signals in the spectrum to achieve minimum interference, and thus, to increase the capacity [1]. Signal identification is considered as the core of intelligent radios and represents the process of determining main parameters describing the structure of the received signals, such as transmission scheme, modulation type, and number of transmit antennas. Signal identification has been initially employed for military applications, such as radio surveillance and electronic warfare. Recently, it has been considered also for several commercial applications, such as software-defined radio and spectrum awareness in cognitive radio [2–5].

Extensive studies have been devoted to signal identification problems for single-input single-output (SISO) scenarios [6–12]. However, with the rapid adoption of the multiple-input multiple-output (MIMO) technology, additional signal identification problems have been introduced, such as estimation of the number of transmit antennas and identification of the space-time block codes (STBCs). Moreover, existing algorithms for modulation identification in SISO scenarios cannot be employed for signals transmitted with multiple antennas, and new algorithms are required. Investigation of MIMO signal identification is at an early stage; modulation identification has been addressed in [13–16], estimation of the number of transmit antennas in [17–20], and STBC identification in [21–27]. Most of these studies considered single carrier transmissions over frequency-flat fading channels [13–15, 17–19, 21–24], which is not practically valid for high data rate applications. A few recent works studied orthogonal frequency division multiplexing (OFDM) signals

over frequency-selective fading channels [16, 20, 25–27]. For STBC identification, the algorithms developed for OFDM signals [25–27] assumed intelligent radios equipped with multiple receive antennas, which is not always a practical case due to power, cost, and size limitations. Second-order statistics were employed as discriminating features.

To the best of the authors' knowledge, there exists no study in the literature for the identification of single carrier frequency division multiple access (SC-FDMA) signals transmitted with multiple antennas. SC-FDMA represents an alternative to OFDM, being used in uplink LTE and LTE-A [28].

This paper fills in the gap regarding the identification of STBC for SC-FDMA signals. We propose a fourth-order statistic-based algorithm to identify spatial multiplexing (SM) and Alamouti (AL) STBC for SC-FDMA signals when the receiver is equipped with a single antenna. A theoretical analysis of the identification performance is performed and a closed form expression for the probability of correct identification is obtained. The proposed algorithm provides a good identification performance without requiring STBC/SC-FDMA block synchronization or knowledge of the modulation, channel, and noise power. Furthermore, it has the advantage of being robust to spatially correlated fading.

The rest of this paper is organized as follows. The system model is introduced in Section 5.3, and the properties of AL and SM SC-FDMA signals, leading to the discriminating feature, are presented in Section 5.4. The proposed identification algorithm is described in Section 5.5, and the corresponding theoretical performance analysis is given in Section 5.6. Finally, simulation results are reported in Section 5.7, and conclusions are drawn in Section 5.8.

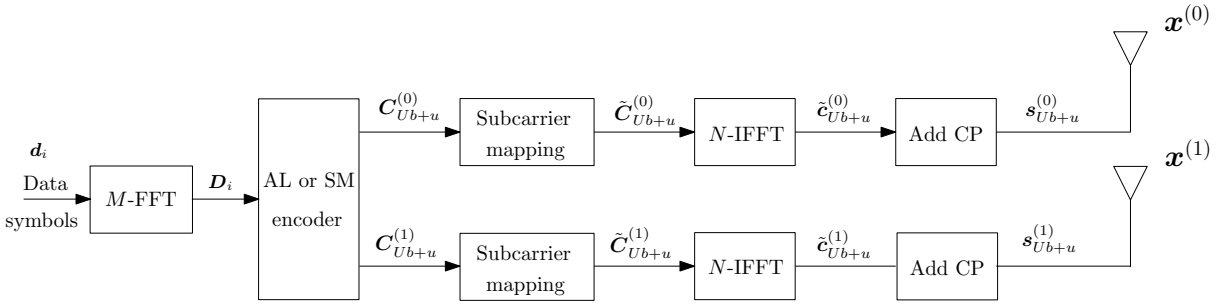

Fig. 5.1: Block diagram of an AL/ SM SC-FDMA transmitter equipped with two antennas [29].

5.3 System model

The block diagram of a transmitter using either AL or SM SC-FDMA signals and equipped with two antennas is shown in Fig. 5.1. The modulated data symbols, which are randomly and independently generated from an Ω-point constellation, $\Omega > 4$, are considered as a stream of M-length blocks, i.e., the ith data block is $\boldsymbol{d}_i = [d_i(0), ..., d_i(M-1)]$. Each block is input to an M-point fast Fourier transform (FFT) leading to a stream of M-length blocks representing the frequency-domain symbols corresponding to the modulated data blocks, $\boldsymbol{D}_i = [D_i(0), ..., D_i(M-1)]$. Each two consecutive frequency-domain blocks, i.e., with $i = 2b, 2b+1$, are encoded using a space-time coding matrix which is respectively defined for AL and SM STBCs as

$$\mathbb{G}^{(\mathrm{AL})}\left([\boldsymbol{D}_{2b+0}, \boldsymbol{D}_{2b+1}]\right) = \begin{bmatrix} \boldsymbol{D}_{2b+0} & -\boldsymbol{D}^*_{2b+1} \\ \boldsymbol{D}_{2b+1} & \boldsymbol{D}^*_{2b+0} \end{bmatrix} = \begin{bmatrix} \boldsymbol{C}^{(0)}_{2b+0} & \boldsymbol{C}^{(0)}_{2b+1} \\ \boldsymbol{C}^{(1)}_{2b+0} & \boldsymbol{C}^{(1)}_{2b+1} \end{bmatrix}, \tag{5.1}$$

and

$$\mathbb{G}^{(\mathrm{SM})}\left([\boldsymbol{D}_{2b+0}, \boldsymbol{D}_{2b+1}]\right) = \begin{bmatrix} \boldsymbol{D}_{2b+0} \\ \boldsymbol{D}_{2b+1} \end{bmatrix} = \begin{bmatrix} \boldsymbol{C}^{(0)}_{2b+0} \\ \boldsymbol{C}^{(1)}_{2b+0} \end{bmatrix}, \tag{5.2}$$

where $\boldsymbol{C}^{(f)}_{Ub+u}$ represents the $(Ub+u)$th block of length M transmitted from the fth

antenna, $f = 0, 1$, b is an integer denoting the STBC block index, U is the length of the STBC ($U = 2$ for AL and $U = 1$ for SM), u is the slot index within the bth STBC block, $u = 0, 1, ..., U-1$, and * denotes the complex conjugate.

For each transmit branch, a distributed subcarrier mapping is used to assign the M symbols within the block $\boldsymbol{C}_{Ub+u}^{(f)}$ to N subcarriers, $N > M$. Note that $N = \lambda M$, with λ as an integer representing the expansion factor, and the unoccupied subcarriers are set to zero [28]. The mapped block $\tilde{\boldsymbol{C}}_{Ub+u}^{(f)}$ is converted into a time-domain sequence $\tilde{\boldsymbol{c}}_{Ub+u}^{(f)} = [\tilde{c}_{Ub+u}^{(f)}(0), ..., \tilde{c}_{Ub+u}^{(f)}(N-1)]$ using an N-point inverse FFT (IFFT). Then, the cyclic prefix of length ν is added to the block $\tilde{\boldsymbol{c}}_{Ub+u}^{(f)}$ by appending the last ν samples as a prefix, leading to $\boldsymbol{s}_{Ub+u}^{(f)} = [\tilde{c}_{Ub+u}^{(f)}(N-\nu), ..., \tilde{c}_{Ub+u}^{(f)}(N-1), \tilde{c}_{Ub+u}^{(f)}(0), ..., \tilde{c}_{Ub+u}^{(f)}(N-1)]$, with components expressed as

$$s_{Ub+u}^{(f)}(n) = \frac{1}{\sqrt{N}} \sum_{p=0}^{N-1} \tilde{C}_{Ub+u}^{(f)}(p) e^{\frac{j2\pi p(n-\nu)}{N}}, \quad n = 0, 1, .., N+\nu-1. \tag{5.3}$$

Accordingly, the transmitted sequence from the fth antenna can be expressed as $\boldsymbol{x}^{(f)} = [\boldsymbol{s}_0^{(f)}, \boldsymbol{s}_1^{(f)}, \boldsymbol{s}_2^{(f)}...]$. We consider a receiver equipped with a single antenna, where the kth sample can be expressed as

$$y(k) = \boldsymbol{h}\boldsymbol{x}_k^T + w(k), \tag{5.4}$$

where the superscript T denotes transpose, $\boldsymbol{h} = [h_0(0), h_0(1), ..., h_0(L_h-1), h_1(0), ..., h_1(L_h-1)]$, $\boldsymbol{x}_k = [x^{(0)}(k), x^{(0)}(k-1), ..., x^{(0)}(k-L_h-1), x^{(1)}(k), ..., x^{(1)}(k-L_h-1)]$, with L_h as the number of propagation paths, $h_f(l)$ as the channel coefficient corresponding to the lth path between the transmit antenna f and the receive antenna, $l = 0, 1, ..., L_h - 1$, and $x^{(f)}(k-l)$ as the $(k-l)$th element of the sequence transmitted via the fth antenna, and $w(k)$ represents the zero-mean complex additive white Gaussian noise (AWGN) with variance σ_w^2.

5.4 Properities of AL and SM SC-FDMA signals and discriminating feature

In this section, we first introduce properties exhibited by the AL and SM SC-FDMA signals, which we then employ to obtain the feature for their identification.

Property 1. For the distributed subcarrier mapping, the time-domain samples $\tilde{c}^{(f)}_{Ub+u}(v),\ v = 0, 1, ..., N-1$, corresponding to $\boldsymbol{D}_{Ub+u}$ (AL and SM) and $\boldsymbol{D}^{*}_{Ub+u}$ (AL) are respectively expressed as

$$\tilde{c}^{(f)}_{Ub+u}(v = m + aM) = \frac{1}{\sqrt{\lambda}} d_{Ub+u}(m), \quad m = 0, 1, ..., M-1, a = 0, 1, ..., \lambda - 1, \tag{5.5}$$

and

$$\tilde{c}^{(f)}_{Ub+u}(v = m + aM) = \frac{1}{\sqrt{\lambda}} d^{*}_{Ub+u}(mod(-m, M)), \quad m = 0, 1, ..., M-1, a = 0, 1, ..., \lambda - 1, \tag{5.6}$$

where *mod* is the modulo operation.

Proof: See Appendix A. ■

In other words, the transmitted symbols from each antenna belong to the Ω-point constellation, scaled by a factor of $\frac{1}{\sqrt{\lambda}}$; it should be noted that this also holds after adding the cyclic prefix.

Property 2. Based on the structure of the AL coding matrix and by following [27], one can easily show for the AL SC-FDMA signal that

$$s^{(0)}_{2b+0}(n) = s^{(1)^{*}}_{2b+1}(mod(-(n-\nu), N) + \nu), \qquad \forall n = 0, 1, ..., N + \nu - 1. \tag{5.7}$$

Property 3. Let $\boldsymbol{x}^{(f,\tau)}$ denote the sequence with components $x^{(f,\tau)}(k) = x^{(f)}(k+\tau)$, $\tau = 0, 1, ..., N+\nu-1$. This is split into consecutive $(N+\nu)$-length blocks, i.e., $\boldsymbol{x}^{(f,\tau)} = [\boldsymbol{s}_0^{(f,\tau)}, \boldsymbol{s}_1^{(f,\tau)}, ..., \boldsymbol{s}_{i-1}^{(f,\tau)}, \boldsymbol{s}_i^{(f,\tau)}, \boldsymbol{s}_{i+1}^{(f,\tau)}, ...]$.

By using *Property 1* and *Property 2*, and following the analysis in [27], for the AL SC-FDMA signal, it can be shown that the components of $\boldsymbol{s}_i^{(0,\tau)}$ and $\boldsymbol{s}_{i+1}^{(1,\tau)}$ satisfy[1]

$$s_i^{(0,\tau)}(n) = s_{i+1}^{(1,\tau)^*}(mod(-(n-\nu), N) + \nu), \tag{5.8}$$

if and only if

- $\tau = 0$, $i = 2b$, and $n = 0, 1, ..., N+\nu-1$,
- $\tau = N/4$, $i = 2b$, and $n = 0, 1, ..., \nu$, $n = N/4+\nu+1, ..., 3N/4+\nu-1$,
- $\tau = N/2$, $i = 2b$, and $n = 0, 1, ..., \nu$,
- $\tau = N/2+\nu$, $i = 2b-1$, and $n = \frac{N}{2}, \frac{N}{2}+1, ..., \frac{N}{2}+2\nu$,
- $\tau = 3N/4$, $i = 2b$, and $n = 0, 1, ..., \nu$,
- $\tau = 3N/4+\nu$, $i = 2b-1$, and $n = N/4, ..., 3N/4+2\nu$.

Proof: See Appendix B. ■

Fig. 5.2 illustrates *Property 3* while also using *Properties* 1 and 2, by showing an example for $\tau = N/4$, with $N = 8$ and $\nu = 1$. The correlated samples are indicated through braces, whereas "•" is employed for components of data blocks other than $\boldsymbol{d}_i$.

With a single receive antenna, it can be easily shown that the second-order statistics cannot provide discriminating features, and thus, one needs to resort to fourth-order

[1]Henceforth, $\lambda = 2$ is considered; note that this is a typical value, as larger values of λ result in reduced spectral efficiency [29]. A brief discussion on $\lambda > 2$ is provided in Appendix B.

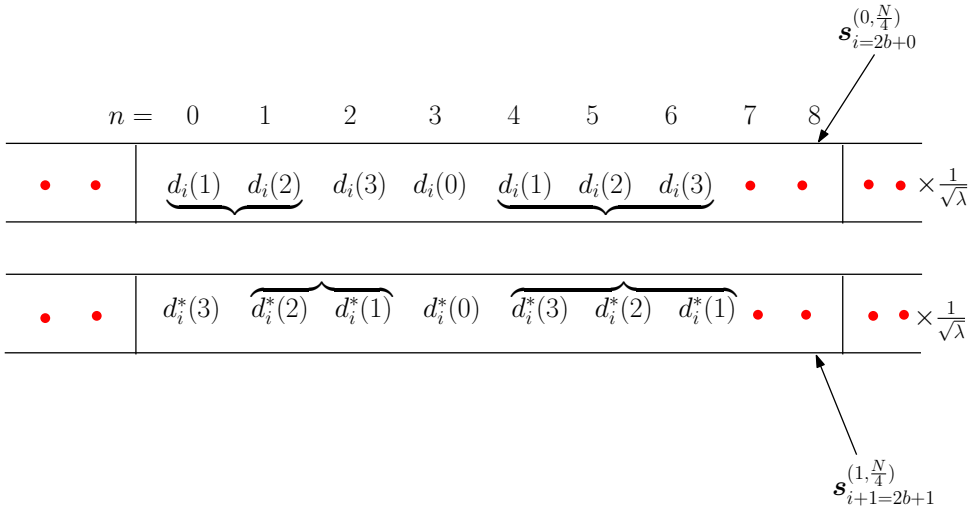

Fig. 5.2: Illustrative example for *Property 3* when $\tau = \frac{N}{4}$, with $N = 8$ and $\nu = 1$.

statistics.[2] We first introduce the proposed fourth-order statistic of the transmitted sequence, and then the one of the received sequence.

We define the fourth-order statistic of the transmitted sequence as

$$\mathcal{A}_s(\tau) = \mathrm{E}\left\{\left[\boldsymbol{s}_i^{(0,\tau)} \circ \boldsymbol{s}_i^{(0,\tau)}\right]\left[\bar{\boldsymbol{s}}_{i+1}^{(1,\tau)} \circ \bar{\boldsymbol{s}}_{i+1}^{(1,\tau)}\right]^T\right\}, \tag{5.9}$$

where $\bar{\boldsymbol{s}}_{i+1}^{(1,\tau)} = [\bar{s}_{i+1}^{(1,\tau)}(0), ..., \bar{s}_{i+1}^{(1,\tau)}(N+\nu-1)]$, with $\bar{s}_{i+1}^{(1,\tau)}(n) = s_{i+1}^{(1,\tau)}(mod(-(n-\nu), N)+\nu)$, $n = 0, 1, ..., N+\nu-1$, and E and $\circ$ denote the statistical expectation and the Hadmard product, respectively.

Based on (5.3), *Property 1*, and *Property 3*, one can show that

[2]It is worth noting that one should start investigating the lowest order statistic as discriminating feature [4]; due to the summetry of the signal constellation, the first and third order statistics are zero.

$$\mathcal{A}_s^{\mathrm{AL}}(\tau) = \begin{cases} \frac{\kappa_{d,4,2}}{4}(N+\nu), & \tau = 0, \\ \frac{\kappa_{d,4,2}}{4}(\frac{N}{2}+\nu), & \tau = \frac{N}{4}, \\ \frac{\kappa_{d,4,2}}{4}(\nu+1), & \tau = \frac{N}{2}, \\ \frac{\kappa_{d,4,2}}{4}(2\nu+1), & \tau = \frac{N}{2}+\nu, \\ \frac{\kappa_{d,4,2}}{4}(\nu+1), & \tau = \frac{3N}{4}, \\ \frac{\kappa_{d,4,2}}{4}(\frac{N}{2}+2\nu+1), & \tau = \frac{3N}{4}+\nu, \\ 0 & \text{otherwise}, \end{cases} \tag{5.10}$$

where $\kappa_{d,4,2}$ represents the (4,2) cumulant [2] of the modulated data symbols.[3] From Fig. 5.2, one can see the correlation between $N/2+\nu = 5$ components of $\boldsymbol{s}_i^{(0,\tau)}$ and $\boldsymbol{s}_{i+1}^{(1,\tau)}$ for $\tau = N/4$, with $N = 8$ and $\nu = 1$.

On the other hand, due to the fact that the transmitted SM SC-FDMA blocks from the two antennas are independent, it can be easily shown that

$$\mathcal{A}_s^{\mathrm{SM}}(\tau) = 0, \qquad \forall \tau = 0, 1, ..., N+\nu-1. \tag{5.11}$$

At the receive-side, the following assumptions and definitions are first introduced:

1. Without loss of generality we assume that the first intercepted sample corresponds to the start of an SC-FDMA block, and the total number of received samples is a multiple integer of the SC-FDMA block length, i.e., $K = N_B(N+\nu)$, where N_B is the number of received SC-FDMA blocks. This assumption will be relaxed later in the paper.

2. Define the vector $\boldsymbol{y}^{(\tau)}$ with $y^{(\tau)}(k) = y(k+\tau)$, $\tau = 0, 1, ..., N+\nu-1$. This vector is then divided into consecutive blocks each of length $(N+\nu)$, i.e., $\boldsymbol{y}^{(\tau)} =$

[3]Note that when $\nu = N/4$, the fourth-order statistic at $\tau = 3N/4$ is given by the summation of the fourth and fifth branches in (5.10).

$[\boldsymbol{r}_0^{(\tau)}, \boldsymbol{r}_1^{(\tau)}, \boldsymbol{r}_2^{(\tau)}, ..., \boldsymbol{r}_{N_B-1}^{(\tau)}]$, where $\boldsymbol{r}_i^{(\tau)} = [r_i^{(\tau)}(0), ..., r_i^{(\tau)}(N+\nu-1)]$, with $r_i^{(\tau)}(n) = y^{(\tau)}(n+i(N+\nu)),\ n = 0, 1, ..., N+\nu-1,\ i = 0, 1, ..., N_B-1$.

3. Define the fourth-order statistic

$$\mathcal{A}_r(\tau) = \mathrm{E}\left\{ \left[\boldsymbol{r}_i^{(\tau)} \circ \boldsymbol{r}_i^{(\tau)} \right] \left[\bar{\boldsymbol{r}}_{i+1}^{(\tau)} \circ \bar{\boldsymbol{r}}_{i+1}^{(\tau)} \right]^T \right\}, \tag{5.12}$$

where $\bar{\boldsymbol{r}}_{i+1}^{(\tau)} = [\bar{r}_{i+1}^{(\tau)}(0), ..., \bar{r}_{i+1}^{(\tau)}(N+\nu-1)]$, with $\bar{r}_{i+1}^{(\tau)}(n) = r_{i+1}^{(\tau)}(mod(-(n-\nu), N)+\nu)$, $n = 0, 1, ..., N+\nu-1$.

By using (5.4), (5.8), and (5.10), one can express $\mathcal{A}_r(\tau)$ for the AL SC-FDMA signal as

$$\mathcal{A}_r^{\mathrm{AL}}(\tau) = \begin{cases} (N+\nu)\Psi(\tau), & \tau = 0, 1, ..., L_h-1, \\ (\frac{N}{2}+\nu)\Psi(\tau-\frac{N}{4}), & \tau = \frac{N}{4}, \frac{N}{4}+1, ..., \frac{N}{4}+L_h-1, \\ (\nu+1)\Psi(\tau-\frac{N}{2}), & \tau = \frac{N}{2}, \frac{N}{2}+1, ..., \frac{N}{2}+L_h-1, \\ (2\nu+1)\Psi(\tau-\frac{N}{2}-\nu), & \tau = \frac{N}{2}+\nu, \frac{N}{2}+\nu+1, ..., \frac{N}{2}+\nu+L_h-1, \\ (\nu+1)\Psi(\tau-\frac{3N}{4}), & \tau = \frac{3N}{4}, \frac{3N}{4}+1, ..., \frac{3N}{4}+L_h-1, \\ (\frac{N}{2}+2\nu+1)\Psi(\tau-\frac{3N}{4}-\nu), & \tau = \frac{3N}{4}+\nu, \frac{3N}{4}+\nu+1, ..., \frac{3N}{4}+\nu+L_h-1, \\ 0 & \text{otherwise}, \end{cases} \tag{5.13}$$

where $\Psi(\tau) = \frac{\kappa_{d,4,2}}{4} \sum_{l,l'=0}^{L_h-1} (h_0^2(l) h_1^2(l')) \delta(2\tau - l - l')$.

On the other hand, due to the fact that the transmitted SM SC-FDMA blocks from the two antennas are independent, it can be easily shown that

$$\mathcal{A}_r^{\mathrm{SM}}(\tau) = 0, \qquad \forall \tau = 0, 1, ..., N+\nu-1. \tag{5.14}$$

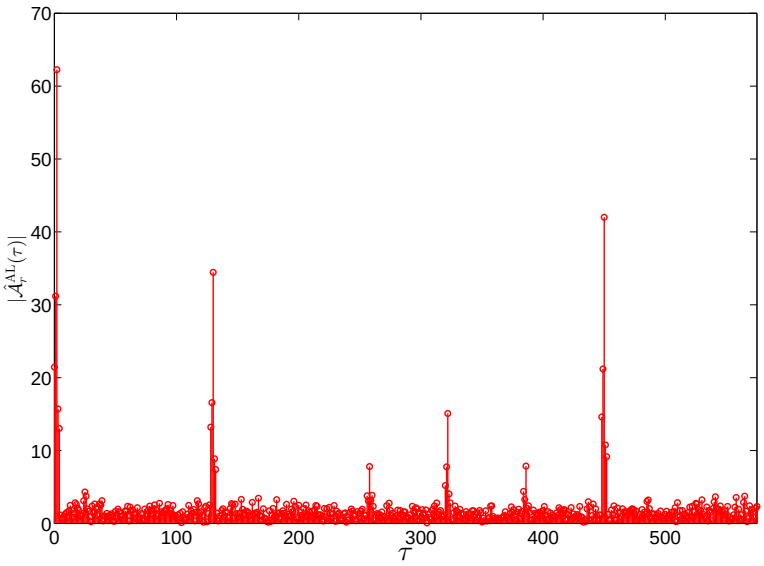

Fig. 5.3: $|\hat{\mathcal{A}}_r^{\mathrm{AL}}(\tau)|$ with QPSK modulation, $N = 512$, $\lambda = 2$, $\nu = N/8$, and $N_B = 4000$ at SNR= 25 dB over multipath Rayleigh fading channel, $L_h = 3$, for the AL SC-FDMA signal.

Fig. 5.3 shows the magnitude of the estimated fourth-order statistic, $|\hat{\mathcal{A}}_r^{\mathrm{AL}}(\tau)|$, with $N = 512$, $M = N/2$, $\nu = N/8$, $N_B = 4000$, and quadrature phase-shift-keying (QPSK) modulation over multipath Rayleigh fading channel with $L_h = 3$ at SNR= 25 dB. Apparently, the results match with the theoretical findings discussed above.

It is worth noting that if the first received sample does not correspond to the start of an SC-FDMA block, the discriminating peaks shown in Fig. 5.3 will be shifted with the delay between the first received sample and the start of the next SC-FDMA block. Indeed, this shift does not affect the identification performance, as the statistically significant peaks still exist.

5.5 Proposed identification algorithm

5.5.1 Proposed algorithm

Based on the aforementioned discussion, the presence of significant peaks in $|\hat{\mathcal{A}}_r^{\mathrm{AL}}(\tau)|$ provides a discriminating feature that can be employed to identify AL and SM SC-FDMA signals. Here we propose a statistical test to detect the peak presence in $|\hat{\mathcal{A}}_r(\tau)|$,[4] and develop the identification algorithm accordingly.

The fourth-order statistic defined in (5.12) can be estimated as

$$\hat{\mathcal{A}}_r(\tau) = \frac{1}{N_B} \sum_{i=0}^{N_B-1} \left[\boldsymbol{r}_i^{(\tau)} \circ \boldsymbol{r}_i^{(\tau)}\right] \left[\bar{\boldsymbol{r}}_{i+1}^{(\tau)} \circ \bar{\boldsymbol{r}}_{i+1}^{(\tau)}\right]^T. \tag{5.15}$$

By following [30, 31], this can be expressed as

$$\hat{\mathcal{A}}_r(\tau) = \mathcal{A}_r(\tau) + \epsilon(\tau), \tag{5.16}$$

where the estimation error $\epsilon(\tau)$ has an asymptotic zero-mean complex Gaussian distribution with variance σ_ϵ^2.

Based on (5.13) and (5.14), the identification process can be formulated as a binary hypothesis testing problem:

$$\begin{aligned} \text{Hypothesis } \mathcal{H}_0: \quad & \forall \tau = 0, 1, ..., N+\nu-1, \quad \hat{\mathcal{A}}_r(\tau) = \epsilon(\tau), \text{ and the} \\ & \text{SM SC-FDMA signal is decided to be received,} \end{aligned}$$

and

$$\begin{aligned} \text{Hypothesis } \mathcal{H}_1: \quad & \text{For at least one value of } \tau = 0, 1, ..., N+\nu-1 \\ & \hat{\mathcal{A}}_r(\tau) = \mathcal{A}_r(\tau) + \epsilon(\tau), \text{ and the} \\ & \text{AL SC-FDMA signal is decided to be received.} \end{aligned}$$

[4] The superscript AL is dropped, as one does not know if the received signal is AL or SM.

We define the test function $\mathcal{G}(\tau)$ as

$$\mathcal{G}(\tau) = \frac{2|\hat{\mathcal{A}}_r(\tau)|^2}{\frac{1}{N+\nu}\sum_{\tau'=0}^{N+\nu-1}|\hat{\mathcal{A}}'_r(\tau')|^2}, \quad \tau = 0, 1, ..., N+\nu-1, \tag{5.17}$$

with

$$\hat{\mathcal{A}}'_r(\tau') = \frac{1}{N_B}\sum_{i=0}^{N_B-1}\left[\boldsymbol{r}_i^{(\tau')} \circ \boldsymbol{r}_i^{(\tau')}\right]\left[\bar{\boldsymbol{r}}_{i+4}^{(\tau')} \circ \bar{\boldsymbol{r}}_{i+4}^{(\tau')}\right]^T. \tag{5.18}$$

Note that the denominator in (5.17) is an estimate of σ_ϵ^2 regardless of the transmitted signal (there are no statistically significant peaks). Also, for the AL SC-FDMA signal, the peak positions in $\mathcal{G}(\tau)$ are the same as in $\mathcal{A}(\tau)$. Moreover, under hypothesis $\mathcal{H}_0$, $\hat{\mathcal{A}}_r(\tau) = \epsilon(\tau)$ has an asymptotic zero-mean complex Gaussian distribution with variance σ_ϵ^2. Accordingly, and considering the denominator of (5.17) as a constant, σ_ϵ^2, $\mathcal{G}(\tau)$ has an asymptotic central chi-square distribution with the degree of freedom equal to two [32].

We further define the test statistic Γ as

$$\Gamma = \max_{\tau=0,1,...,N+\nu-1}\mathcal{G}(\tau). \tag{5.19}$$

By using the fact that the cumulative distribution function (CDF) of the maximum value Γ is the product of the CDFs of $\mathcal{G}(\tau)$, $\tau = 0, 1, ..., N+\nu-1$ [32], we can set a threshold, γ corresponding to a certain probability of false alarm, $P_f = P(\Gamma > \gamma|\mathcal{H}_0)$, i.e.,

$$1 - P_f = (1 - e^{\frac{-\gamma}{2}})^{(N+\nu)}. \tag{5.20}$$

Then, the threshold can be calculated as

$$\gamma = -2\ln(1 - (1 - P_f)^{\frac{1}{N+\nu}}). \tag{5.21}$$

5.5.2 Computational complexity

The required number of floating point operations (flops) [33] is employed as a measure of the computational complexity of the proposed algorithm. It can be easily found that the proposed algorithm requires $36N_B(N+\nu)^2+4(N+\nu)(N_B+2)$ flops. As an example, with $N = 512$, $\nu = N/8$, and $N_B = 1000$, it can be seen that 1.19×10^{10} flops are required. As such, the calculations needed for the proposed algorithm can be done in approximately 6.36 $m$sec if a microprocessor with 1.87 Tera-flops[5] is used.

5.6 Theoretical Performance analysis

The identification process is done by comparing the test statistic, Γ, with a threshold, γ. If $\Gamma > \gamma$, then the AL SC-FDMA signal is declared present; otherwise, SM SC-FDMA is chosen. As the threshold γ is determined according to a constant probability of false alarm, P_f, the probability of correctly identifying the SM SC-FDMA signal is determined as

$$P(\zeta = \text{SM}|\text{SM}) = 1 - P_f, \tag{5.22}$$

where ζ is the estimated signal type.

On the other hand, the probability of correctly identifying the AL SC-FDMA signal is $P(\zeta = \text{AL}|\text{AL}) = P(\Gamma > \gamma|\mathcal{H}_1) = 1 - P(\Gamma \leq \gamma|\mathcal{H}_1)$. As Γ is the maximum of $\mathcal{G}(\tau)$, $P(\Gamma \leq \gamma|\mathcal{H}_1)$ is the probability that $\mathcal{G}(\tau) \leq \gamma$, $\forall \tau = 0, 1, ..., N+\nu-1$. Furthermore, under hypothesis $\mathcal{H}_1$, $\mathcal{G}(\tau)$ has significant peaks around $\tau = 0, N/4, N/2, N/2+\nu, 3N/4, 3N/4+\nu$ and has nulls at other values of τ. Let Λ be the set of τ values for which $\mathcal{G}(\tau)$ is non-zero. According to (5.13), the cardinality of the set Λ is $6L_h$; as such, $N + \nu - 6L_h$ points of $\mathcal{G}(\tau)$, $\tau \notin \Lambda$, have an asymptotic central chi-square distribution with two degrees of

[5][online], available: http://www.nvidia.ca/object/tesla-servers.html

freedom, and one can write

$$P(\mathcal{G}(\tau) \leq \gamma, \tau \notin \Lambda | \mathcal{H}_1) = (1 - e^{-\gamma/2})^{N+\nu-6L_h}. \tag{5.23}$$

For $\tau \in \Lambda$, the corresponding values of $\mathcal{G}(\tau)$ have a non-central chi-square distribution with the non-centrality parameter, $\mathcal{P}_\tau$, which can be written based on (5.17) as

$$\mathcal{P}_\tau = \frac{2|\mathcal{A}_r(\tau)|^2}{\sigma_\epsilon^2}. \tag{5.24}$$

For the PSK modulated data symbols with unit variance constellation,[6] σ_ϵ^2 is given by (see Appendix C for the proof)

$$\begin{aligned} \sigma_\epsilon^2 \; &= \tfrac{N+\nu}{N_B}\Big[\tfrac{1}{\lambda^4} \parallel (\boldsymbol{h} \otimes \boldsymbol{h}) \otimes (\boldsymbol{h} \otimes \boldsymbol{h}) \parallel_F^2 + 8\tfrac{\sigma_w^2}{\lambda^3} \parallel (\boldsymbol{h} \otimes \boldsymbol{h}) \otimes \boldsymbol{h} \parallel_F^2 \\ &\quad + 20\tfrac{\sigma_w^4}{\lambda^2} \parallel (\boldsymbol{h} \otimes \boldsymbol{h}) \parallel_F^2 + 16\tfrac{\sigma_w^6}{\lambda} \parallel \boldsymbol{h} \parallel_F^2 + 4\sigma_w^8\Big], \end{aligned} \tag{5.25}$$

where $\otimes$ and $\| \cdot \|_F$ denote the Kronecker product and the Frobenius norm, respectively.

Based on the CDF of the non-central chi-square distribution with two degrees of freedom, the probability that $\mathcal{G}(\tau) \leq \gamma$, $\tau \in \Lambda$, for certain channel coefficients is

$$P(\mathcal{G}(\tau) \leq \gamma, \tau \in \Lambda | \mathcal{H}_1, \boldsymbol{h}) = \prod_{\tau \in \Lambda} (1 - Q_1(\sqrt{\mathcal{P}_\tau}, \sqrt{\gamma})), \tag{5.26}$$

where $Q_1(\cdot, \cdot)$ is the generalized Marcum Q function [34].

Based on (5.23) and (5.26), the probability of correctly identifying the AL SC-FDMA signal for certain channel coefficients can be expressed as

$$P(\zeta = \text{AL} | \text{AL}, \boldsymbol{h}) = 1 - \left[(1 - e^{-\gamma/2})^{N+\nu-6L_h} \prod_{\tau \in \Lambda} (1 - Q_1(\sqrt{\mathcal{P}_\tau}, \sqrt{\gamma})) \right]. \tag{5.27}$$

[6]Note that in this case both second-order/ one-conjugate and fourth-order/ two-conjugate moments are equal to one [2], and a simple analytical expression can be obtained.

Then, the probability of correctly identifying the AL SC-FDMA signal can be calculated as $P(\zeta = \text{AL}|\text{AL}) = \int_{\boldsymbol{h}} P(\zeta = \text{AL}|\text{AL}, \boldsymbol{h}) p(\boldsymbol{h}) d\boldsymbol{h}$, where $p(\boldsymbol{h})$ is the probability density function of $\boldsymbol{h}$. Finally, the average probability of correct identification represents the average of $P(\zeta = \text{AL}|\text{AL})$ and $P(\zeta = \text{SM}|\text{SM})$ when AL and SM SC-FDMA are considered to be received with equal probability.

5.7 Simulation results

5.7.1 Simulation setup

The evaluation of the proposed identification algorithm was done by considering the LTE SC-FDMA signal with a useful duration of 66.66 μsec and subcarrier spacing of 15 kHz. Unless otherwise mentioned, QPSK modulation, $N = 512$ (5 MHz double sided bandwidth), $\nu = N/8$, $\lambda = 2$, $N_B = 1000$, and $P_f = 10^{-3}$ were used. The received signal was affected by frequency-selective Rayleigh fading channel with $L_h = 3$ statistically independent taps and an exponential power delay profile [35], $\sigma^2(l) = \exp(-l/5)$, where $l = 0, ..., L_h - 1$. The out-of-band noise was removed at the receive-side with a Butterworth filter, and the SNR was considered at the output of this filter. The average probability of correct identification, $P_c = 0.5[P(\zeta = \text{AL}|\text{AL}) + P(\zeta = \text{SM}|\text{SM})]$, was used as a measure of the identification performance. This was calculated based on 1000 trials for each signal.

5.7.2 Effect of the number of subcarriers: Theoretical and simulation results

Fig. 5.4 shows the analytical and simulation results for the probability of correct identification achieved with the proposed algorithm for various number of subcarriers, N.

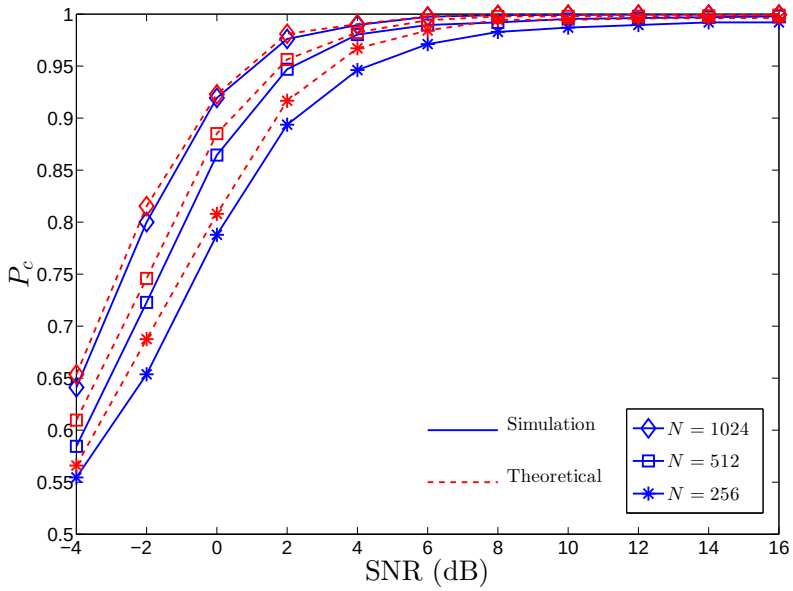

Fig. 5.4: The effect of the number of subcarriers on the probability of correct identification, P_c.

In general, the theoretical findings are in a good agreement with the simulation results. A slight difference between the theoretical and simulation results can be observed for $N = 256$ when compared with larger values of N. This is because of the difference between the estimated variance in the denominator of (5.17) and the actual value shown in (5.25). Indeed, this difference is decreased by increasing N, as better estimate of the variance, σ_ϵ^2 is achieved in such cases. On the other hand, it can be seen that the identification performance significantly improves by increasing N. This is can be easily noticed from (5.13), as the peak values in $\mathcal{A}_r^{\mathrm{AL}}(\tau)$ are proportional to $(N + \nu)$.

5.7.3 Effect of the factor λ and the number of SC-FDMA blocks

Fig. 5.5 presents the average probability of correct identification, P_c, of the proposed algorithm for various number of SC-FDMA blocks, N_B with $\lambda = 2, 4$. It can be noticed that the performance does not depend on λ. This can be explained, as although the

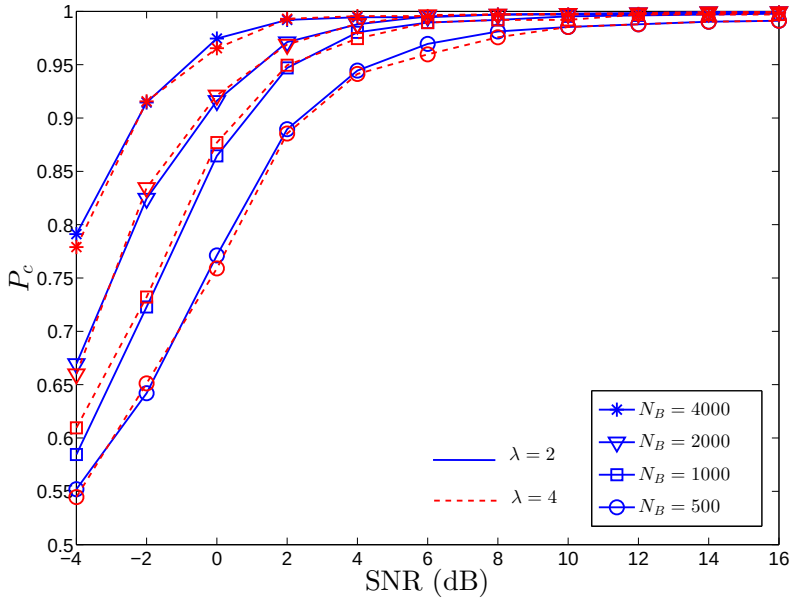

Fig. 5.5: The effect of the factor λ and the number of SC-FDMA blocks on the average probability of correct identification, P_c.

magnitudes of statistically discriminating peaks decrease by increasing λ, the noise power is also decreased to keep the same SNR.[7] Furthermore, the performance of the proposed algorithm improves with N_B, as a more accurate estimate of the discriminating peaks in $\mathcal{A}_r^{\mathrm{AL}}(\tau)$ is achieved. A very good performance of the proposed algorithm ($P_c \approx 1$) is obtained at SNR = 6 dB with $N_B = 1000$, while the same performance can be reached with $N_B = 4000$ at SNR = 2 dB.

5.7.4 Effect of the modulation format

The effect of the modulation format on the average probability of correct identification, P_c, is illustrated in Fig. 5.6 with $N_B = 2000$. As can be seen, the same performance is achieved for the PSK modulations, i.e., QPSK and 8-PSK, while a performance degradation is seen for 16-QAM and 64-QAM modulations. The dependence of the proposed

[7]Based on *Property 1*, the transmitted signal power decreases by increasing λ.

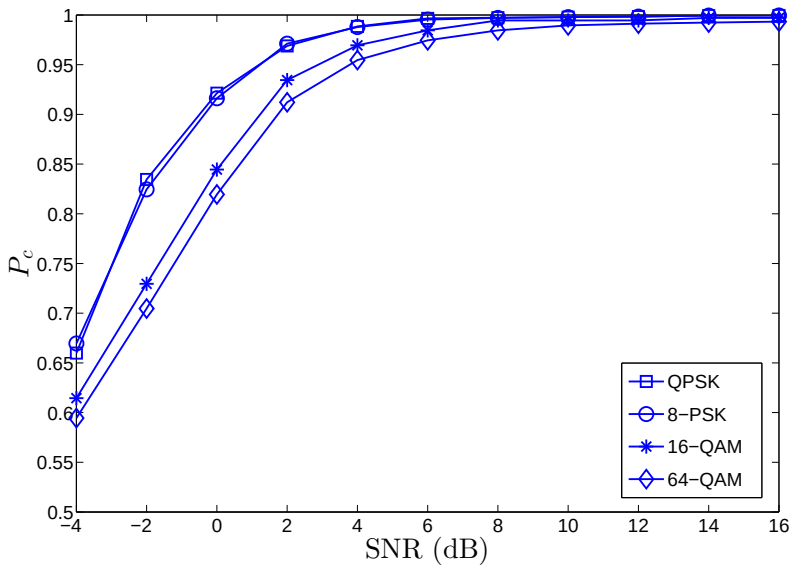

Fig. 5.6: The effect of the modulation format on the average probability of correct identification, P_c.

algorithm on the modulation format can be explained, as the values of the discriminating peaks in $\mathcal{A}_r^{\mathrm{AL}}(\tau)$ are directly proportional to $\kappa_{d,4,2}$. Theoretical values of $\kappa_{d,4,2}$ are given in [2] for various unit variance constellations. For example, this equals $\kappa_{d,4,2} = -1$ for QPSK and 8-PSK, and $\kappa_{d,4,2} = -0.68$ and $\kappa_{d,4,2} = -0.619$ for 16-QAM and 64-QAM, respectively [2].

5.7.5 Effect of the timing offset

Fig. 5.7 presents the effect of the timing offset on the average probability of correct identification, P_c. When the timing offset is a fraction of the sampling interval, its effect is modeled as a two path channel $[1-\mu, \mu]$, where $0 \leq \mu < 1$ is the normalized timing offset [22]. Results for $\mu = 0, 0.25, 0.5$ are shown in Fig. 5.7. A slight degradation in the identification performance is observed at lower SNRs when μ increases. However, the performance is not affected by the timing offset at higher SNRs. This is because the effect of timing offset can be modeled as an additional noise component that affects the

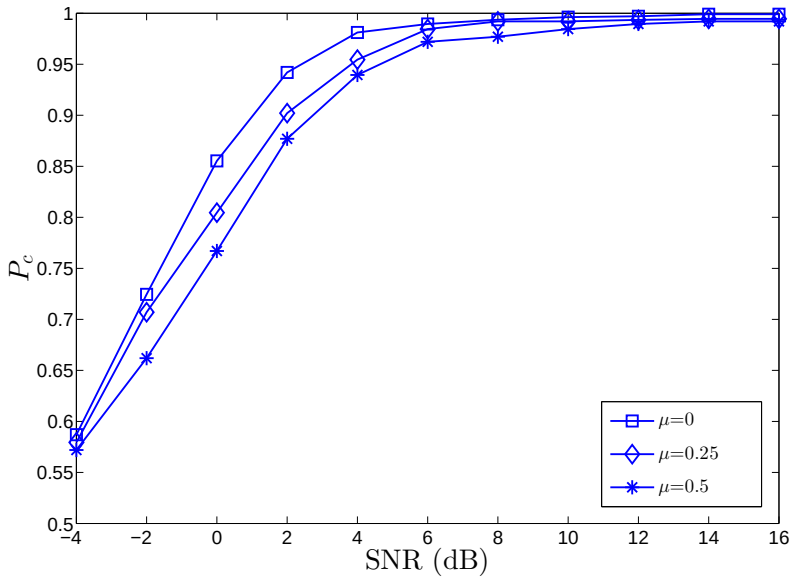

Fig. 5.7: The effect of the timing offset on the average probability of correct identification, P_c.

discriminating peaks in $\mathcal{A}_r^{\mathrm{AL}}(\tau)$; the effect of such a noise component vanishes at high SNRs. On the other hand, with a timing offset equivalent to multiple integer of the sampling interval, the discriminating peaks in $\mathcal{A}_r^{\mathrm{AL}}(\tau)$ are shifted by that offset, which does not affect the performance.

5.7.6 Effect of the frequency offset

Fig. 5.8 shows the average probability of correct identification, P_c, versus the frequency offset normalized to the subcarrier spacing, Δf, for $N_B = 600, 1000$ at SNR= 10 dB. Apparently, the proposed algorithm is sensitive to frequency offset. Although the frequency offset does not affect the identification of SM SC-FDMA, it affects the identification of the AL SC-FDMA signal, as the discriminating peaks reduce when increasing the frequency offset. Hence, the algorithm requires carrier frequency recovery.

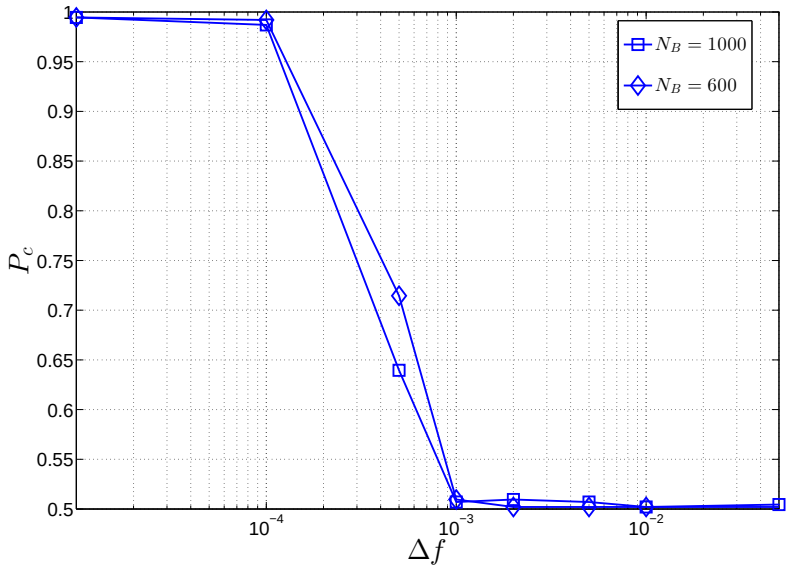

Fig. 5.8: The effect of the frequency offset on the average probability of correct identification, P_c at SNR=10 dB.

5.7.7 Effect of spatial correlation

Fig. 5.9 depicts the average probability of correct identification, P_c, versus the correlation coefficient between $h_0(l), l = 0, 1, ..., L_h - 1$ and $h_1(l'), l' = 0, 1, ..., L_h - 1$ at SNR = 10 dB, 4 dB, and 0 dB. It can be seen that the identification performance is not affected by spatial correlation. This can be noticed from (5.13) and (5.17), where the spatial correlation does not change the discriminating peaks.

5.8 Conclusion

The identification of SM SC-FDMA and AL SC-FDMA signals was addressed in this paper for single receive antenna scenarios. A fourth-order statistic of the received signal was employed as a discriminating feature. It was shown that the proposed statistic exhibits significant peaks for the AL SC-FDMA signal, while it does not for the SM SC-FDMA signal. Furthermore, a constant false alarm criterion was developed for decision making.

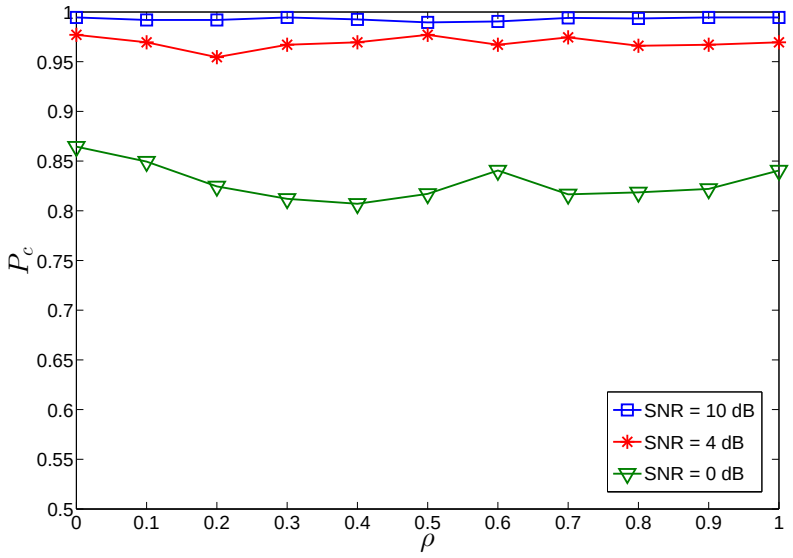

Fig. 5.9: The effect of the spatially correlated fading on the average probability of correct identification, P_c, at SNR=10 dB, 4 dB, and 0 dB.

Analytical results for the identification performance of the proposed algorithm were derived. It was shown that simulation and theoretical findings match. The applicability of the proposed algorithm was proved through extensive simulations; this does not require estimation of noise power or channel coefficients, block timing synchronization, and modulation identification.

Appendix A: Proof of *Property 1*

The frequency samples after distributed subcarrier mapping, $\tilde{C}^{(f)}_{Ub+u}(p)$, $p = 0, 1, ..., N-1$, can be represented as

$$\tilde{C}^{(f)}_{Ub+u}(p) = \begin{cases} C^{(f)}_{Ub+u}(q), & p = q\lambda, \;\; q = 0, 1, ..., M-1, \\ 0, & \text{otherwise.} \end{cases} \tag{5.28}$$

After applying the N-point IFFT, the time samples, $\tilde{c}_{Ub+u}^{(f)}(v)$, $v = 0, 1, ..., N-1$, can be expressed as

$$\tilde{c}_{Ub+u}^{(f)}(v) = \frac{1}{\sqrt{N}} \sum_{p=0}^{N-1} \tilde{C}_{Ub+u}^{(f)}(p) e^{2\pi jvp/N}. \tag{5.29}$$

Let $v = m + aM$, $m = 0, 1, ..., M-1$, $a = 0, 1, ..., \lambda - 1$; by substituting (5.28) into (5.29), one obtains

$$\tilde{c}_{Ub+u}^{(f)}(v) = \frac{1}{\sqrt{\lambda}} \frac{1}{\sqrt{M}} \sum_{q=0}^{M-1} C_{Ub+u}^{(f)}(q) e^{2\pi j(m+aM)q/M}. \tag{5.30}$$

If $\boldsymbol{C}_{Ub+u}^{(f)} = \boldsymbol{D}_{Ub+u}$, it is straightforward to find that $\tilde{c}_{Ub+u}^{(f)}(v = m+aM) = \frac{1}{\sqrt{\lambda}} d_{Ub+u}(m)$. On the other hand, if $\boldsymbol{C}_{Ub+u}^{(f)} = \boldsymbol{D}_{Ub+u}^{*}$, after some mathematical manipulations, it is easy to find that $\tilde{c}_{Ub+u}^{(f)}(v = m + aM) = \frac{1}{\sqrt{\lambda}} d_{Ub+u}^{*}(mod(-m, M))$.

Appendix B: Proof of *Property 3*

Based on the definition of $\boldsymbol{x}^{(f,\tau)}$ and the structure of the AL coding matrix, the samples of the $(N+\nu)$-length blocks transmitted from the two antennas, $\boldsymbol{s}_i^{(0,\tau)}$ and $\boldsymbol{s}_{i+1}^{(1,\tau)}$ can be respectively expressed as

$$s_i^{(0,\tau)}(n) = \begin{cases} s_i^{(0)}(n+\tau), & n = 0, 1, ..., N+\nu-\tau-1, \\ s_{i+1}^{(0)}(n+\tau-N-\nu), & n = N+\nu-\tau, ..., N+\nu-1, \end{cases} \tag{5.31}$$

and

$$s_{i+1}^{(1,\tau)}(n') = \begin{cases} s_{i+1}^{(1)}(n'+\tau), & n' = 0, 1, ..., N+\nu-\tau-1, \\ s_{i+2}^{(1)}(n'+\tau-N-\nu), & n' = N+\nu-\tau, ..., N+\nu-1. \end{cases} \tag{5.32}$$

It can be noticed that $\boldsymbol{s}_i^{(0,\tau)}$ and $\boldsymbol{s}_{i+1}^{(1,\tau)}$ belong to the same bth AL block for $n, n' = 0, 1, ..., N+\nu-\tau-1$ when $i = 2b$, whereas this occurs for $n, n' = N+\nu-\tau, ..., N+\nu-1$ when $i = 2b-1$.

According to [27], *Property 3* is valid for the following cases:

- $i = 2b$, $n + n' = 2\nu$ or $N + 2\nu$, and $n + n' + 2\tau = 2\nu$ or $N + 2\nu$
- $i = 2b-1$, $n + n' = 2\nu$ or $N + 2\nu$, and $n + n' + 2\tau - 2N - 2\nu = 2\nu$ or $N + 2\nu$.

Hence, similar to [27], the cases for $\tau = 0,\ N/2,\ N/2+\nu$ can be obtained. The remaining three cases in (5.8), i.e., $\tau = N/4,\ 3N/4$, and $3N/4+\nu$, can be proved as follows.

For $\lambda = 2$, according to Appendix A, the transmitted blocks $\boldsymbol{s}_{i=Ub+u}^{(f)}$ corresponding to $\boldsymbol{D}_{i=Ub+u}$ and $\boldsymbol{D}_{i=Ub+u}^{*}$ are respectively given as

$$\frac{1}{\sqrt{\lambda}}\left[\underbrace{d_i(M-\nu),...,d_i(M-1)}_{CP},\underbrace{d_i(0),d_i(1),...,d_i(M-1)}_{\{d_i(m)\}_{m=0}^{M-1}},\underbrace{d_i(0),d_i(1),...d_i(M-1)}_{\{d_i(m)\}_{m=0}^{M-1}}\right], \tag{5.33}$$

and

$$\frac{1}{\sqrt{\lambda}}\left[\underbrace{d_i^*(\nu),...,d_i^*(1)}_{CP},\underbrace{d_i^*(0),d_i^*(M-1),...,d_i^*(1)}_{\{d_i^*(mod(-m,M))\}_{m=0}^{M-1}},\underbrace{d_i^*(0),d_i^*(M-1),...d_i^*(1)}_{\{d_i^*(mod(-m,M))\}_{m=0}^{M-1}}\right]. \tag{5.34}$$

Note that there is a repetition of the symbols (twice for $\lambda = 2$) in each transmitted block. By taking this into account and following the analysis in [27], it can be shown that

- When $i = 2b$, $s_i^{(0,\tau)}(n) = s_{i+1}^{(1,\tau)^*}(n' = mod(-(n-\nu),N)+\nu)$ if n and τ satisfy $n + n' = 2\nu,\ N + 2\nu$ and $n \pm N/2 + n' + 2\tau = 2\nu,\ N+\nu$. Note that the term $N/2$ appears due to the repetition in the transmitted block ($\lambda = 2$). If $n + n' = 2\nu$ and

$n+N/2+n'+2\tau = N+2\nu$, then $\tau = N/4$, $n = 0, 1, .., \nu$, $N/4+\nu-1, ..., 3N/4+\nu-1$. Furthermore, if $n + n' = 2\nu$ and $n - N/2 + n' + 2\tau = N + 2\nu$, then $\tau = 3N/4$, $n = 0, 1, .., \nu$. For the other cases, one can see that either the value of τ or n is out of range. For example, if $n + n' = N + 2\nu$ and $n + N/2 + n' + 2\tau = 2\nu$, then $\tau = -3N/4$, which is out of range.

- When $i = 2b - 1$, $s_i^{(0,\tau)}(n) = s_{i+1}^{(1,\tau)^*}(n' = mod(-(n-\nu), N) + \nu)$ if n and τ satisfy $n + n' = 2\nu,\ N + 2\nu$ and $n \pm N/2 + n' + 2\tau - 2N - 2\nu = 2\nu,\ N + 2\nu$. If both $n + n'$ and $n + N/2 + n' + 2\tau - 2N - 2\nu$ are either equal to 2ν or $N + 2\nu$, then $\tau = 3N/4 + \nu$, $n = N/4, ..., 3N/4 + 2\nu$. For the other cases, it can be easily shown that either the value of τ or n is out of range.

It is worth noting that when $\lambda > 2$, one can show that a λ time repetition of the symbols occurs in (5.33) and (5.34). By following the above analysis, it can be shown that (5.8) holds for more and possibly different values of τ.

Appendix C:

Proof of the variance σ_ϵ^2

The proof for the variance σ_ϵ^2 given in (5.25) is provided in this appendix.[8] The fourth-order statistic $\mathcal{A}_r(\tau)$ when there are no statistically significant peaks can be estimated as

$$\hat{\mathcal{A}'}_r(\tau) = \frac{1}{N_B} \sum_{i=0}^{N_B-1} \left[\boldsymbol{r}_i^{(\tau)} \circ \boldsymbol{r}_i^{(\tau)}\right] \left[\bar{\boldsymbol{r}}_{i+4}^{(\tau)} \circ \bar{\boldsymbol{r}}_{i+4}^{(\tau)}\right]^T. \tag{5.35}$$

Note that both $\left[\boldsymbol{r}_i^{(\tau)} \circ \boldsymbol{r}_i^{(\tau)}\right]$ and $\left[\bar{\boldsymbol{r}}_{i+4}^{(\tau)} \circ \bar{\boldsymbol{r}}_{i+4}^{(\tau)}\right]$ are $(N+\nu)$-length vectors whose components are independent and expressed by $(y^{(\tau)}(k+i(N+\nu)))^2$ and $(y^{(\tau)}(k+(i+4)(N+\nu)))^2$,

[8] Through extensive simulations, it was noticed that σ_ϵ^2 has similar values for both SM and AL SC-FDMA signals when $\tau \notin \Lambda$; hence, and due to simplicity, the analytical results are obtained for the SM SC-FDMA signal.

$k = 0, 1, ..., N + \nu - 1$, respectively.

According to (5.4), and taking into account that the symbols in the vectors $\boldsymbol{r}_i^{(\tau)}$ and $\boldsymbol{r}_{i+4}^{(\tau)}$ are independent, it can be shown that

$$\begin{aligned}
\sigma_\epsilon^2 &= var\left[\hat{\mathcal{A}'}_r(\tau)\right] \\
&= var\left[\frac{1}{N_B}\sum_{i=0}^{N_B-1}\left[\boldsymbol{r}_i^{(\tau)} \circ \boldsymbol{r}_i^{(\tau)}\right]\left[\bar{\boldsymbol{r}}_{i+4}^{(\tau)} \circ \bar{\boldsymbol{r}}_{i+4}^{(\tau)}\right]^T\right] \\
&= var\left[\frac{1}{N_B}\sum_{k=0}^{N+\nu-1}\sum_{i=0}^{N_B-1}\left(y^{(\tau)}(k+i(N+\nu))\right)^2\left(y^{(\tau)}(k+(i+4)(N+\nu))\right)^2\right] \\
&= \frac{N+\nu}{N_B^2}\sum_{i=0}^{N_B-1} var\left[\left(y^{(\tau)}(k+i(N+\nu))\right)^2\left(y^{(\tau)}(k+(i+4)(N+\nu))\right)^2\right],
\end{aligned} \tag{5.36}$$

where $var[\cdot]$ denotes the variance of a random variable.

By using that $y^{(\tau)}(k) = y(k+\tau)$ along with (5.4), it is easy to express $\left[\left(y^{(\tau)}(k+i(N+\nu))\right)^2\left(y^{(\tau)}(k+(i+4)(N+\nu))\right)^2\right]$, in terms of the channel coefficients, transmitted sequence, and noise, and after some mathematical manipulations, to obtain the expression in (5.25) for σ_ϵ^2.

References

[1] A. Gorcin and H. Arslan, "Signal identification for adaptive spectrum hyperspace access in wireless communications systems," *IEEE Commun. Mag.*, vol. 52, pp. 134–145, Oct. 2014.

[2] O. A. Dobre, A. Abdi, Y. Bar-Ness, and W. Su, "Survey of automatic modulation classification techniques: Classical approaches and new trends," *IET Commun.*,

vol. 1, pp. 137–156, Apr. 2007.

[3] J. L. Xu, W. Su, and M. Zhou, "Software-defined radio equipped with rapid modulation recognition," *IEEE Trans. Veh. Technol.*, vol. 59, pp. 1659–1667, May 2010.

[4] O. A. Dobre, "Signal identification for emerging intelligent radios: Classical problems and new challenges," *IEEE Instrum. Meas. Mag.*, vol. 18, pp. 11–18, Apr. 2015.

[5] B. Wang and K. Liu, "Advances in cognitive radio networks: A survey," *IEEE J. Sel. Topics Signal Process.*, vol. 5, pp. 5–23, Feb. 2011.

[6] A. Swami and B. M. Sadler, "Hierarchical digital modulation classification using cumulants," *IEEE Trans. Commun.*, vol. 48, pp. 416–429, Mar. 2000.

[7] H.-C. Wu, M. Saquib, and Z. Yun, "Novel automatic modulation classification using cumulant features for communications via multipath channels," *IEEE Trans. Wireless Commun.*, vol. 7, pp. 3098–3105, Aug. 2008.

[8] K. Hassan, I. Dayoub, W. Hamouda, and M. Berbineau, "Automatic modulation recognition using wavelet transform and neural networks in wireless systems," *EURASIP J. Adv. Sig. Proc.*, vol. 2010, pp. 1–13, 2010.

[9] A. Punchihewa, Q. Zhang, O. A. Dobre, C. Spooner, S. Rajan, and R. Inkol, "On the cyclostationarity of OFDM and single carrier linearly digitally modulated signals in time dispersive channels: theoretical developments and application," *IEEE Trans. Wireless Commun.*, vol. 9, pp. 2588–2599, Aug. 2010.

[10] Q. Zhang, O. A. Dobre, Y. A. Eldemerdash, S. Rajan, and R. Inkol, "Second-order cyclostationarity of BT-SCLD signals: Theoretical developments and applications to signal classification and blind parameter estimation," *IEEE Trans. Wireless Commun.*, vol. 12, pp. 1501–1511, Apr. 2013.

[11] A. Al-Habashna, O. A. Dobre, R. Venkatesan, and D. C. Popescu, "Second-order cyclostationarity of mobile WiMAX and LTE OFDM signals and application to spectrum awareness in cognitive radio systems," *IEEE J. Sel. Topics Signal Process.*, vol. 6, pp. 26–42, Feb. 2012.

[12] W. A. Jerjawi, Y. A. Eldemerdash, and O. A. Dobre, "Second-order cyclostationarity-based detection of LTE SC-FDMA signals for cognitive radio systems," *IEEE Trans. Instrum. Meas.*, vol. 64, pp. 823–833, Mar. 2015.

[13] V. Choqueuse, S. Azou, K. Yao, and G. Burel, " Blind modulation recognition for MIMO systems," *J. Military Technical Academy Review*, vol. XIX, pp. 183–196, Jun. 2009.

[14] K. Hassan, I. Dayoub, W. Hamouda, C. N. Nzeza, and M. Berbineau, "Blind digital modulation identification for spatially-correlated MIMO systems," *IEEE Trans. Wireless Commun.*, vol. 11, pp. 683–693, Feb. 2012.

[15] M. S. Mühlhaus, M. Öner, O. A. Dobre, and F. K. Jondral, "A low complexity modulation classification algorithm for MIMO systems," *IEEE Commun. Lett.*, vol. 17, pp. 1881–1884, Oct. 2013.

[16] H. Agirman-Tosun, Y. Liu, A. M. Haimovich, O. Simeone, W. Su, J. Dabin, and E. Kanterakis, "Modulation classification of MIMO-OFDM signals by independent component analysis and support vector machines," in *Proc. IEEE ASILOMAR*, 2011, pp. 1903–1907.

[17] M. Shi, Y. Bar-Ness, and W. Su, "Adaptive estimation of the number of transmit antennas," in *Proc. IEEE MILCOM*, 2007, pp. 1–5.

[18] K. Hassan, C. N. Nzeza, R. Gautier, E. Radoi, M. Berbineau, and I. Dayoub, "Blind detection of the number of transmitting antennas for spatially-correlated MIMO systems," in *Proc. IEEE ITST*, 2011, pp. 458–462.

[19] M. Mohammadkarimi, E. Karami, and O. A. Dobre, "A novel algorithm for blind detection of the number of transmit antennas," in *Proc. CROWNCOM*, 2015.

[20] E. Ohlmer, T.-J. Liang, and G. Fettweis, "Algorithm for detecting the number of transmit antennas in MIMO-OFDM systems," in *Proc. IEEE VTC Spring*, 2008, pp. 478–482.

[21] V. Choqueuse, M. Marazin, L. Collin, K. C. Yao, and G. Burel, "Blind recognition of linear space–time block codes: A likelihood-based approach," *IEEE Trans. Signal Process.*, vol. 58, pp. 1290–1299, Mar. 2010.

[22] V. Choqueuse, K. Yao, L. Collin, and G. Burel, "Hierarchical space-time block code recognition using correlation matrices," *IEEE Trans. Wireless Commun.*, vol. 7, pp. 3526–3534, Sep. 2008.

[23] Y. A. Eldemerdash, M. Marey, O. A. Dobre, G. Karagiannidis, and R. Inkol, "Fourth-order statistics for blind classification of spatial multiplexing and Alamouti space-time block code signals," *IEEE Trans. Commun.*, vol. 61, pp. 2420–2431, Jun. 2013.

[24] M. Mohammadkarimi and O. A. Dobre, "Blind identification of spatial multiplexing and Alamouti space-time block code via Kolmogorov-Smirnov (KS) test," *IEEE Commun. Lett.*, vol. 18, pp. 1711–1714, Oct. 2014.

[25] E. Karami and O. A. Dobre, "Identification of SM-OFDM and AL-OFDM signals based on their second-order cyclostationarity," *IEEE Trans. Veh. Technol.*, vol. 64, pp. 942–953, Mar. 2015.

[26] M. Marey, O. A. Dobre, and R. Inkol, "Blind STBC identification for multiple-antenna OFDM systems," *IEEE Trans. Commun.*, vol. 62, pp. 1554–1567, May 2014.

[27] Y. A. Eldemerdash, O. A. Dobre, and B. J. Liao, "Blind identification of SM and Alamouti STBC-OFDM signals," *IEEE Trans. Wireless Commun.*, vol. 14, pp. 972–982, Feb. 2015.

[28] A. Ghosh and R. Ratasuk, *Essentials of LTE and LTE-A*. Cambridge University Press, 2011.

[29] H. G. Myung and D. J. Goodman, *Single Carrier FDMA: A New Air Interface for Long Term Evolution*. Wiley, 2008, vol. 8.

[30] S. M. Kay, *Fundamentals of Statistical Signal Processing: Estimation Theory* . Prentice Hall, 1993.

[31] D. R. Brillinger, *Time Series: Data Analysis and Theory*. Society for Industrial and Applied Mathematics, 2001.

[32] A. Papoulis and S. Pillai, *Probability, Random Variables and Stochastic Processes*. McGraw-Hill, 2001.

[33] D. Watkins, *Fundamentals of Matrix Computations*. Wiley, 2002.

[34] P. Cantrell and A. Ojha, "Comparison of generalized q-function algorithms (corresp.)," *IEEE Trans. Inf. Theory*, vol. 33, pp. 591–596, Jul. 1987.

[35] M. Patzold, A. Szczepanski, and N. Youssef, "Methods for modeling of specified and measured multipath power-delay profiles," *IEEE Trans. Veh. Technol.*, vol. 51, pp. 978–988, Sep. 2002.

Chapter 6

Conclusions

In this final chapter, we summarize the contributions presented in the dissertation and discuss several potential extensions to our work.

6.1 Conclusions

The following conclusions can be drawn from the dissertation:

- For the STBC identification capability of a radio equipped with a single receive antenna for single carrier (SC) systems, it was shown that the fourth-order moment (FOM) and the discrete Fourier transform (DFT) of a fourth-order lag product (FOLP) can be efficiently used to blindly identify spatial multiplexing (SM) and Alamouti STBCs. Based on this result, four identification algorithms were proposed. The first algorithm is FOM-based and employs the likelihood ratio test (LRT) for decision-making. Unfortunately, its practical implementation is complicated by the requirement for knowledge of the channel coefficients, modulation, and noise power. To avoid this requirement, we further proposed three algorithms which are based on the DFT of the FOLP and are referred to as the FOLP-based algo-

rithms, named FOLP-A, -B, and -C. Their common idea is that the DFT of the FOLP exhibits peaks at certain frequencies for the AL-STBC signals, but not for the SM-STBC signal. Different decision criteria on the presence of such peaks are used for the three algorithms. In particular, the position of the maximum value of the DFT of the FOLP, comparison with a threshold that corresponds to a certain probability of false alarm, and the distance between the two maximum values of the DFT of the FOLP are employed for the FOLP-A, -B, and -C algorithms, respectively. We investigated the performance of the proposed algorithms in the presence of diverse model mismatches, such as spatially correlated fading and time and frequency offsets. It was shown that the FOLP-C algorithm is more robust to the frequency offset impairment when compared with the other algorithms. Moreover, the FOLP algorithms have lower sensitivity to timing offset when compared with the FOM algorithm. A significant performance enhancement is provided by the proposed algorithms when compared with algorithms in the literature.

- The FOLP-C approach was extended to include more STBCs. The proposed algorithm shows a good performance and robustness to the frequency offset impairment.

- We investigated the problem of STBC identification for OFDM systems with multiple receive antenna, $N_r \geq 2$. It was shown that the second-order cross-correlation function can be used as a discriminating feature to identify SM-OFDM and AL-OFDM signals. The proposed algorithm requires neither modulation identification nor estimation of the channel coefficients and noise power. Further, it outperforms algorithms in the literature, needs a reduced observation period, and is less sensitive to the frequency offset impairment. Moreover, it has a low sensitivity to timing offset.

- We addressed the problem of STBC identification for SC-FDMA signals. A fourth-

order statistic was employed as a discriminating feature, and a novel constant false alarm decision criterion was developed based on the statistical properties of the feature estimate. The theoretical performance analysis of the proposed algorithm was presented. The proposed algorithm achieves a good identification performance with the advantages of not requiring a priori knowledge of the transmission parameters. The proposed algorithm has a low sensitivity to the timing offset, while for the frequency offset it is more sensitive.

6.2 Possible Directions of Research

As the work on the identification of signals transmitted with multiple antennas is only at an early stage, there can be different directions to extend our work, which can be briefly outlined as follows:

- The parameters describing the MIMO signals, e.g., STBC, modulation scheme, and number of transmit antennas, are identified separately in the literature; it may be worth exploring the joint identification of STBC with other parameters.

- The work devoted to STBC-OFDM signal identification assumes multiple receive antennas. Studying such a problem for a single receive antenna scenario would be of interest.

- Most signal identification approaches proposed for MIMO systems consider generic signals. As MIMO systems are already adopted in several wireless standards, such as LTE and LTE-A, exploiting the characteristics imposed by the employed communication standard may provide additional information for the purpose of signal identification.

- As new and innovative transmission techniques emerge within the context of MIMO, the existing MIMO signal identification methodologies would need to be extended to include those. Spatial modulation [1–3] and filter bank multicarrier (FBMC) [4,5] are two promising transmission methods that have been drawing considerable interest. Spatial modulation exploits the space dimension in a novel way, by mapping part of the information bits on the transmit antenna indices. FBMC, on the other hand, can be considered as a multicarrier transmission methodology that, unlike OFDM, does not require a cyclic prefix, increasing the spectral efficiency of the transmission. Both previously mentioned transmission techniques present new challenges to signal identification, which would need to be addressed, especially since they are considered for 5G systems.

References

[1] R. Y. Mesleh, H. Haas, S. Sinanovic, C. W. Ahn, and S. Yun, "Spatial modulation," *IEEE Trans. Veh. Technol.*, vol. 57, pp. 2228–2241, Jul. 2008.

[2] E. Basar, U. Aygolu, E. Panayirci, and H. V. Poor, "Space-time block coded spatial modulation," *IEEE Trans. Commun.*, vol. 59, pp. 823–832, Mar. 2011.

[3] P. Yang, M. Di Renzo, Y. Xiao, S. Li, and L. Hanzo, "Design guidelines for spatial modulation," *IEEE Commun. Surveys Tuts.*, vol. 17, pp. 6–26, Mar. 2015.

[4] H. Saeedi-Sourck, Y. Wu, J. W. Bergmans, S. Sadri, and B. Farhang-Boroujeny, "Complexity and performance comparison of filter bank multicarrier and OFDM in uplink of multicarrier multiple access networks," *IEEE Trans. Signal Process.*, vol. 59, pp. 1907–1912, Apr. 2011.

[5] B. Farhang-Boroujeny, "OFDM versus filter bank multicarrier," *IEEE Signal Process. Mag.*, vol. 28, pp. 92–112, May 2011.

References

Chapter 1

[1] S. Haykin, "Cognitive radio: brain-empowered wireless communications," *IEEE J. Sel. Areas Commun.*, vol. 23, pp. 201–220, Feb. 2005.

[2] B. Wang and K. Liu, "Advances in cognitive radio networks: A survey," *IEEE J. Sel. Topics Signal Process.*, vol. 5, pp. 5–23, Feb. 2011.

[3] D. Cabric, "Cognitive Radios: System Design Perspective," Ph.D. dissertation, University of California, Berkeley, USA, 2007.

[4] T. Yucek and H. Arslan, "A survey of spectrum sensing algorithms for cognitive radio applications," *IEEE Commun. Surveys Tuts.*, vol. 11, pp. 116–130, Mar. 2009.

[5] H. Celebi, I. Guvenc, S. Gezici, and H. Arslan, "Cognitive-radio systems for spectrum, location, and environmental awareness," *IEEE Antennas Propag. Mag.*, vol. 52, pp. 41–61, Aug. 2010.

[6] E. Axell, G. Leus, E. G. Larsson, and H. Poor, "Spectrum sensing for cognitive radio: State-of-the-art and recent advances," *IEEE Signal Process. Mag.*, vol. 29, pp. 101–116, May 2012.

[7] J. L. Xu, W. Su, and M. Zhou, "Software-defined radio equipped with rapid modulation recognition," *IEEE Trans. Veh. Technol.*, vol. 59, pp. 1659–1667, May 2010.

[8] O. A. Dobre, A. Abdi, Y. Bar-Ness, and W. Su, "Survey of automatic modulation classification techniques: Classical approaches and new trends," *IET Commun.*, vol. 1, pp. 137–156, Apr. 2007.

[9] F. Hameed, O. Dobre, and D. Popescu, "On the likelihood-based approach to modulation classification," *IEEE Trans. Wireless Commun.*, vol. 8, pp. 5884–5892, Dec. 2009.

[10] Q. Shi and Y. Karasawa, "Noncoherent maximum likelihood classification of quadrature amplitude modulation constellations: Simplification, analysis, and extension," *IEEE Trans. Wireless Commun.*, vol. 10, pp. 1312–1322, Apr. 2011.

[11] A. Swami and B. M. Sadler, "Hierarchical digital modulation classification using cumulants," *IEEE Trans. Commun.*, vol. 48, pp. 416–429, Mar. 2000.

[12] H.-C. Wu, M. Saquib, and Z. Yun, "Novel automatic modulation classification using cumulant features for communications via multipath channels," *IEEE Trans. Wireless Commun.*, vol. 7, pp. 3098–3105, Aug. 2008.

[13] M. Pedzisz and A. Mansour, "Automatic modulation recognition of MPSK signals using constellation rotation and its 4th order cumulant," *Elsevier: Digital Signal Processing*, vol. 15, pp. 295–304, Jan. 2005.

[14] W. Su, "Feature space analysis of modulation classification using very high-order statistics," *IEEE Commun. Lett.*, vol. 17, pp. 1688–1691, Sep. 2013.

[15] O. A. Dobre, M. Oner, S. Rajan, and R. Inkol, "Cyclostationarity-based robust algorithms for QAM signal identification," *IEEE Commun. Lett.*, vol. 16, pp. 12–15, Jan. 2012.

[16] K. Hassan, I. Dayoub, W. Hamouda, and M. Berbineau, "Automatic modulation recognition using wavelet transform and neural networks in wireless systems," *EURASIP J. Adv. Sig. Proc.*, vol. 2010, pp. 1–13, 2010.

[17] T. Yucek and H. Arslan, "Ofdm signal identification and transmission parameter estimation for cognitive radio applications," in *Proc. IEEE GLOBCOM*, 2007, pp. 4056–4060.

[18] M. Shi, A. Laufer, Y. Bar-Ness, and W. Su, "Fourth order cumulants in distinguishing single carrier from ofdm signals," in *Proc. IEEE MILCOM*, 2008, pp. 1–6.

[19] A. Punchihewa, Q. Zhang, O. A. Dobre, C. Spooner, S. Rajan, and R. Inkol, "On the cyclostationarity of OFDM and single carrier linearly digitally modulated signals in time dispersive channels: theoretical developments and application," *IEEE Trans. Wireless Commun.*, vol. 9, pp. 2588–2599, Aug. 2010.

[20] P. D. Sutton, K. E. Nolan, and L. E. Doyle, "Cyclostationary signatures in practical cognitive radio applications," *IEEE J. Sel. Areas Commun.*, vol. 26, pp. 13–24, Jan. 2008.

[21] A. Al-Habashna, O. A. Dobre, R. Venkatesan, and D. C. Popescu, "Second-order cyclostationarity of mobile WiMAX and LTE OFDM signals and application to spectrum awareness in cognitive radio systems," *IEEE J. Sel. Topics Signal Process.*, vol. 6, pp. 26–42, Feb. 2012.

[22] M. Wax and T. Kailath, "Detection of signals by information theoretic criteria," *IEEE Trans. Acoust., Speech, Signal Process.*, vol. 33, pp. 387–392, Apr. 1985.

[23] S. Valaee and P. Kabal, "An information theoretic approach to source enumeration in array signal processing," *IEEE Trans. Signal Process.*, vol. 52, pp. 1171–1178, May 2004.

[24] B. Nadler, "Nonparametric detection of signals by information theoretic criteria: performance analysis and an improved estimator," *IEEE Trans. Signal Process.*, vol. 58, pp. 2746–2756, May 2010.

[25] L. Huang and S. Wu, "Low-complexity MDL method for accurate source enumeration," *IEEE Signal Process. Lett.*, vol. 14, pp. 581–584, Sep. 2007.

[26] E. Fishler, M. Grosman, and H. Messer, "Determining the number of discrete alphabet sources from sensor data," *EURASIP J. Adv. Sig. Proc.*, vol. 2005, pp. 4–12, Jan. 2005.

[27] F. Haddadi, M. Malek-Mohammadi, M. M. Nayebi, and M. R. Aref, "Statistical performance analysis of MDL source enumeration in array processing," *IEEE Trans. Signal Process.*, vol. 58, pp. 452–457, Jan. 2010.

[28] R. Nee, V. K. Jones, G. Awater, A. Zelst, J. Gardner, and G. Steele, "The 802.11n MIMO-OFDM standard for wireless LAN and beyond," *Wireless Personal Comm.*, vol. 37, pp. 445–453, May 2006.

[29] A. Ghosh and R. Ratasuk, *Essentials of LTE and LTE-A*. Cambridge University Press, 2011.

[30] V. Choqueuse, M. Marazin, L. Collin, K. C. Yao, and G. Burel, "Blind recognition of linear space–time block codes: A likelihood-based approach," *IEEE Trans. Signal Process.*, vol. 58, pp. 1290–1299, Mar. 2010.

[31] V. Choqueuse, K. Yao, L. Collin, and G. Burel, "Blind recognition of linear space time block codes," in *Proc. IEEE ICASSP*, 2008, pp. 2833–2836.

[32] V. Choqueuse, K. Yao, L. Collin, and G. Burel, "Hierarchical space-time block code recognition using correlation matrices," *IEEE Trans. Wireless Commun.*, vol. 7, pp. 3526–3534, Sep. 2008.

[33] M. Luo, L. Gan, and L. Li, "Blind recognition of space-time block code using correlation matrices in a high dimensional feature space," *J. Inf. Comput. Sci*, vol. 9, pp. 1469–1476, Jun. 2012.

[34] M. Marey, O. A. Dobre, and B. Liao, "Classification of STBC systems over frequency-selective channels," *IEEE Trans. Veh. Technol.,* DOI: 10.1109/TVT.2014.2335415, 2014.

[35] G. Qian, L. Li, M. Luo, H. Liao, and H. Zhang, "Blind recognition of space-time block code in MISO system," *EURASIP JWCN*, vol. 1, pp. 164–176, Jun. 2013.

[36] M. Shi, Y. Bar-Ness, and W. Su, "STC and BLAST MIMO modulation recognition," in *Proc. IEEE GLOBECOM*, 2007, pp. 3034–3039.

[37] M. Marey, O. A. Dobre, and R. Inkol, "Cyclostationarity-based blind classification of stbcs for cognitive radio systems," in *Proc. IEEE ICC*. IEEE, 2012, pp. 1715–1720.

[38] ——, "Classification of space-time block codes based on second-order cyclostationarity with transmission impairments," *IEEE Trans. Wireless Commun.*, vol. 11, pp. 2574–2584, Jul. 2012.

[39] A. Turan, M. Oner, and H. Cirpan, "Space time block code classification for MIMO signals exploiting cyclostationarity," *accepted in IEEE ICC*, 2015.

[40] M. DeYoung, R. Heath, and B. Evans, "Using higher order cyclostationarity to identify space-time block codes," in *Proc. IEEE GLOBECOM*, 2008, pp. 1–5.

[41] M. Mohammadkarimi and O. A. Dobre, "Blind identification of spatial multiplexing and Alamouti space-time block code via Kolmogorov-Smirnov (KS) test," *IEEE Commun. Lett.*, vol. 18, pp. 1711–1714, Oct. 2014.

[42] ——, "A novel non-parametric method for blind identification of STBC codes," in *Proc. IEEE CWIT*, 2015.

[43] M. Marey, O. A. Dobre, and R. Inkol, "Novel algorithm for stbc-ofdm identification in cognitive radios," in *Proc. IEEE ICC*. IEEE, 2013, pp. 2770–2774.

[44] ——, "Blind STBC identification for multiple-antenna OFDM systems," *IEEE Trans. Commun.*, vol. 62, pp. 1554–1567, May 2014.

[45] E. Karami and O. A. Dobre, "Identification of SM-OFDM and AL-OFDM signals based on their second-order cyclostationarity," *IEEE Trans. Veh. Technol.*, vol. 64, pp. 942–953, Mar. 2015.

[46] O. Somekh, O. Simeone, Y. Bar-Ness, and W. Su, "Detecting the number of transmit antennas with unauthorized or cognitive receivers in MIMO systems," in *Proc. IEEE MILCOM*, 2007, pp. 1–5.

[47] K. Hassan, C. N. Nzeza, R. Gautier, E. Radoi, M. Berbineau, and I. Dayoub, "Blind detection of the number of transmitting antennas for spatially-correlated MIMO systems," in *Proc. IEEE ITST*, 2011, pp. 458–462.

[48] M. Shi, Y. Bar-Ness, and W. Su, "Adaptive estimation of the number of transmit antennas," in *Proc. IEEE MILCOM*, 2007, pp. 1–5.

[49] K. Hassan, I. Dayoub, W. Hamouda, C. N. Nzeza, and M. Berbineau, "Blind digital modulation identification for spatially-correlated MIMO systems," *IEEE Trans. Wireless Commun.*, vol. 11, pp. 683–693, Feb. 2012.

[50] M. S. Mühlhaus, M. Öner, O. A. Dobre, H. U. Jäkel, and F. K. Jondral, "Automatic modulation classification for MIMO systems using fourth-order cumulants," in *Proc. IEEE VTC(Fall)*, 2012, pp. 1–5.

[51] M. Muhlhaus, M. Oner, O. A. Dobre, H. Jakel, and F. K. Jondral, "A novel algorithm for mimo signal classification using higher-order cumulants," in *Proc. IEEE RWS*, 2013, pp. 7–9.

[52] M. S. Mühlhaus, M. Öner, O. A. Dobre, and F. K. Jondral, "A low complexity modulation classification algorithm for MIMO systems," *IEEE Commun. Lett.*, vol. 17, pp. 1881–1884, Oct. 2013.

[53] S. Kharbech, I. Dayoub, M. Zwingelstein-Colin, E. Simon, and K. Hassan, "Blind digital modulation identification for time-selective mimo channels," *IEEE Wireless Commun. lett.*, vol. 3, pp. 373–376, Aug. 2014.

[54] J. Vía and I. Santamaría, "Correlation matching approaches for blind ostbc channel estimation," *IEEE Trans. Signal Process.*, vol. 56, pp. 5950–5961, Aug. 2008.

[55] V. Choqueuse, A. Mansour, G. Burel, L. Collin, and K. Yao, "Blind channel estimation for STBC systems using higher-order statistics," *IEEE Trans. Wireless Commun.*, vol. 10, pp. 495–505, Feb. 2011.

[56] A. V. Dandawate and G. B. Giannakis, "Statistical tests for presence of cyclostationarity," *IEEE Trans. Signal Process.*, vol. 42, pp. 2355–2369, Sep. 1994.

[57] J. Lundén, V. Koivunen, A. Huttunen, and H. V. Poor, "Spectrum sensing in cognitive radios based on multiple cyclic frequencies," in *Proc. IEEE CrownCom*, 2007, pp. 37–43.

[58] J.-F. Cardoso and A. Souloumiac, "Blind beamforming for non-gaussian signals," in *Proc. IEE FRSP)*, vol. 140, no. 6, 1993, pp. 362–370.

[59] Y. G. Li, J. H. Winters, and N. R. Sollenberger, "MIMO-OFDM for wireless communications: signal detection with enhanced channel estimation," *IEEE Trans. Commun.*, vol. 50, pp. 1471–1477, Sep. 2002.

Chapter 2

[1] B. Wang and K. Liu, "Advances in cognitive radio networks: A survey," *IEEE J. Sel. Topics Signal Process.*, vol. 5, pp. 5–23, Feb. 2011.

[2] A. B. MacKenzie et al. , "Cognitive radio and networking research at Virginia Tech," *Proc. of the IEEE, invited paper*, vol. 97, pp. 660–688, Apr. 2009.

[3] D. Cabric, "Cognitive Radios: System Design Perspective," Ph.D. dissertation, University of California, Berkeley, USA, 2007.

[4] D. Cabric, S. Mishra, and R. Brodersen, "Implementation issues in spectrum sensing for cognitive radios," in *Proc. IEEE ASILOMAR*, 2004, pp. 772–776.

[5] T. Yucek and H. Arslan, "A survey of spectrum sensing algorithms for cognitive radio applications," *IEEE Commun. Surveys Tuts.*, vol. 11, pp. 116–130, Mar. 2009.

[6] Y. Zheng, Y.-C. Liang, A. T. Hoang, and R. Zhang, "A review on spectrum sensing for cognitive radio: Challenges and solutions," *EURASIP J. Adv. Sig. Proc.,* DOI:10.1155/2010/381465, 2010.

[7] E. Axell, G. Leus, E. G. Larsson, and H. Poor, "Spectrum sensing for cognitive radio: State-of-the-art and recent advances," *IEEE Signal Process. Mag.*, vol. 29, pp. 101–116, May 2012.

[8] O. A. Dobre, A. Abdi, Y. Bar-Ness, and W. Su, "Survey of automatic modulation classification techniques: Classical approaches and new trends," *IET Commun.*, vol. 1, pp. 137–156, Apr. 2007.

[9] H.-C. Wu, M. Saquib, and Z. Yun, "Novel automatic modulation classification using cumulant features for communications via multipath channels," *IEEE Trans. Wireless Commun.*, vol. 7, pp. 3098–3105, Aug. 2008.

[10] M. Oner and F. Jondral, "On the extraction of the channel allocation information in spectrum pooling systems," *IEEE J. Sel. Areas Commun.*, vol. 25, pp. 558–565, Apr. 2007.

[11] A. Swami and B. M. Sadler, "Hierarchical digital modulation classification using cumulants," *IEEE Trans. Commun.*, vol. 48, pp. 416–429, Mar. 2000.

[12] A. Punchihewa, Q. Zhang, O. Dobre, C. Spooner, S. Rajan, and R. Inkol, "On the cyclostationarity of OFDM and single carrier linearly digitally modulated signals in time dispersive channels: theoretical developments and application," *IEEE Trans. Wireless Commun.*, vol. 9, pp. 2588–2599, Aug. 2010.

[13] F. Hameed, O. Dobre, and D. Popescu, "On the likelihood-based approach to modulation classification," *IEEE Trans. Wireless Commun.*, vol. 8, pp. 5884–5892, Dec. 2009.

[14] V. Chavali and C. R. da Silva, "Maximum-likelihood classification of digital amplitude-phase modulated signals in flat fading non-gaussian channels," *IEEE Trans. Commun.*, vol. 59, pp. 2051–2056, Aug. 2011.

[15] W. C. Headley and C. R. da Silva, "Asynchronous classification of digital amplitude-phase modulated signals in flat-fading channels," *IEEE Trans. Commun.*, vol. 59, pp. 7–12, Jan. 2011.

[16] A. Al-Habashna, O. A. Dobre, R. Venkatesan, and D. C. Popescu, "Second-order cyclostationarity of mobile WiMAX and LTE OFDM signals and application to spectrum awareness in cognitive radio systems," *IEEE J. Sel. Topics Signal Process.*, vol. 6, pp. 26–42, Feb. 2012.

[17] M. Shi, Y. Bar-Ness, and W. Su, "Adaptive estimation of the number of transmit antennas," in *Proc. IEEE MILCOM*, 2007, pp. 1–5.

[18] O. Somekh, O. Simeone, Y. Bar-Ness, and W. Su, "Detecting the number of transmit antennas with unauthorized or cognitive receivers in MIMO systems," in *Proc. IEEE MILCOM*, 2007, pp. 1–5.

[19] V. Choqueuse, S. Azou, K. Yao, and G. Burel, " Blind modulation recognition for MIMO systems," *J. Military Technical Academy Review*, vol. XIX, pp. 183–196, Jun. 2009.

[20] K. Hassan, I. Dayoub, W. Hamouda, C. N. Nzeza, and M. Berbineau, "Blind digital modulation identification for spatially-correlated MIMO systems," *IEEE Trans. Wireless Commun.*, vol. 11, pp. 683–693, Feb. 2012.

[21] V. Choqueuse, M. Marazin, L. Collin, K. C. Yao, and G. Burel, "Blind recognition of linear space–time block codes: A likelihood-based approach," *IEEE Trans. Signal Process.*, vol. 58, pp. 1290–1299, Mar. 2010.

[22] V. Choqueuse, K. Yao, L. Collin, and G. Burel, "Hierarchical space-time block code recognition using correlation matrices," *IEEE Trans. Wireless Commun.*, vol. 7, pp. 3526–3534, Sep. 2008.

[23] V. Choqueuse, K. Yao, L. Collin, and G. Burel, "Blind recognition of linear space time block codes," in *Proc. IEEE ICASSP*, 2008, pp. 2833–2836.

[24] M. Shi, Y. Bar-Ness, and W. Su, "STC and BLAST MIMO modulation recognition," in *Proc. IEEE GLOBECOM*, 2007, pp. 3034–3039.

[25] M. Marey, O. A. Dobre, and R. Inkol, "Classification of space-time block codes based on second-order cyclostationarity with transmission impairments," *IEEE Trans. Wireless Commun.*, vol. 11, pp. 2574–2584, Jul. 2012.

[26] M. DeYoung, R. Heath, and B. Evans, "Using higher order cyclostationarity to identify space-time block codes," in *Proc. IEEE GLOBECOM*, 2008, pp. 1–5.

[27] M. Jankiraman, *Space-Time Codes and MIMO Systems*. Artech House, 2004.

[28] V. Tarokh, H. Jafarkhani, and A. R. Calderbank, "Space-time block codes from orthogonal designs," *IEEE Trans. Inf. Theory*, vol. 45, pp. 1456–1467, Jul. 1999.

[29] S. M. Alamouti, "A simple transmit diversity technique for wireless communications," *IEEE J. Sel. Areas Commun.*, vol. 16, pp. 1451–1458, Oct. 1998.

[30] J. Mendel, "Tutorial on higher-order statistics (spectra) in signal processing and system theory: Theoretical results and some applications," *Proceedings of the IEEE*, vol. 79, pp. 278–305, Mar. 1991.

[31] D. R. Brillinger, *Time Series: Data Analysis and Theory*. Society for Industrial and Applied Mathematics, 2001.

[32] J. G. Proakis and M. Salehi, *Communication Systems Engineering*. Prentice Hall, 2002.

[33] P. J. Davis, and P. Rabinowitz, *Methods of Numerical Integration*. Academic Press, 1975, vol. 1.

[34] H. Van Trees, *Detection, Estimation, and Modulation Theory: Detection, Estimation, and Linear Modulation Theory*. Wiley, 2001.

[35] A. Papoulis and S. Pillai, *Probability, Random Variables and Stochastic Processes*. McGraw-Hill, 2001.

[36] N. C. Beaulieu and C. Cheng, "Efficient Nakagami-m fading channel simulation," *IEEE Trans. Veh. Technol.*, vol. 54, pp. 413–424, Mar. 2005.

[37] D. Watkins, *Fundamentals of Matrix Computations*. Wiley, 2002.

[38] M. E. Johnson, *Multivariate Statistical Simulation*. Wiley, 1987.

Chapter 3

[1] J. L. Xu, W. Su, and M. Zhou, "Software-defined radio equipped with rapid modulation recognition," *IEEE Trans. Veh. Technol.*, vol. 59, pp. 1659–1667, May 2010.

[2] T. Yucek and H. Arslan, "A survey of spectrum sensing algorithms for cognitive radio applications," *IEEE Commun. Surveys Tuts.*, vol. 11, pp. 116–130, Mar. 2009.

[3] O. A. Dobre, A. Abdi, Y. Bar-Ness, and W. Su, "Survey of automatic modulation classification techniques: Classical approaches and new trends," *IET Commun.*, vol. 1, pp. 137–156, Apr. 2007.

[4] L. Korowajczuk, *LTE, WiMAX and WLAN Network Design, Optimization and Performance Analysis*. Wiley, 2011.

[5] M. Shi, Y. Bar-Ness, and W. Su, "Adaptive estimation of the number of transmit antennas," in *Proc. IEEE MILCOM*, 2007, pp. 1–5.

[6] O. Somekh, O. Simeone, Y. Bar-Ness, and W. Su, "Detecting the number of transmit antennas with unauthorized or cognitive receivers in MIMO systems," in *Proc. IEEE MILCOM*, 2007, pp. 1–5.

[7] V. Choqueuse, S. Azou, K. Yao, and G. Burel, " Blind modulation recognition for MIMO systems," *J. Military Technical Academy Review*, vol. XIX, pp. 183–196, Jun. 2009.

[8] K. Hassan, I. Dayoub, W. Hamouda, C. N. Nzeza, and M. Berbineau, "Blind digital modulation identification for spatially-correlated MIMO systems," *IEEE Trans. Wireless Commun.*, vol. 11, pp. 683–693, Feb. 2012.

[9] M. S. Mühlhaus, M. Öner, O. A. Dobre, H. U. Jäkel, and F. K. Jondral, "Automatic modulation classification for MIMO systems using fourth-order cumulants," in *Proc. IEEE VTC(Fall)*, 2012, pp. 1–5.

[10] M. Muhlhaus, M. Oner, O. A. Dobre, H. Jakel, and F. K. Jondral, "A novel algorithm for mimo signal classification using higher-order cumulants," in *Proc. IEEE RWS*, 2013, pp. 7–9.

[11] V. Choqueuse, M. Marazin, L. Collin, K. C. Yao, and G. Burel, "Blind recognition of linear space–time block codes: A likelihood-based approach," *IEEE Trans. Signal Process.*, vol. 58, pp. 1290–1299, Mar. 2010.

[12] V. Choqueuse, K. Yao, L. Collin, and G. Burel, "Hierarchical space-time block code recognition using correlation matrices," *IEEE Trans. Wireless Commun.*, vol. 7, pp. 3526–3534, Sep. 2008.

[13] V. Choqueuse, K. Yao, L. Collin, and G. Burel, "Blind recognition of linear space time block codes," in *Proc. IEEE ICASSP*, 2008, pp. 2833–2836.

[14] Y. A. Eldemerdash, M. Marey, O. A. Dobre, G. Karagiannidis, and R. Inkol, "Fourth-order statistics for blind classification of spatial multiplexing and Alamouti space-time block code signals," *IEEE Trans. Commun.*, vol. 61, pp. 2420–2431, Jun. 2013.

[15] M. DeYoung, R. Heath, and B. Evans, "Using higher order cyclostationarity to identify space-time block codes," in *Proc. IEEE GLOBECOM*, 2008, pp. 1–5.

[16] M. Shi, Y. Bar-Ness, and W. Su, "STC and BLAST MIMO modulation recognition," in *Proc. IEEE GLOBECOM*, 2007, pp. 3034–3039.

[17] M. Marey, O. A. Dobre, and R. Inkol, "Classification of space-time block codes based on second-order cyclostationarity with transmission impairments," *IEEE Trans. Wireless Commun.*, vol. 11, pp. 2574–2584, Jul. 2012.

[18] E. Larsson and P. Stoica, *Space-Time Block Coding for Wireless Communication*. Cambridge Press, 2003.

[19] V. Tarokh, H. Jafarkhani, and A. R. Calderbank, "Space-time block codes from orthogonal designs," *IEEE Trans. Inf. Theory*, vol. 45, pp. 1456–1467, Jul. 1999.

[20] A. Papoulis and S. Pillai, *Probability, Random Variables and Stochastic Processes*. McGraw-Hill, 2001.

[21] N. C. Beaulieu and C. Cheng, "Efficient Nakagami-m fading channel simulation," *IEEE Trans. Veh. Technol.*, vol. 54, pp. 413–424, Mar. 2005.

[22] M. E. Johnson, *Multivariate Statistical Simulation*. Wiley, 1987.

[23] D. Watkins, *Fundamentals of Matrix Computations*. Wiley, 2002.

Chapter 4

[1] O. A. Dobre, A. Abdi, Y. Bar-Ness, and W. Su, "Survey of automatic modulation classification techniques: Classical approaches and new trends," *IET Commun.*, vol. 1, pp. 137–156, Apr. 2007.

[2] D. Cabric, "Addressing feasibility of cognitive radios," *IEEE Signal Process. Mag.*, vol. 25, pp. 85–93, Nov. 2008.

[3] J. L. Xu, W. Su, and M. Zhou, "Software-defined radio equipped with rapid modulation recognition," *IEEE Trans. Veh. Technol.*, vol. 59, pp. 1659–1667, May 2010.

[4] H.-C. Wu, M. Saquib, and Z. Yun, "Novel automatic modulation classification using cumulant features for communications via multipath channels," *IEEE Trans. Wireless Commun.*, vol. 7, pp. 3098–3105, Aug. 2008.

[5] W. Su, "Feature space analysis of modulation classification using very high-order statistics," *IEEE Commun. Lett.*, vol. 17, pp. 1688–1691, Sep. 2013.

[6] W. Su, J. L. Xu, and M. Zhou, "Real-time modulation classification based on maximum likelihood," *IEEE Commun. Lett.*, vol. 12, pp. 801–803, Nov. 2008.

[7] O. A. Dobre, M. Oner, S. Rajan, and R. Inkol, "Cyclostationarity-based robust algorithms for QAM signal identification," *IEEE Commun. Lett.*, vol. 16, pp. 12–15, Jan. 2012.

[8] D. Grimaldi, S. Rapuano, and L. De Vito, "An automatic digital modulation classifier for measurement on telecommunication networks," *IEEE Trans. Instrum. Meas.*, vol. 56, pp. 1711–1720, Oct. 2007.

[9] Q. Zhang, O. A. Dobre, Y. A. Eldemerdash, S. Rajan, and R. Inkol, "Second-order cyclostationarity of BT-SCLD signals: Theoretical developments and applications to signal classification and blind parameter estimation," *IEEE Trans. Wireless Commun.*, vol. 12, pp. 1501–1511, Apr. 2013.

[10] A. Bouzegzi, P. Ciblat, and P. Jallon, "New algorithms for blind recognition of OFDM based systems," *Elsevier Signal Processing*, vol. 90, pp. 900–913, Mar. 2010.

[11] A. Al-Habashna, O. A. Dobre, R. Venkatesan, and D. C. Popescu, "Second-order cyclostationarity of mobile WiMAX and LTE OFDM signals and application to spectrum awareness in cognitive radio systems," *IEEE J. Sel. Topics Signal Process.*, vol. 6, pp. 26–42, Feb. 2012.

[12] T. Xia and H.-C. Wu , "Blind identification of nonbinary LDPC codes using average LLR of syndrome a posteriori probability," *IEEE Commun. Lett.*, vol. 17, pp. 1301–1304, Jul. 2013.

[13] ——, "Novel blind identification of LDPC codes using average LLR of syndrome a posteriori probability," *IEEE Trans. Signal Process.*, vol. 62, pp. 632–640, Feb. 2014.

[14] ——, "Joint blind frame synchronization and encoder identification for low-density parity-check codes," *IEEE Commun. Lett.*, vol. 18, pp. 352–355, Feb. 2014.

[15] H.-C. Wu, X. Huang, and D. Xu, "Pilot-free dynamic phase and amplitude estimations for wireless ICI self-cancellation coded OFDM systems," *IEEE Trans. Broadcast.*, vol. 51, pp. 94–105, Mar. 2005.

[16] L. Korowajczuk, *LTE, WiMAX and WLAN Network Design, Optimization and Performance Analysis.* Wiley, 2011.

[17] M. Shi, Y. Bar-Ness, and W. Su, "Adaptive estimation of the number of transmit antennas," in *Proc. IEEE MILCOM*, 2007, pp. 1–5.

[18] O. Somekh, O. Simeone, Y. Bar-Ness, and W. Su, "Detecting the number of transmit antennas with unauthorized or cognitive receivers in MIMO systems," in *Proc. IEEE MILCOM*, 2007, pp. 1–5.

[19] K. Hassan, I. Dayoub, W. Hamouda, C. N. Nzeza, and M. Berbineau, "Blind digital modulation identification for spatially-correlated MIMO systems," *IEEE Trans. Wireless Commun.*, vol. 11, pp. 683–693, Feb. 2012.

[20] V. Choqueuse, S. Azou, K. Yao, and G. Burel, " Blind modulation recognition for MIMO systems," *J. Military Technical Academy Review*, vol. XIX, pp. 183–196, Jun. 2009.

[21] M. S. Mühlhaus, M. Öner, O. A. Dobre, and F. K. Jondral, "A low complexity modulation classification algorithm for MIMO systems," *IEEE Commun. Lett.*, vol. 17, pp. 1881–1884, Oct. 2013.

[22] V. Choqueuse, K. Yao, L. Collin, and G. Burel, "Hierarchical space-time block code recognition using correlation matrices," *IEEE Trans. Wireless Commun.*, vol. 7, pp. 3526–3534, Sep. 2008.

[23] V. Choqueuse, M. Marazin, L. Collin, K. C. Yao, and G. Burel, "Blind recognition of linear space–time block codes: A likelihood-based approach," *IEEE Trans. Signal Process.*, vol. 58, pp. 1290–1299, Mar. 2010.

[24] M. Marey, O. A. Dobre, and R. Inkol, "Classification of space-time block codes based on second-order cyclostationarity with transmission impairments," *IEEE Trans. Wireless Commun.*, vol. 11, pp. 2574–2584, Jul. 2012.

[25] M. Luo, L. Gan, and L. Li, "Blind recognition of space-time block code using correlation matrices in a high dimensional feature space," *J. Inf. Comput. Sci*, vol. 9, pp. 1469–1476, Jun. 2012.

[26] G. Qian, L. Li, M. Luo, H. Liao, and H. Zhang, "Blind recognition of space-time block code in MISO system," *EURASIP JWCN*, vol. 1, pp. 164–176, Jun. 2013.

[27] Y. A. Eldemerdash, M. Marey, O. A. Dobre, G. Karagiannidis, and R. Inkol, "Fourth-order statistics for blind classification of spatial multiplexing and Alamouti space-time block code signals," *IEEE Trans. Commun.*, vol. 61, pp. 2420–2431, Jun. 2013.

[28] H. Agirman-Tosun, Y. Liu, A. M. Haimovich, O. Simeone, W. Su, J. Dabin, and E. Kanterakis, "Modulation classification of MIMO-OFDM signals by independent component analysis and support vector machines," in *Proc. IEEE ASILOMAR*, 2011, pp. 1903–1907.

[29] M. Marey, O. A. Dobre, and R. Inkol, "Novel algorithm for stbc-ofdm identification in cognitive radios," in *Proc. IEEE ICC*. IEEE, 2013, pp. 2770–2774.

[30] ——, "Blind STBC identification for multiple-antenna OFDM systems," *IEEE Trans. Commun.*, vol. 62, pp. 1554–1567, May 2014.

[31] E. Karami and O. A. Dobre, "Identification of SM-OFDM and AL-OFDM signals based on their second-order cyclostationarity," *IEEE Trans. Veh. Technol.*, vol. 64, pp. 942–953, Mar. 2015.

[32] Y. G. Li, J. H. Winters, and N. R. Sollenberger, "MIMO-OFDM for wireless communications: signal detection with enhanced channel estimation," *IEEE Trans. Commun.*, vol. 50, pp. 1471–1477, Sep. 2002.

[33] A. Punchihewa, V. K. Bhargava, and C. Despins, "Blind estimation of OFDM parameters in cognitive radio networks," *IEEE Trans. Wireless Commun.*, vol. 10, pp. 733–738, Mar. 2011.

[34] S. M. Kay, *Fundamentals of Statistical Signal Processing: Estimation Theory* . Prentice Hall, 1993.

[35] D. R. Brillinger, *Time Series: Data Analysis and Theory*. Society for Industrial and Applied Mathematics, 2001.

[36] A. Papoulis and S. Pillai, *Probability, Random Variables and Stochastic Processes*. McGraw-Hill, 2001.

[37] M. K. Simon, *Probability Distributions Involving Gaussian Random Variables: A Handbook for Engineers and Scientists*. Springer, 2007.

[38] J. Stoer and R. Bulirsch, *Introduction to Numerical Analysis*. Springer, 2002.

[39] D. Watkins, *Fundamentals of Matrix Computations*. Wiley, 2002.

[40] M. Patzold, A. Szczepanski, and N. Youssef, "Methods for modeling of specified and measured multipath power-delay profiles," *IEEE Trans. Veh. Technol.*, vol. 51, pp. 978–988, Sep. 2002.

Chapter 5

[1] A. Gorcin and H. Arslan, "Signal identification for adaptive spectrum hyperspace access in wireless communications systems," *IEEE Commun. Mag.*, vol. 52, pp. 134–145, Oct. 2014.

[2] O. A. Dobre, A. Abdi, Y. Bar-Ness, and W. Su, "Survey of automatic modulation classification techniques: Classical approaches and new trends," *IET Commun.*, vol. 1, pp. 137–156, Apr. 2007.

[3] J. L. Xu, W. Su, and M. Zhou, "Software-defined radio equipped with rapid modulation recognition," *IEEE Trans. Veh. Technol.*, vol. 59, pp. 1659–1667, May 2010.

[4] O. A. Dobre, "Signal identification for emerging intelligent radios: Classical problems and new challenges," *IEEE Instrum. Meas. Mag.*, vol. 18, pp. 11–18, Apr. 2015.

[5] B. Wang and K. Liu, "Advances in cognitive radio networks: A survey," *IEEE J. Sel. Topics Signal Process.*, vol. 5, pp. 5–23, Feb. 2011.

[6] A. Swami and B. M. Sadler, "Hierarchical digital modulation classification using cumulants," *IEEE Trans. Commun.*, vol. 48, pp. 416–429, Mar. 2000.

[7] H.-C. Wu, M. Saquib, and Z. Yun, "Novel automatic modulation classification using cumulant features for communications via multipath channels," *IEEE Trans. Wireless Commun.*, vol. 7, pp. 3098–3105, Aug. 2008.

[8] K. Hassan, I. Dayoub, W. Hamouda, and M. Berbineau, "Automatic modulation recognition using wavelet transform and neural networks in wireless systems," *EURASIP J. Adv. Sig. Proc.*, vol. 2010, pp. 1–13, 2010.

[9] A. Punchihewa, Q. Zhang, O. A. Dobre, C. Spooner, S. Rajan, and R. Inkol, "On the cyclostationarity of OFDM and single carrier linearly digitally modulated signals in time dispersive channels: theoretical developments and application," *IEEE Trans. Wireless Commun.*, vol. 9, pp. 2588–2599, Aug. 2010.

[10] Q. Zhang, O. A. Dobre, Y. A. Eldemerdash, S. Rajan, and R. Inkol, "Second-order cyclostationarity of BT-SCLD signals: Theoretical developments and applications to signal classification and blind parameter estimation," *IEEE Trans. Wireless Commun.*, vol. 12, pp. 1501–1511, Apr. 2013.

[11] A. Al-Habashna, O. A. Dobre, R. Venkatesan, and D. C. Popescu, "Second-order cyclostationarity of mobile WiMAX and LTE OFDM signals and application to spectrum awareness in cognitive radio systems," *IEEE J. Sel. Topics Signal Process.*, vol. 6, pp. 26–42, Feb. 2012.

[12] W. A. Jerjawi, Y. A. Eldemerdash, and O. A. Dobre, "Second-order cyclostationarity-based detection of LTE SC-FDMA signals for cognitive radio systems," *IEEE Trans. Instrum. Meas.*, vol. 64, pp. 823–833, Mar. 2015.

[13] V. Choqueuse, S. Azou, K. Yao, and G. Burel, " Blind modulation recognition for MIMO systems," *J. Military Technical Academy Review*, vol. XIX, pp. 183–196, Jun. 2009.

[14] K. Hassan, I. Dayoub, W. Hamouda, C. N. Nzeza, and M. Berbineau, "Blind digital modulation identification for spatially-correlated MIMO systems," *IEEE Trans. Wireless Commun.*, vol. 11, pp. 683–693, Feb. 2012.

[15] M. S. Mühlhaus, M. Öner, O. A. Dobre, and F. K. Jondral, "A low complexity modulation classification algorithm for MIMO systems," *IEEE Commun. Lett.*, vol. 17, pp. 1881–1884, Oct. 2013.

[16] H. Agirman-Tosun, Y. Liu, A. M. Haimovich, O. Simeone, W. Su, J. Dabin, and E. Kanterakis, "Modulation classification of MIMO-OFDM signals by independent component analysis and support vector machines," in *Proc. IEEE ASILOMAR*, 2011, pp. 1903–1907.

[17] M. Shi, Y. Bar-Ness, and W. Su, "Adaptive estimation of the number of transmit antennas," in *Proc. IEEE MILCOM*, 2007, pp. 1–5.

[18] K. Hassan, C. N. Nzeza, R. Gautier, E. Radoi, M. Berbineau, and I. Dayoub, "Blind detection of the number of transmitting antennas for spatially-correlated MIMO systems," in *Proc. IEEE ITST*, 2011, pp. 458–462.

[19] M. Mohammadkarimi, E. Karami, and O. A. Dobre, "A novel algorithm for blind detection of the number of transmit antennas," in *Proc. CROWNCOM*, 2015.

[20] E. Ohlmer, T.-J. Liang, and G. Fettweis, "Algorithm for detecting the number of transmit antennas in MIMO-OFDM systems," in *Proc. IEEE VTC Spring*, 2008, pp. 478–482.

[21] V. Choqueuse, M. Marazin, L. Collin, K. C. Yao, and G. Burel, "Blind recognition of linear space–time block codes: A likelihood-based approach," *IEEE Trans. Signal Process.*, vol. 58, pp. 1290–1299, Mar. 2010.

[22] V. Choqueuse, K. Yao, L. Collin, and G. Burel, "Hierarchical space-time block code recognition using correlation matrices," *IEEE Trans. Wireless Commun.*, vol. 7, pp. 3526–3534, Sep. 2008.

[23] Y. A. Eldemerdash, M. Marey, O. A. Dobre, G. Karagiannidis, and R. Inkol, "Fourth-order statistics for blind classification of spatial multiplexing and Alamouti space-time block code signals," *IEEE Trans. Commun.*, vol. 61, pp. 2420–2431, Jun. 2013.

[24] M. Mohammadkarimi and O. A. Dobre, "Blind identification of spatial multiplexing and Alamouti space-time block code via Kolmogorov-Smirnov (KS) test," *IEEE Commun. Lett.*, vol. 18, pp. 1711–1714, Oct. 2014.

[25] E. Karami and O. A. Dobre, "Identification of SM-OFDM and AL-OFDM signals based on their second-order cyclostationarity," *IEEE Trans. Veh. Technol.*, vol. 64, pp. 942–953, Mar. 2015.

[26] M. Marey, O. A. Dobre, and R. Inkol, "Blind STBC identification for multiple-antenna OFDM systems," *IEEE Trans. Commun.*, vol. 62, pp. 1554–1567, May 2014.

[27] Y. A. Eldemerdash, O. A. Dobre, and B. J. Liao, "Blind identification of SM and Alamouti STBC-OFDM signals," *IEEE Trans. Wireless Commun.*, vol. 14, pp. 972–982, Feb. 2015.

[28] A. Ghosh and R. Ratasuk, *Essentials of LTE and LTE-A*. Cambridge University Press, 2011.

[29] H. G. Myung and D. J. Goodman, *Single Carrier FDMA: A New Air Interface for Long Term Evolution*. Wiley, 2008, vol. 8.

[30] S. M. Kay, *Fundamentals of Statistical Signal Processing: Estimation Theory* . Prentice Hall, 1993.

[31] D. R. Brillinger, *Time Series: Data Analysis and Theory*. Society for Industrial and Applied Mathematics, 2001.

[32] A. Papoulis and S. Pillai, *Probability, Random Variables and Stochastic Processes*. McGraw-Hill, 2001.

[33] D. Watkins, *Fundamentals of Matrix Computations*. Wiley, 2002.

[34] P. Cantrell and A. Ojha, "Comparison of generalized q-function algorithms (corresp.)," *IEEE Trans. Inf. Theory*, vol. 33, pp. 591–596, Jul. 1987.

[35] M. Patzold, A. Szczepanski, and N. Youssef, "Methods for modeling of specified and measured multipath power-delay profiles," *IEEE Trans. Veh. Technol.*, vol. 51, pp. 978–988, Sep. 2002.

Chapter 6

[1] R. Y. Mesleh, H. Haas, S. Sinanovic, C. W. Ahn, and S. Yun, "Spatial modulation," *IEEE Trans. Veh. Technol.*, vol. 57, pp. 2228–2241, Jul. 2008.

[2] E. Basar, U. Aygolu, E. Panayirci, and H. V. Poor, "Space-time block coded spatial modulation," *IEEE Trans. Commun.*, vol. 59, pp. 823–832, Mar. 2011.

[3] P. Yang, M. Di Renzo, Y. Xiao, S. Li, and L. Hanzo, "Design guidelines for spatial modulation," *IEEE Commun. Surveys Tuts.*, vol. 17, pp. 6–26, Mar. 2015.

[4] H. Saeedi-Sourck, Y. Wu, J. W. Bergmans, S. Sadri, and B. Farhang-Boroujeny, "Complexity and performance comparison of filter bank multicarrier and OFDM in uplink of multicarrier multiple access networks," *IEEE Trans. Signal Process.*, vol. 59, pp. 1907–1912, Apr. 2011.

[5] B. Farhang-Boroujeny, "OFDM versus filter bank multicarrier," *IEEE Signal Process. Mag.*, vol. 28, pp. 92–112, May 2011.